8-2018

Exploring Interspecific Interactions of Reniform Nematode (*Rotylenchulus reniformis*) and Host Roots

Nathan Wayne Redding
Clemson University, nwreddi@g.clemson.edu

EXPLORING INTERSPECIFIC INTERACTIONS OF RENIFORM NEMATODE (*ROTYLENCHULUS RENIFORMIS*) AND HOST ROOTS

A dissertation
Presented to
the Graduate School of
Clemson University

In Partial Fulfillment
of the Requirements for the Degree
Doctor of Philosophy
Plant and Environmental Sciences

---

by
Nathan Wayne Redding
August 2018

Accepted by:
Paula Agudelo, Co-chair
Christina Wells, Co-chair
Julia Frugoli
Patrick Gerard

ABSTRACT

The semi-endoparastic reniform nematode (*Rotylenchulus reniformis*) infects over 300 plant species. Females penetrate host roots and induce formation of complex, multinucleate feeding sites called syncytia. While anatomical changes associated with syncytia morphology are well documented, little is known about their molecular basis or the local impact on root development. Using a soybean (*Glycine max*) split-root system across a twelve-day time course, we identified over 6,000 genes that were differentially expressed between inoculated and control roots (FDR = 0.01, $|\log2FC| \geq 1$) and 507 gene sets that were significantly enriched or depleted in inoculated roots (FDR = 0.05). Numerous genes up-regulated during syncytium formation had previously been associated with rhizobia nodulation. These included the nodule-initiating transcription factors CYCLOPS, NSP1, NSP2, and NIN, as well as multiple nodulins associated with the plant-derived peribacteroid membrane. Nodulation-related NIP aquaporins and SWEET sugar transporters, CLAVATA3/ESR-related (CLE) signaling proteins, and cell cycle regulators such as CCS52A and E2F were induced. Greenhouse growth studies showed that the roots of young soybean plants produced more new lateral roots per unit length when infected with reniform nematode. A pre-selected set of 440 genes with documented roles in lateral root formation were examined, and 131were differentially expressed in response to parasitism on at least one sampling date. These included genes for auxin biosynthetic proteins and transporters, as well as transcription factors such as LATERAL ROOT PRIMORDIUM 1, LATERAL ORGAN BOUNDARIES, SOMBRERO, SHORT-ROOT, RPT2a, and several MADS-box genes. Finally, RNAseq

data from infected soybean and cotton (*Gossypium hirsutum*) roots were used to assemble reniform nematode transcriptomes and identify putative nematode effectors based on sequence homology. A total of 3,485 and 4,852 reniform nematode protein-coding genes were assembled from infected soybean and cotton roots, respectively. One hundred and two of these genes shared homology to published plant parasitic nematode effectors, including CLEs, CTLs, FARs, VAPs, cell wall modifying enzymes, and putative secretory proteins of unknown function. The nematode and host genes identified here offer insight into reniform nematode parasitism and provide numerous avenues for further exploration.

ACKNOWLEDGMENTS

I would like to thank all those who have helped me reach this point in my academic career. To my committee, thank you for your guidance and for pushing me to grow through thoughtful discussions, questions, and conversations that we have shared. To Dr. Agudelo and Dr. Wells, I appreciate the opportunity that you gave me to pursue a PhD degree at Clemson University. Your investment in me through your time and energy has made the experience possible. Dr. Gerard your knowledge of statistical inference and experimental design was invaluable in developing the analysis for my study. Thanks also to Dr. Frugoli for her insights into nodulation and root formation, whose conversations pushed me to go deeper and expand my knowledge of plant biology.

I am also grateful to Dr. Cohen, Dr. DeWalt, Dr. Ballard, and the Clemson Department of Biological Sciences for the opportunity to develop my teaching skills as a Teaching Assistant and Instructor of Record. I have thoroughly enjoyed working with students in numerous sections the Biology of Plants class.

I would like to acknowledge the faculty, staff, and students within Plant and Environmental Science for their support. I want to thank the Clemson University Nematology Lab group for the input, advice, and encouragement throughout the program.

Finally, I would like to thank my friends and family for their unconditional love and support. To my parents, thank you so much for all that you have done. I would not be where I am today without all that you have taught me. To my wife, Krista, words cannot express my gratitude for all the ways you have and continue to bless me. Thank you for giving me the strength and reassurance to tackle each and every challenge.

TABLE OF CONTENTS

Table of Contents (Continued)

Page

LIST OF TABLES

LIST OF FIGURES

CHAPTER ONE

MULTIPLE NODULATION GENES ARE UP-REGULATED DURING ESTABLISHMENT OF RENIFORM NEMATODE FEEDING SITES IN SOYBEAN*

INTRODUCTION

Reniform nematode, *Rotylenchulus reniformis* (Linford and Oliveira), is a sedentary plant-parasitic nematode with a broad host range. Unlike more host-specific nematode parasites, reniform nematode infects over 300 species from numerous plant families in tropical, subtropical, and warm-temperate regions (Heald and Robinson 1990; Robinson et al. 1997). Among its hosts are multiple economically important crops, including soybean, cotton, and pineapple. Reniform nematode (RN) has a significant impact on global crop production and food security; in the United States alone, its infection causes millions of dollars in annual yield losses (Robinson 2007).

Similar to other sedentary plant-parasitic nematodes, reniform nematode induces the formation of permanent feeding structures in host root tissue. Immature females penetrate the epidermis and cortex of a host root, stopping when they reach an endodermal cell. There, they insert their stylet and release a proteinaceous secretion that promotes development of a permanent feeding site. Partial cell wall lysis begins at the initial endodermal cell and progresses to multiple cells in the pericycle, ultimately creating a multinucleate syncytium. The amalgamated cells undergo multiple structural and metabolic changes over the course of several days, giving rise to a metabolically active feeding site that nourishes the nematode during her development and reproduction (Rebois 1980; Rebois et al. 1975).

*Chapter published in Phytopathology 108(2):275-291

The anatomical changes associated with reniform nematode syncytia have been extensively documented (Agudelo et al. 2005; Jones and Dropkin 1975; Rebois 1980; Rebois et al. 1975), but less is known about their molecular basis, especially in comparison to better-studied parasites like the cyst nematodes (*Heterodera* and *Globodera* spp.) and root-knot nematodes (*Meloidogyne* spp.). Cyst nematodes (CN) manipulate host genes to orchestrate partial cell wall lysis in procambium or young vascular tissue, inducing the formation of a multinucleate, hypermetabolic syncytium. Root-knot nematodes (RKN) alter the expression of host genes involved in cell cycle control, cell wall modification, and hormone regulation to induce the formation of "giant cells" in root galls (Cabrera et al. 2015; Engler et al. 2015; Wieczorek 2015). Both groups of nematodes suppress defense-related signaling pathways throughout the lifetime of the feeding structure (Jaouannet et al. 2013; Quentin et al. 2013). Whether reniform nematode manipulates host genes in a manner analogous to that of CN or RKN is unknown, although recent work suggests that broadly similar groups of genes may be involved (Li et al. 2015).

Previous work has highlighted overlap in physiology and gene expression between rhizobia root nodules and CN/RKN feeding sites. RKN giant cells in *Medicago truncatula* exhibit altered expression of the nodule-associated transcriptional regulators PHAN and KNOX, the early nodulin ENOD40, the cell cycle regulator CCS52a, and the cytokinin primary-response gene ARR5 (Lohar et al. 2004). Hypernodulated (*har1*) *Lotus japonicus* mutants exhibit both increased nodulation and increased RKN infection (Lohar and Bird 2003). Similarly, the production of rhizobia-signaling isoflavonoids is

up-regulated during CN infection, and a beet CN resistance gene is highly expressed during both CN and rhizobia infection (Kennedy et al. 1999; Mitra et al. 2004).

Mounting evidence supports the hypothesis that diverse belowground symbionts and parasites have evolved to manipulate a similar genetic toolkit in their hosts. Genes normally involved in lateral root development and substrate transport are co-opted to support the formation of root nodules, mycorrhizae, and feeding sites (Lohar and Bird 2003; Lohar et al. 2004; Mathesius 2003; Wasson et al. 2009). In the context of nodulation, these genes have been termed nodulins. They include many sugar, nutrient, amino acid, and hormone transport proteins, as well as transcription factors, phosphatidylinositol transfer family proteins, and cell cycle regulators (Denance et al. 2014; Desbrosses and Stougaard 2011; Ferguson et al. 2010; Ghosh et al. 2015; Maroti and Kondorosi 2014; Verma et al. 1986). While most extensively studied in the context of nodulation, nodulins and nodule-associated genes are also present in the genomes of non-leguminous plants and are expressed in non-nodulation contexts (Denance et al. 2014; Reddy et al. 1999; Vieira-de-Mello et al. 2011).

Here we report the reference-guided assembly of a soybean (*Glycine max*) transcriptome from control and reniform nematode infected roots over a twelve-day time course. We describe a split-root growth system that allows us to harvest infected and non-infected control roots from the same plant. We identify individual genes and gene sets whose expression is altered in reniform nematode-infected roots, and we report the up-regulation of multiple well-known nodulins and nodule-associated genes during reniform nematode parasitism of soybean.

MATERIALS AND METHODS

Split-root growth system and nematode inoculation

To minimize the effects of plant-to-plant variation on identification of genes related to reniform nematode infection, we developed a split-root growth system that permitted the collection of infected and control root tissue from the same plant. Surface sterilized seeds of the reniform nematode-susceptible *Glycine max* cultivar 'Hutcheson' were germinated on sterilized vermiculite and maintained in a growth room at 28 ± 2°C and 50% relative humidity (RH) with a 14-h/10-h (light/dark) photoperiod. The soybean seed had been grown and collected in our greenhouses and was not coated with the rhizobial inoculum commonly present on commercial seed. After cotyledon emergence, a horizontal cut was made at the base of each primary root to encourage lateral root proliferation. After one week, the lateral roots were grouped into two equal bundles, threaded through the arms of a Y-shaped plastic tube (diameter 2.22 cm), and directed into adjacent 300 cm^3 pots filled with pasteurized fine sand. Plants were grown for one week, and twelve uniform plants were then selected for use in the experiment.

Reniform nematode inoculum was prepared from soil collected in a St. Matthews, SC agricultural field that had been under cotton and corn rotation for many years. Nematodes were extracted by sugar centrifugal flotation, rinsed, and collected in a 500µm mesh sieve (Jenkins 1964). Following inspection and quantification, nematodes were suspended in tap water at a concentration of 1500 individuals/ml. One pot in each split-root system was selected at random and inoculated with 2ml of the nematode

suspension (3,000 individuals); the other pot received an equivalent volume of tap water as a negative control.

Three replicate plants were harvested at 3, 6, 9 and 12 days after inoculation for microscopy and RNA extraction as described below. Thorough examination of scanned root images on each harvest date confirmed that no nodules were present on any root samples (Supplemental File 1.8). Additional inoculated and non-inoculated plants that were grown for 18 days in the same pasteurized sand system also showed no evidence of nodulation (Supplemental File 1.8).

Microscopy

Inoculated root samples were obtained from three replicate plants on each harvest date. Roots were gently rinsed free of soil, cleared with chloride bleach, and stained with acid fuchsin following the protocol of Bybd et al. 1983. Briefly, cleaned root samples were incubated in 0.9% NaOCl for 4 minutes, rinsed, and placed in tap water for 15 minutes to remove residual bleach. After a second rinse, roots were heated to boiling in beakers with 30 ml of tap water and 1 ml of acid fuchsin stain (3.5g acid fuchsin, 250 ml acetic acid, 750 ml water). After boiling for 30 seconds, the beakers were cooled to room temperature, and the roots were rinsed in tap water, placed in acidified glycerol, and heated until destained. Once cooled, roots and stained nematodes were photographed on an inverted microscope at 100x magnification (Motic AE2000 with Cannon EOS Rebel T3i camera). Neither nodules nor nodule primordia were observed in any root sample.

Transcriptome sequencing

Approximately 500 mg fresh weight (FW) of infected and control root tissue was harvested from each of three replicate plants at 3, 6, 9, and 12 days after reniform nematode inoculation (DAI), for a total of 24 samples (2 infection statuses x 4 dates x 3 biological replicates). Tissue was stored in RNA*later*® Stabilization Reagent (Ambion, Austin, TX) and sent to the University of Arizona Genetics Core (Tucson, AZ). RNA was extracted using the Qiagen RNAeasy Mini Kit, and RNA quality was assessed with the Agilent 2100 Bioanalyzer prior to 100-bp paired-end library preparation with the Illumina TruSeq 2 RNA kit. Samples were sequenced across two lanes of the Illumina HiSeq 2000 platform (Illumina, San Diego, CA).

A total of 619 million paired-end 100-bp reads were generated across the experiment, with an average of 25.8 million reads per sample. Read quality was assessed with FastQC v0.10.1, sequencing adaptors were trimmed with Trimmomatic v0.32 (Bolger et al. 2014), and low-quality bases were removed using the default settings of ConDeTri v2.2 (Smeds and Kunstner 2011). The average per-read PHRED quality score after trimming was 36.7, and the minimum per-read score was 36.02. All raw reads were uploaded to the NCBI Sequence Read Archive under accession number SRP091708.

Transcriptome Assembly and Annotation

Trimmed reads from each sample were mapped to the Wm82.a1.v1 build of the soybean reference genome using Bowtie2 v2.1.0 and TopHat v2.0.11 with default parameters (Trapnell et al. 2012). The -G option was used to supply TopHat with the

Glyma1.0 reference gene models as a GTF file (Schmutz et al. 2010). Transcripts were assembled separately for each sample using Cufflinks v2.2.1, then merged with the Glyma1.0 reference annotation to generate a soybean root transcriptome that included both previously described and newly assembled transcripts (Trapnell et al. 2012). The new reference transcriptome was annotated in Blast2GO Pro v3.0, which performs a BLASTx search against the NCBI nr protein database and assigns sequence descriptions, gene ontology (GO) terms, Interpro IDs, enzyme codes (EC), and KEGG pathways to transcripts with significant blast hits ($E < 10^{-6}$) (Conesa et al. 2005).

Gene expression was quantified by mapping reads from individual samples back to the new transcriptome using HTSeq v0.6.1 (Anders et al. 2015). Reads from all splice forms of a given gene were pooled, and count data were imported to DESeq2 for differential expression analysis using default parameters (Love et al. 2014). Data were analyzed separately by date to identify genes differentially expressed between inoculated and non-inoculated roots, while controlling for the effect of individual plants (FDR = 0.01). Genes were considered to be significantly differentially expressed when they fulfilled two criteria: (1) an FDR-adjusted *p*-value of ≤ 0.01 and (2) an $|\log_2(\text{fold change})|$ estimate of ≥ 1. The $\log_2$FC estimates were calculated in DESeq2 and implemented empirical Bayes shrinkage to permit accurate comparison of effect sizes across all genes (Love et al. 2014).

In parallel with the identification of individual DE genes, gene set enrichment analysis (GSEA) was performed to identify pre-defined gene sets whose expression was significantly enriched or depleted in inoculated roots (Subramanian et al. 2005). A

custom GSEA database of 1,499 pre-defined gene sets, each containing at least 15 genes, was created from GO terms, enzyme codes, and KEGG pathway annotations of the root transcriptome. Gene sets whose expression was enriched or depleted in inoculated roots on each date were identified using a FDR of 0.05.

To assess the possibility of rhizobial contamination, raw reads from individual soybean root samples were mapped to the sequenced genomes of rhizobial bacteria and other prokaryotic and eukaryotic model organisms. The reference genomes of eight nodulating bacterial species (*Bradyrhizobium diazoefficiens*, *B. elkanii*, *B. japonicum*, *Mesorhizobium loti*, *Rhizobium etli*, *R. leguminosarum*, *Sinorhizobium fredii*, and *S. meliloti*) and six additional model organisms (*Escherichia coli*, *Saccharomyces cerevisiae*, *Drosophila melanogaster*, *Xenopus laevis*, *Danio rerio*) were obtained from NCBI. Trimmed reads from each soybean root sample were mapped to each reference genome using Bowtie2 v2.1.0 with default parameters (Langmead and Salzberg 2012). The percentage of reads from each sample that mapped to each genome was calculated with HTSeq v0.6.1. Two-way ANOVAs were used to test for differences in percent mapped reads between inoculated and control samples for each genome and date.

The percent reads that could be successfully aligned to these non-plant genomes was extremely low, never exceeding 2.06E-05 percent for any sample (Suppl. 1.9). Across all dates and genomes, there were no significant differences in the percent mapped reads between inoculated and control samples. The percent reads that could be aligned to nodulating bacterial genomes (range: 0 to 2.06E-05) were similar in magnitude to the percent that could be aligned to *E.coli*, animal, and fungal genomes (range: 0 to

2.01E-05). It is likely that these reads derive from genes and gene segments that are highly conserved across species.

RESULTS

Microscopy

Histology of infected roots documented the progress of reniform nematode infection through time and provided context for the gene expression results (Fig. 1). At 3 DAI, all inoculated samples contained multiple vermiform females embedded in the root cortex with their head regions adjacent to the stele. At 6 DAI, individual root samples contained a mixture of infection stages: both vermiform females and swollen females were present, indicating a mixture of new and mature feeding sites. At 9 DAI, all females were swollen into the characteristic mature reniform shape, and at 12 DAI, egg masses were present at the majority of infection sites. In no samples was there evidence of rhizobial nodules or nodule primordia.

Assembly and Differential Gene Expression

Illumina sequencing of 24 RNA samples from reniform nematode-inoculated and control roots generated over 619 million 100-bp reads. After filtering and trimming, clean reads from all samples were mapped back to the soybean reference genome, and transcripts were assembled using soybean reference gene models as guidance. The final soybean root transcriptome contained both previously annotated and novel transcripts. In total, we assembled 46,995 unique genes and 120,565 alternate splice forms of these genes, with an N50 of 1430 bp and a mean length of 984 bp. Ninety-seven percent of the assembled genes received a significant hit to the NCBI nr database ($E < 10^{-6}$), and 79% were annotated with at least one GO term. Enzyme codes and KEGG pathways were

assigned to 21% and 26% of the assembled genes, respectively. The FASTA sequences of all assembled transcripts are provided in Supplementary File 1.1, and Blast2GO transcript annotations, including Glyma names of previously annotated genes, are provided in Supplementary File 1.2.

Overall patterns of differential gene expression

Exploratory data visualization with principal components analysis (PCA) confirmed that samples could be separated by infection status along one of the first two principal components at 3, 9 and 12 DAI (Fig.2). There was no clear separation of samples by infection status at 6 DAI (see below). Sequence descriptions, normalized counts, $\log_2$FC estimates, and FDR-adjusted *p*-values for all genes on all dates are provided in Supplementary Files 1.3-1.6.

A total of 6,628 genes were differentially expressed (DE) between inoculated and control roots on at least one sampling date (Fig. 3; FDR = 0.01; $|\log_2 FC| \geq 1$). The greatest number of DE genes (6,021) was observed early in the infection process on DAI 3. There were far fewer DE genes on later dates (Fig. 3). The magnitude of differential expression was also highest on DAI 3, when estimated $\log_2$FC values for individual DE genes ranged from -5.24 to 8.75. The fold changes of DE genes on subsequent dates were orders of magnitude smaller: $\log_2$FC ranges were -3.38 to 4.11 (DAI 6), -4.05 to 4.06 (DAI 9) and -3.00 to 4.72 (DAI 12).

More genes were up-regulated than down-regulated in infected roots: 4,000 up-regulated vs. 2,021 down-regulated (3 DAI), 773 vs. 296 (9 DAI), and 458 vs. 64 (12

DAI). The exception occurred on DAI 6, when only a small number of DE genes were identified, and more were down-regulated (72 vs. 138). In a separate experiment, we observed a similar phenomenon during reniform nematode infection of cotton roots: high variability among samples and fewer DE genes at 6 DAI compared to 3, 9 and 12 DAI. This result may reflect the presence of multiple infection stages at 6 DAI (Fig. 1), a result we have documented histologically in both soybean and cotton.

Top differentially expressed genes

Tables 1 and 2 present the top twenty DE genes with the largest positive and negative $\log_2$FC estimates on each sampling date. Data for all DE genes can be found in Supplementary Files 1.3-1.6. Many of the top twenty up-regulated genes on each date coded for nodulins, nodulation-specific proteins, and/or proteins with a documented role in nodulation (Table 1). This trend was most apparent at 3 DAI, when sixteen of the top twenty up-regulated genes were known to be associated with nodulation. Five, eight and eleven of the top twenty up-regulated genes at 6, 9 and 12 DAI also had documented roles in nodulation. The magnitude of up-regulation for some nodulation-related genes was extremely high: at 3 DAI, $\log_2$FC estimates for eight nodulation-related genes were greater than 8.0 (i.e. a 256-fold increase).

The top up-regulated gene list contained nodulin-16 (a membrane protein), nodulin-21 (an iron transporter), nodulin-41 (an aspartic protease), and nodulin-61 (a FluG glutamate-ammonia ligase). Other well-known nodulation genes included CERBERUS/LIN-1, the NODULE INCEPTION transcription factor NIN, the nodule-

specific zinc transporter ZIP1, and a soybean homolog of ROOT DETERMINED NODULATION 1.

The top up-regulated gene list also contained multiple genes related to defense (defensin- and thaumatin-like proteins, endochitinase, and tmv resistance protein), stress and reactive oxygen detoxification (universal stress protein A, numerous peroxidases, and GDP-mannose-epimerase), modification and degradation of proteins (several proteases and ring-h2 finger proteins), and the metabolism of gibberellic acid (ent-copalyl diphosphate synthase and gibberellin 20 oxidase 1) and ethylene (1-aminocyclopropane-1-carboxylate oxidase).

Two strongly induced genes coded for transcription factors: NIN and a bHLH30-like transcription factor. In contrast, 12 transcription factors appeared on the top down-regulated gene list, three of them ethylene response factors (ERFs, Table 2). ERFs control plant responses to pathogens through the regulation of jasmonate (JA)/ethylene (ET) responsive defense genes (Huang et al. 2016); their down-regulation is consistent with nematode-induced suppression of the plant immune system. Also strongly down-regulated were genes associated with jasmonic acid metabolism (12-oxophytodienoate reductase and cytochrome p450 94a1) and the transport and response to auxin (ATP binding cassette B family member 4, auxin-induced protein 5NG4, and cryptochrome 1). Numerous cell wall genes were down-regulated, including those associated with lignin metabolism (laccases), hemicellulose metabolism (glucomannan 4-β-mannosyltransferase, mannan endo-β-1,4-mannosidase, and UDP-glucuronate:xylan

alpha-glucuronosyltransferase), cell adhesion (fasciclin-like arabinogalactan proteins), and cell wall strengthening (extensins and hydroxyproline-rich glycoproteins).

Gene set enrichment analysis

In parallel with the identification of individual DE genes, gene set enrichment analysis (GSEA) was used to identify pre-defined gene sets whose expression differed between inoculated and control roots on each date (FDR = 0.05; Fig. 4). While DESeq2 identifies individual genes with large, statistically significant fold changes, GSEA identifies gene sets whose individual members show concordant, but potentially smaller, differences in expression between treatments (Subramanian et al. 2005). Five hundred and seven gene sets were significantly enriched or depleted in infected roots on at least one sampling date: 303 enriched in infected roots, 169 depleted, and 35 either enriched or depleted, depending on the date. The top 20 gene sets significantly enriched in infected roots on each date are presented in Table 3, and normalized enrichment scores for all gene sets are provided in Supplementary File 1.7.

Some enriched gene sets confirmed the results of the differential gene expression analysis. The gene set GO:0009877 (Nodulation) was significantly enriched in infected roots on all sampling dates and was among the top twenty enriched gene sets at 6 and 9 DAI (Table 3). The related gene set GO:0009399 (Nitrogen fixation) was also significantly enriched on all sampling dates. BLASTx results confirmed that all genes with these GO annotations were plant genes, most of them previously annotated in the soybean reference genome. None were of bacterial origin.

The gene set MAP00940 (Phenylpropanoid biosynthesis) was significantly enriched in infected roots on all dates, and the related gene sets GO:0016210 (Naringenin-chalcone synthase activity), MAP00943 (Isoflavonoid biosynthesis), MAP00941 (Flavonoid biosynthesis), and GO:0009813 (Flavonoid biosynthetic process) were all significantly enriched at 3 DAI. While flavonoids in general have broad roles in plant development and defense, isoflavonoids such as narigenin serve as chemical messengers between legumes and their bacterial symbionts and have been shown to increase during nematode infection (Hutangura et al. 1999; Kennedy et al. 1999; Liu and Murray 2016).

By far the largest number of top enriched gene sets were related to DNA: its packaging, modification, and replication, as well as the accompanying process of mitosis (Table 3). Many of these sets were significantly enriched on at least three dates, including GO:0003678 (DNA helicase activity), GO:0006270 (DNA replication initiation), GO:0000786 (Nucleosome), GO:0051567 (Histone H3-K9 methylation), GO:0042555 (MCM Complex), and GO:0010389 (Regulation of G2/M transition of mitotic cell cycle).

Enrichment at 3 DAI of gene sets related to large ribosomal subunits (GO:0015934), small ribosomal subunits (GO:0015935), and rRNA binding (GO:0019843) suggested that early stages of reniform nematode symbiosis were characterized by wholesale induction of translational machinery and *de novo* protein synthesis (Table 3). Enrichment of genes sets related to aerobic respiration (GO:0009060, GO:0005747, GO:0004129) on multiple dates was consistent with enhanced energy

demand and cellular respiration. Enrichment of gene sets related to pectin catabolism suggested that pectin degradation may occur in cell walls and middle lamellae during reniform nematode infection (EC:3.1.1.11, GO:0030599, GO:0045490).

While pectin catabolism genes were enriched, far more cell wall-related gene sets were depleted. At 3 DAI, four gene sets related to 1,3-beta-glucan (callose) synthase activity were depleted in infected roots (Table 4). At 6 DAI, expression of multiple cell wall gene sets was depleted, including those associated with general wall properties (GO:0042546, GO:0071555), pectin synthesis (GO:004589, EC.2.4.1.43), hemicellulose synthesis (GO:0010417, GO:0010413), and lignin metabolism (EC:1.10.3.2, GO:0046274). Many of these same sets were enriched at 12 DAI, consistent with a switch from wall thinning and lysing in early infection to later wall thickening in mature feeding sites (Supplemental Table 1.7; Rebois et al. 1975).

Also depleted in infected roots were gene sets related to blue light signaling. These included phototropism (GO: 0009638), blue light signaling pathway (GO:0009785), and blue light photoreceptor activity (GO: 0009882). Inspection of the leading edge genes from the depleted sets (i.e. the specific genes responsible for the depletion signal) showed that in all cases the signal was related to repression of four cryptochrome 1 genes (XLOC_009646, XLOC_014716, XLOC_034413, and XLOC_037027), two cryptochrome 2 genes (XLOC_039443 and XLOC_002396), and one phytochrome A gene (XLOC_025512). Down-regulation of these genes was most marked at 3 DAI but, in some cases, continued into later stages of syncytium formation (Supplemental Tables 1.3-1.6).

Expression of nodulation-related genes

Of the 59 genes in the Nodulation (GO:0009877) gene set, 50 contributed to its leading edge on at least one date. Expression data for these and 81 additional nodulation-related genes identified from the assembled transcriptome are presented as clustered heat maps in Fig. 5 (up-regulated genes) and Fig. 6 (down-regulated and unchanged genes). The most pronounced differences in nodulation-related gene expression occurred early in the infection process at 3 DAI. Ninety-nine putative nodulation-related genes were significantly up-regulated at 3 DAI, compared with six, twenty, and eighteen at 6, 9, and 12 DAI, respectively. Nineteen nodulation-related genes were down-regulated at 3 DAI, compared to three, five, and zero at 6, 9, and 12 DAI.

Multiple genes that participate in the canonical signal transduction pathway of nodule initiation were strongly up-regulated in infected roots. These included the transcriptional activator CYCLOPS (up-regulated 5.5-fold at 3 DAI) and four soybean homologs of the NODULE INCEPTION (NIN) transcription factor to which CYCLOPS binds (up-regulated 6 to 188.7 fold at 3 DAI). Also induced were soybean homologs of the GRAS-family transcription factors NODULATION SIGNALING PATHWAY 1 (NSP1, up 3.5-fold) and NODULATION SIGNALING PATHWAY 2 (NSP2, up 10.3-fold), which bind the promoters of early nodulin genes. Components of signal transduction events associated with the Autoregulation of Nodulation (AON) program were also induced. These included a homolog of ROOT DETERMINED NODULATION 1 (RDN1, up 123.6-fold at 3 DAI) and five plant CLAVATA3/ESR family (CLE) proteins (up 2.7 to 8.3-fold at 3 DAI).

Additional nodulins and nodulation-related genes, many of which act downstream of the transcription factors above, were also induced by reniform nematode parasitism. These spanned a wide range of functions, from membrane transporters (NIP aquaglyceroporins, SWEET bidirectional sugar uniporters, vacuolar iron transporters, and a nodule-specific zinc transporter) to lipid raft components (remorins and flotillins) to proteins involved in remodeling of the extracellular matrix (pectate lyases and extensin-like/proline-rich proteins). Some were nodulins of unknown function that have been previously annotated only as peribacteroid membrane components (e.g. ENOD 55-2, nodulin-24, nodulin-20, and nodulin-16). Others were associated with cell cycle control and endoreduplication (cyclin-dependent kinase inhibitor 7, E2Fa, and FIZZY-RELATED 3). Of particular interest was the significant up-regulation of nodulation genes that have no obvious role in nematode parasitism, such as the three leghemoglobin genes induced 8.3 to 11.5-fold at 3 DAI. It is unclear whether these genes are required for reniform nematode parasitism, or whether their induction is incidental to nematode manipulation of high level regulatory programs also involved with nodulation.

A smaller number of putative nodulation-related genes were down-regulated during reniform nematode infection. Several were from families also present in the up-regulated gene set, such as remorins, SWEET sugar transporters, a CLAVATA/ESR (CLE) protein, and an RDN-1/o-arabinosyltransferase. Others were from families not present in the up-regulated gene list, and many of these had putative roles in defense. Five of the down-regulated nodulation-related genes coded for phospholipase D, which generates phosphatidic acid (PA) in response to bacterial Nod factors, and functions in

perception and response to bacterial, fungal, and nematode pathogens (Zhao 2015). Two genes coding for Nodulin-related Protein 1, previously linked to heat stress and defense signaling, were also significantly down-regulated during infection (Fu et al. 2010).

DISCUSSION

Reniform nematode infection begins when an immature female penetrates the root epidermis and cortex to reach an endodermal "initial cell." There she inserts her stylet and releases a mixture of effectors, including both CLE and CEP peptide mimics (Eves-Van den Akker et al. 2016; Wubben et al. 2015). The initial cell and adjacent pericycle cells exhibit areas of cell wall lysing, which ultimately converge into full breaks, allowing multiple cytoplasms to coalesce into a single syncytium. Previous work suggests that feeding site formation is initiated by 2 to 3 DAI and that syncytia are well established by 6 to 9 DAI (Agudelo et al. 2005; Jones and Dropkin 1975; Rebois 1980; Rebois et al. 1975). Our histological results were consistent with this time course.

Uninfected root pericycle cells are dominated by a large central vacuole, with a relatively small amount of cytoplasm confined to the cell periphery. During feeding site formation, the central vacuoles of affected cells are disassembled and the numbers of ribosomes, mitochondria, plastids, and small vacuoles increase. Together with an increase in the size of endoplasmic reticula and nuclei, these changes fill syncytial cells with a dense, organelle-rich cytoplasm (Agudelo et al. 2005; Rebois et al. 1975). The number of incorporated pericycle cells increases outwardly from the initial cell as the syncytium develops, ultimately encompassing 100 to 200 cells. Remaining portions of the syncytial cell walls thicken and may display in-growths and complex "boundary formations" (Agudelo et al. 2005; Rebois et al. 1975). Although the broad ultrastructural changes that accompany infection have been documented, relatively little is known about infection-related changes in plant gene expression.

General trends in gene expression during reniform nematode infection

The most substantial changes in gene expression occurred early in infection. A subset of genes was differentially expressed throughout the full twelve-day time course, but the largest number of DE genes and the largest differences in gene expression were observed at 3 DAI.

Many DE genes and gene sets were consistent with ultrastructural changes previously reported during infection. Genes involved in cell wall synthesis and organization were suppressed early in infection when cell walls have been shown to lyse, then up-regulated in later stages when they have been reported to thicken and develop ingrowths (Agudelo et al. 2005; Rebois et al. 1975). Likewise, genes and gene sets associated with aerobic respiration and ribosomal biogenesis were markedly up-regulated in infected roots, consistent with the documented proliferation of mitochondria and ribosomes in syncytial cells. It should be noted that we sampled whole infected roots, not syncytia alone. Gene expression changes therefore represent the aggregate response of the root system as a whole, including - but not limited to - the responses of syncytial cells.

Many genes and gene sets induced during infection had previously-documented roles in rhizobial nodule formation. Nodulation-related genes are not unique to legumes, nor are they expressed only during nodulation (Denance et al. 2014). They have been most extensively studied in the context of legume nodulation, but they have homologs in non-legume species and function in multiple developmental and symbiotic contexts. Many instances of overlap among genes involved in mycorrhization, nodulation, and

nematode parasitism have been reported previously (reviewed in Mathesius 2003). For example, nodulin *N-26*, which encodes an aquaglyceroporin, is also induced during mycorrhizal infection, RKN gall formation, and reniform nematode parasitism (Albrecht et al. 1999; Favery et al. 2002). Likewise, the leucine-rich repeat (LRR) receptor kinase SYMRK/NORK is part of a receptor complex that functions in plant perception of rhizobia, mycorrhizal fungi, and RKN (Endre et al. 2002; Stracke et al. 2002; Weerasinghe et al. 2005). Nonetheless, the number and magnitude of differentially expressed nodulation-related genes observed during reniform nematode parasitism of soybean was unexpected.

Reniform nematodes may exploit aspects of the same signal exchange pathways used by rhizobia to communicate with their legume hosts. This possibility has previously been raised for the endoparasitic RKN *Meloidogyne incognita,* which possesses a horizontally acquired gene homologous to that of rhizobial nodL (Bellafiore et al. 2008; McCarter et al. 2003). In response to root-derived flavonoids, rhizobial nodL promotes production of Nod factors that trigger nodule formation on host roots. It is not yet clear whether the *M. incognita* nodL gene promotes synthesis of nematode "Nod factors" that similarly trigger aspects of feeding site formation. Nonetheless, the wholesale induction of nodulation-related genes reported here suggests that reniform nematode may also modulate high-level regulators shared with the nodulation program.

Nodulation-related genes: early signaling events and Autoregulation of Nodulation

Legumes signal to rhizobia through the secretion of specific flavonoids that promote synthesis and release of bacterial Nod factors (Ferguson et al. 2010). In *L. japonica,* Nod factors diffuse to the root epidermis, where they bind to a receptor complex consisting of NFR1, NFR5, and SYMRK/NORK recruited by flotillin FLOT4 to lipid rafts (Madsen et al. 2003). Protein interactions and phosphorylations generate a signaling cascade that ultimately initiates a cytosolic calcium spike perceived by Calcium/Calmodulin-Dependent Protein Kinase (CCaMK). CCaMK binds and phosphorylates the transcription factor CYCLOPS, which in turn induces expression of NIN, a transcriptional regulator of multiple nodulation genes including pectate lyase (Singh et al. 2014; Xie et al. 2012). GRAS family transcription factors NSP1 and NSP2 are also induced by the calcium spike and promote expression of early nodulation genes (Catoira et al. 2000; Oldroyd and Long 2003). Finally, CERBERUS, a putative E3 ubiquitin-protein ligase, is expressed early in nodule formation and appears to be required for proper infection thread development (Yano et al. 2009).

Soybean homologs of many genes described above were differentially expressed in response to reniform nematode infection, including FLOT4, CYCLOPS, NIN, pectate lyase, NSP1, NSP2, and CERBERUS (Fig. 5). Early events in reniform nematode infection appear to share components of the signal transduction pathways involved in perception of rhizobial Nod factors. Indeed, the evolution of these signal transduction pathways may pre-date both nematode parasitism and rhizobial nodulation, as a recent review suggests that nodulation arose through co-option of genes involved in the ancient mycorrhizal symbiosis (Suzaki et al. 2015).

Once formed, nodules can be costly to maintain. The extent of rhizobial nodulation is therefore limited through the Autoregulation of Nodulation (AON) program, a long-distance feedback loop in which NIN promotes synthesis of CLE signaling peptides that negatively regulate nodule number (Soyano et al. 2014; Suzaki et al. 2015). Also involved in AON is the o-arabinosyltransferase, RDN1, which adds arabinose to CLE peptides (Kassaw et al. 2015).

Infection by reniform nematode (RN) was associated with induction of both NIN and RDN1, as well as up-regulation of five CLE peptides and down-regulation of one CLE peptide (Fig. 5). All CLE peptides were of plant origin and had been previously annotated in the soybean reference genome. Two CLE receptors, homologs of CALVATA1 and ACR4, were also down-regulated (Fig. 6).

This is not the first evidence for a role of CLE peptides in nematode parasitism: previous studies have documented the production of CLE peptide mimics by CN, RKN, and RN (Bakhetia et al. 2007; Guo et al. 2015; Patel et al. 2008; Wang et al. 2005; Wubben et al. 2015). Hg-SYV46 was the first nematode-derived CLE to be identified from the secretions of the soybean CN *Heterodera glycines* (Wang et al. 2005). Its role and that of other CLE mimics was subsequently established through RNAi and receptor knockout studies (Bakhetia et al. 2007; Guo et al. 2015; Patel et al. 2008). RKNs secrete the CLE-like peptide 16D10, and its RNAi silencing causes lower RKN infection (Huang et al. 2006a; Huang et al. 2006b). Recently, the presence of at least three CLE-motif genes has been demonstrated in the dorsal esophageal gland cell of sedentary reniform

nematode females (Wubben et al. 2015). The present work suggests that the plant's own CLE peptides are also involved in the response to RN parasitism.

Other nodulation-related genes

Multiple transporter genes whose expression changed in response to reniform nematode also had documented roles nodulation: three nodulin 26-like intrinsic proteins (NIPs, a family of aquaporins), two vacuolar iron transporters, a nodule-specific zinc transporter and numerous sugar transporters (Fig. 5). Eight of these sugar transporters belonged to the SWEET (Sugars Will Eventually be Exported Transporters) family of bidirectional sugar uniporters. The first SWEET gene to be identified was a nodulin from *Medicago truncatula* (MtN3), but SWEETs are known to function in a variety of processes, including phloem loading, nectar secretion, pollen nutrition, and seed filling (Eom et al. 2015; Gamas et al. 1996). Their up-regulation by bacterial and fungal pathogens is thought to promote the release of sugars into the apoplast during early infection stages (Chen et al. 2010).

In addition to SWEET sugar transporters, homologs of the sucrose-proton symporters SUT4 and SUC2 were also up-regulated. Both genes have previously been implicated in phloem loading and unloading (Truernit and Sauer 1995; Weise et al. 2000), and their expression has been documented in nodules and nodule-associated phloem (Complainville et al. 2003; Flemetakis et al. 2003). AtSUC2 expression has also been observed in syncytia induced by the sugar beet cyst nematode, *Heterodera schachtii* (Juergensen et al. 2003).

The construction of nodules and syncytia necessitates significant changes to cellular membrane systems. In nodules, these changes involve root hair curling, infection thread formation, and production of a plant-derived peribacteroid membrane (Ferguson et al. 2010). In reniform nematode feeding sites, syncytial cells disassemble their central vacuoles, expand the endoplasmic reticulum membrane system, and increase the number of membrane-bound organelles (Agudelo et al. 2005; Rebois et al. 1975). Multiple genes involved in lipid signaling, membrane trafficking, and membrane organization are up-regulated during both biotic interactions.

Four Sec14-like phosphatidylinositol transfer proteins with the GO term Nodulation (GO:0009877) were up-regulated in infected roots (Fig. 5). Sec14-like proteins coordinate lipid signaling with membrane trafficking and facilitate the non-enzymatic transfer of phostphatidylinositols and phosphatidylcholine monomers between membrane bilayers (Ghosh and Bankaitis 2011). Sec14-nodulins were first identified in *L. japonicus* nodules and have been shown to influence polar membrane trafficking and root hair development in *A. thaliana* (Ghosh et al. 2015). Two up-regulated soybean Sec14-like genes contained a GOLD (Golgi dynamics) domain. In Arabidopsis, such genes are termed patellins and are believed to function in vesicle and membrane trafficking, including cell plate formation during cytokinesis (Peiro et al. 2014; Peterman et al. 2004).

A large number of remorins were also differentially expressed in infected roots: nine up-regulated and four down-regulated (Fig. 5 and 6). While their functions are not fully understood, remorins appear to be associated almost exclusively with plasma

membrane lipid rafts; several members of the family are strongly induced during nodulation in *M. truncatula* and *L. japonicus* (Lefebvre et al. 2010). One nodulation-related remorin is thought to function as a scaffolding protein, mediating spatial relationships among the core Nod factor receptor-like kinases NFP, LYK3, and DMI2 in *M. truncatula*.

Cell cycle and endoreduplication

During rhizobial infection, host cells undergo several rounds of endoreduplication, i.e. replication of the genome without mitosis or cytokinesis, leading to increased nuclear size (Maroti and Kondorosi 2014). The mitotic inhibitor CCS52 is required for this process. It activates the APC ubiquitin protein ligase that degrades mitotic cyclins, blocking the mitotic cell cycle and promoting endoreduplication (Engler and Gheysen 2013; Vinardell et al. 2003).

Reniform nematode infected roots showed up-regulation of two CCS52B homologs (FIZZY-RELATED 3) at DAI 12 (Fig. 5). At 3 DAI, a CCS52A homolog was up-regulated with an FDR-adjusted *p*-value of ≤ 0.01, although it did not meet our $\log_2$FC ≥ 1 cutoff; another CCS52A homolog was up-regulated with an FDR adjusted *p*-value between 0.01 and 0.05 (Supplemental File 1.3). Also up-regulated at 3 DAI was the transcription factor E2Fa, which is required for endoreduplication (Engler and Gheysen 2013; Vinardell et al. 2003) and whose expression in the Arabidopsis pericycle controls lateral root initiation (Benkova and Bielach 2010).

The up-regulation of endoreduplication genes, enrichment of multiple DNA replication-related gene sets, and the increase in nuclear size previously observed in syncytial cells is consistent with endoreduplication in reniform nematode syncytia. This finding comports with studies of RKN and CN, both of whose feeding structures exhibit increased nuclear size, primarily due to endoreduplication (Edgar et al. 2014). Endoreduplication appears to be vital for successful RKN and CN feeding site formation, as a knockdown of CCS52 delays feeding site development and decreases reproduction for both nematodes (Vieira et al. 2013).

Genes associated with nitrogen fixation

While similarities in gene expression between nodulation and reniform nematode parasitism may reflect common developmental mechanisms, extensive nodule-related gene expression in parasitized roots may also be a by-product of nematode interference with nodulation signaling pathways. Some up-regulated nodulation-related genes may be "brought along for the ride" when transcription factors such as CYCLOPS, NIN, NSP1, and NSP2 are induced early in reniform nematode parasitism. Evidence for this hypothesis is provided by the induction of nitrogen fixation genes that have no obvious role in nematode parasitism. A case in point is the expression of three leghemoglobin genes up-regulated from 8.3-fold to 11.5-fold at 3 DAI. Leghemoglobins bind oxygen to protect nitrogenase and to manage the movement of oxygen for bacterial respiration (Ott et al. 2005). They have no documented function outside of nitrogen-fixing root nodules, and it is unclear what role they would play in the absence of nitrogenase or rhizobia.

Several lines of evidence suggest that rhizobial contamination was not responsible for changes in gene expression reported here. Surface sterilized soybean seeds were produced in our lab, free from rhizobial inoculum, and soil was pasteurized prior to seedling transplant. Reniform nematode inoculum was prepared from a field that had been under a continuous non-legume corn and cotton rotation for many years. Careful visual inspection and microscopy revealed no evidence of nodules or nodule primordia on any sample throughout an 18 day time course. The very small percentage of Illumina reads that could be aligned to rhizobial genomes did not differ in magnitude from the percentage that could be aligned to genomes from *E. coli* and a variety of eukaryotic model organisms. In no case did the small percentage of rhizobial-mappable reads differ between inoculated and control root samples. While some microbial RNA is inevitably sequenced in plant tissue transcriptomes, we found no evidence to suggest there was significant rhizobial contamination.

Conclusion

Our understanding of reniform nematode biology and feeding site formation is limited compared to that of other sedentary endoparasitic nematodes such as RKN and CN. Nonetheless, the overall patterns of gene expression reported here share features with transcriptomes from better-studied nematode-host interactions. Many genes affected by reniform nematode infection also share similarities with mutualistic belowground symbioses such as nodulation and mycorrhization, and it has been suggested that multiple belowground symbionts and parasites manipulate aspects of the lateral root

organogenesis program to form symbiotic structures (Mathesius 2003). If an ultimate goal is nematode management, then the similarities among diverse belowground processes may be less important than their specific differences. A comparative approach to the transcriptomic changes induced by lateral root organogenesis, mycorrhization, nodule formation, and nematode parasitism will allow us to pinpoint how one organism induces formation of a beneficial nodule while another induces formation of a harmful feeding site. Breeding and genetic engineering efforts can be focused on disrupting molecular events that are unique to nematode infection while avoiding pathways that function in normal organogenesis and beneficial symbioses.

Table 1.1. Top 20 genes whose expression was significantly up-regulated in reniform nematode-infected soybean roots at four time points after inoculation (FDR = 0.01, genes ranked based on log_2FC estimate). Bolded genes have previously been identified as nodulins or as playing a role in legume-rhizobia nodulation.

Gene ID	Description	Mean Normalized Counts				
		Inoculated	SD	Control	SD	L2FC estimate
3 DAI						
XLOC_003387	ring-h2 finger protein atl34-like	1623	2264	1	1	8.75
XLOC_002605	**prolyl 4-hydroxylase subunit alpha-1**	1048	895	0	0	8.63
XLOC_000614	**casp-like protein**	1456	1448	1	1	8.53
XLOC_012146	**vacuolar iron transporter homolog 4-like/nodulin 21**	2352	2392	3	0	8.44
XLOC_033005	**probable 2-isopropylmalate synthase**	929	1344	0	0	8.35
XLOC_039620	**aspartic protease CDR-1-like /nodulin 41**	637	489	0	0	8.31
XLOC_049195	**2-isopropylmalate synthase**	558	512	0	0	8.07
XLOC_019074	**selenium-binding protein 1**	1998	2542	2	1	8.05
XLOC_005135	**nodulin 16**	808	394	1	0	8.04
XLOC_011554	**carboxy-terminal region remorin**	547	629	0	0	7.92
XLOC_037046	ring-h2 finger protein atl34-like	909	996	1	1	7.76
XLOC_020450	**carboxy-terminal region remorin**	595	585	1	1	7.62
XLOC_009155	**nodule inception protein (NIN)**	1170	861	3	1	7.56
XLOC_028021	**polyol transporter 3/6-like**	344	216	0	0	7.54
XLOC_049849	subtilisin-like serine protease	4337	2568	18	7	7.52
XLOC_012147	**EKN protein**	3489	4401	3	2	7.42
XLOC_013559	**defensin-like protein 1**	289	173	0	0	7.26
XLOC_030420	tmv resistance protein n/ TIR-NBS-LRR	391	449	1	1	7.01
XLOC_028458	**PGN polygalacturonase specific to nodule**	328	305	0	0	7.00

6 DAI						
XLOC_042297	uncharacterized glycosyl transferase	1421	2455	1	2	4.11
XLOC_042566	serine acetyltransferase 2-like	916	1580	1	2	4.10
XLOC_022985	**cell number regulator 2/FW2.2-like**	408	687	0	0	3.61
XLOC_022216	peroxidase 15	342	151	7	5	3.58
XLOC_051027	protein iq-domain 31-like	170	292	0	0	2.69
XLOC_014144	transcription factor bhlh30-like	88	147	1	1	2.44
XLOC_004535	ammonium transporter 3 member 1-like	56	40	3	1	2.43
XLOC_015272	expansin A15	81	134	1	1	2.40
XLOC_031107	putative cyclin-dependent kinase inhibitor 1c-like	239	397	6	8	2.39
XLOC_051990	peroxidase 12-like	424	482	39	17	2.25
XLOC_045581	mitochondrial calcium uniporter	104	179	0	0	2.22
XLOC_035511	**allantoinase 1**	420	720	2	3	2.22
XLOC_051360	**zinc transporter protein ZIP1**	296	394	13	9	2.18
XLOC_040432	g-type lectin s-receptor-like serine threonine-protein kinase SD2-5-like	74	123	0	0	2.18
XLOC_040169	**glutamine synthetase**	745	805	45	18	2.15
XLOC_011394	IRK-interacting protein-like	69	116	0	0	2.03
XLOC_018724	**e3 ubiquitin-protein ligase lin-1/CERBERUS**	42	64	0	0	1.99
XLOC_017748	putative ABC transporter C family member 15	1321	1022	205	39	1.95
XLOC_049982	abc transporter b family member 15	232	374	11	11	1.86
XLOC_050071	hyoscyamine 6-dioxygenase-like	57	15	8	1	1.85
9 DAI						
XLOC_000425	udp-glycosyltransferase 83a1-like	88	107	0	0	4.06
XLOC_019174	SNF1-related serine threonine-protein kinase SRK2A-like	191	243	5	8	3.87
XLOC_045079	subtilisin-like protease SDD1	622	881	25	41	3.85
XLOC_025801	cytochrome P450 geraniol 8-hydroxylase-like	111	147	2	1	3.80
XLOC_048378	**caffeic acid o-methyltransferase**	145	240	2	3	3.80
XLOC_025121	**thaumatin-like protein 1b**	139	232	1	2	3.78

XLOC_049783	**homoglutathione synthetase**	174	200	4	7	3.70
XLOC_041566	NEP1-interacting protein 2	99	129	1	2	3.68
XLOC_029854	**annexin-like protein rj4**	150	157	7	11	3.51
XLOC_038757	p34 thiol protease	49	49	0	0	3.47
XLOC_007899	basic endochitinase-like	563	531	28	34	3.43
XLOC_019850	dirigent protein 9-like	220	159	10	6	3.41
XLOC_001973	**sec14p-like phosphatidylinositol transfer protein**	103	139	2	2	3.41
XLOC_040201	stig1-like protein	92	141	2	3	3.39
XLOC_024512	duf642 family protein	103	107	3	6	3.34
XLOC_011098	**remorin family protein**	64	80	1	2	3.25
XLOC_020628	probable serine threonine-protein kinase	79	43	2	4	3.22
XLOC_035322	**mate efflux family protein LjMATE1-like**	1037	1012	94	102	3.15
XLOC_038934	**14 kda proline-rich protein**	69	75	2	4	3.15
XLOC_013019	squalene monooxygenase	388	420	40	56	3.13
12 DAI						
XLOC_026556	**protein flug/nodulin 61**	1326	2291	3	4	4.72
XLOC_006138	**ent-copalyl diphosphate synthase**	116	100	0	0	4.01
XLOC_043161	**copper diamine oxidase**	5314	5056	159	86	3.99
XLOC_016066	**gibberellin 20 oxidase 1**	207	121	7	3	3.76
XLOC_008289	**pleiotropic drug resistance protein 1-like**	75	16	0	0	3.61
XLOC_034123	universal stress protein a-like protein	285	492	1	1	3.54
XLOC_042753	peroxidase 12-like	189	321	2	4	3.44
XLOC_036762	potassium channel akt1-like	214	368	1	1	3.42
XLOC_033005	**2-isopropylmalate synthase-like**	173	295	0	0	3.40
XLOC_010580	**extensin-like/14 kda proline-rich DC2.15 protein**	433	229	34	21	3.20
XLOC_045110	**extensin-like/14 kda proline-rich DC2.15 protein**	230	226	7	2	3.19
XLOC_043784	**extensin-like/14 kda proline-rich DC2.15 protein**	125	88	7	5	3.16
XLOC_049373	ent-copalyl diphosphate synthase	71	59	1	1	3.09
XLOC_004314	LRR receptor-like protein kinase At3g28040-like	64	62	0	0	3.08
XLOC_022215	peroxidase 15	641	501	31	7	3.07

XLOC_003387	ring-h2 finger protein atl34-like	119	204	1	1	2.93
XLOC_026325	1-aminocyclopropane-1-carboxylate oxidase-like	57	56	0	0	2.89
XLOC_038982	peroxidase 15	204	93	17	2	2.88
XLOC_051032	gdp-mannose-epimerase 1	100	62	6	2	2.85
XLOC_013663	**carbonic anhydrase**	255	404	7	7	2.83

Table 1.2. Top 20 genes whose expression was significantly down-regulated in reniform nematode-infected soybean roots at four time points after inoculation (FDR = 0.01, genes ranked based on log_2FC estimate).

Gene ID	Description	Mean Normalized Counts				
		Inoculated	SD	Control	SD	L2FC estimate
3 DAI						
XLOC_031122	high affinity nitrate transporter 2.4	123	78	4096	2780	-4.91
XLOC_014708	molybdate transporter 1-like	5	3	158	112	-4.37
XLOC_009515	molybdate transporter 1-like	32	5	626	235	-4.09
XLOC_015632	light-dependent short hypocotyls 10-like transcription factor	1	1	55	43	-3.98
XLOC_005541	vinorine synthase	8	4	149	37	-3.80
XLOC_016249	K+ efflux antiporter	2	2	62	16	-3.78
XLOC_044150	12-oxophytodienoate reductase 11	3	4	91	38	-3.75
XLOC_012899	subtilisin-like protease cucumisin-like	13	5	224	110	-3.74
XLOC_022590	LRR receptor-like serine/threonine-protein kinase	3	3	70	11	-3.70
XLOC_012604	CONSTANS-like zinc finger transcription factor	2	4	55	48	-3.63
XLOC_002565	homeobox protein knotted-1-like 6 transcription factor	2	2	53	12	-3.58
XLOC_006330	ethylene-responsive transcription factor erf024-like	10	12	149	44	-3.56
XLOC_049553	ethylene-responsive transcription factor erf024-like	13	9	170	25	-3.43
XLOC_029737	bel1-like homeodomain protein 1 transcription factor	60	8	589	24	-3.21
XLOC_002405	wrky transcription factor 47-like	9	5	103	11	-3.21
XLOC_030749	bel1-like homeodomain protein 1 transcription factor	82	67	766	72	-3.18

XLOC_010357	7-deoxyloganetin glucosyltransferase-like	11	4	112	44	-3.08
XLOC_004579	glutaredoxin C13-like	0	0	17	14	-3.05
XLOC_021885	ABC transporter c family member 3	3	2	44	15	-3.02
XLOC_052219	metal-nicotianamine transporter YSL1	3	1	44	12	-2.99
6 DAI						
XLOC_006330	ethylene-responsive transcription factor erf024-like	13	3	319	236	-3.38
XLOC_010579	extensin-like/14 kda proline-rich DC2.15 protein	0	0	69	65	-2.76
XLOC_007587	cytochrome p450 94a1-like	24	20	247	127	-2.50
XLOC_016551	laccase 17 isoform 1	35	26	304	99	-2.34
XLOC_049553	ethylene-responsive transcription factor erf024-like	10	9	201	190	-2.34
XLOC_012899	subtilisin-like protease cucumisin-like	43	14	336	260	-2.25
XLOC_030148	laccase 5-like	43	25	311	79	-2.25
XLOC_009515	molybdate transporter 1-like	94	60	734	541	-2.25
XLOC_038094	blue copper protein/phytocyanin	88	62	526	199	-2.18
XLOC_025501	germin-like protein 17	68	52	436	56	-2.15
XLOC_051714	probable carboxylesterase 6	62	27	357	46	-2.14
XLOC_021377	palmitoyl-monogalactosyldiacylglycerol delta-7 (FAD5)	156	147	797	387	-2.14
XLOC_045792	laccase 5-like	41	20	263	57	-2.14
XLOC_027563	probable carboxylesterase 17	8	5	72	39	-2.04
XLOC_033266	glucomannan 4-beta-mannosyltransferase 9-like	14	15	97	53	-2.03
XLOC_048157	mannan endo-beta-1,4-mannosidase 6	17	6	130	44	-2.03
XLOC_046719	protein LURP-one-related 15-like	46	33	237	75	-2.02
XLOC_010120	UDP-glucuronate:xylan alpha-glucuronosyltransferase 1-like	27	11	167	35	-2.01
XLOC_035373	sugar transporter ERD6-like 16	15	8	611	985	-2.00
XLOC_025490	ATP binding cassette B family member 4	28	13	147	75	-1.96
9 DAI						

XLOC_006330	ethylene-responsive transcription factor erf024-like	4	2	123	19	-4.05
XLOC_002565	homeobox protein knotted-1-like 6 transcription factor	0	0	38	1	-3.38
XLOC_012899	subtilisin-like protease cucumisin-like	7	5	161	133	-3.23
XLOC_007587	cytochrome p450 94a1-like	31	17	282	82	-2.93
XLOC_049553	ethylene-responsive transcription factor erf024-like	5	3	67	17	-2.89
XLOC_027563	probable carboxylesterase 17	3	1	53	33	-2.85
XLOC_039814	ethylene-responsive transcription factor erf024-like	2	1	44	1	-2.85
XLOC_031122	high affinity nitrate transporter 2.4	129	54	1464	853	-2.72
XLOC_044314	WUSCHEL-related homeobox 4-like	1	1	31	22	-2.58
XLOC_002206	E3 ubiquitin-protein ligase RHA1B-like	29	15	189	55	-2.48
XLOC_019263	auxin-induced protein 5NG4	47	27	278	90	-2.40
XLOC_047728	nitrate transporter 1.2-like	14	3	89	15	-2.28
XLOC_035906	high affinity nitrate transporter 2.4-like	1108	530	7295	4942	-2.27
XLOC_043785	extensin-like/14 kda proline-rich DC2.15 protein	9	10	99	62	-2.25
XLOC_038778	fasciclin-like arabinogalactan protein 11-like	185	220	915	773	-2.20
XLOC_000520	sugar phosphate phosphate translocator at3g11320-like	3	5	39	53	-2.14
XLOC_029801	high affinity nitrate transporter 2.4	458	364	2069	167	-2.14
XLOC_035435	fasciclin-like arabinogalactan protein 11-like	297	303	1435	1140	-2.12
XLOC_030739	momilactone A synthase	63	33	300	86	-2.11
XLOC_030910	pleckstrin domain-containing family N member 1	7	8	46	26	-2.06
12 DAI						
XLOC_036897	alcohol dehydrogenase 1	1	2	49	41	-2.51
XLOC_012481	ring-h2 finger protein ATL78-like	5	2	55	39	-2.23
XLOC_028025	polyol transporter 3-like	285	173	1338	560	-2.11
XLOC_041911	CEN-like protein 1	100	60	465	104	-2.00

XLOC_024315	dehydrin-like protein	7	7	65	81	-1.87
XLOC_020262	trypsin inhibitor A	11	12	178	287	-1.84
XLOC_021091	ring-h2 finger protein ATL78-like	36	22	185	75	-1.83
XLOC_020147	gdsl esterase lipase	78	41	474	341	-1.83
XLOC_007303	glucan endo-1,3-beta-glucosidase-like	996	993	4017	2077	-1.81
XLOC_000098	hydroxyproline-rich glycoprotein	61	43	249	96	-1.78
XLOC_018422	ankyrin repeat protein	12	3	65	16	-1.73
XLOC_043206	late embryogenesis abundant protein LEA5	127	88	771	790	-1.71
XLOC_031220	cysteine-rich repeat secretory protein 38-like	23	12	102	54	-1.65
XLOC_049742	galactinol synthase	434	215	1624	995	-1.64
XLOC_006648	cbl-interacting serine threonine-protein kinase 9-like	32	14	122	42	-1.63
XLOC_013822	LRR receptor-like serine threonine-protein kinase at2g24130-like	57	58	191	76	-1.59
XLOC_013725	cyclic dof factor 3-like transcription factor	69	29	258	132	-1.58
XLOC_039767	ovate family protein transcription factor	70	25	236	64	-1.56
XLOC_003515	LRR receptor-like serine threonine-protein kinase at1g06840-like	161	8	540	163	-1.54
XLOC_014835	cryptochrome 1	71	17	260	105	-1.51

Table 1.3. Top 20 gene sets whose expression was significantly enriched in reniform nematode-infected soybean roots at four time points after inoculation (FDR = 0.05, gene sets ranked by GSEA normalized enrichment score).

Gene Set Name	Gene Set Description	Number of Genes in Set	Type	Normalized Enrichment Score
3 DAI				
GO:0006334	nucleosome assembly	97	BP	2.68
GO:0009853	photorespiration	152	BP	2.50
GO:0008283	cell proliferation	136	BP	2.47
GO:0006270	DNA replication initiation	67	BP	2.39
GO:0080129	proteasome core complex assembly	114	BP	2.32
GO:0043086	negative regulation of catalytic activity	222	BP	2.26
GO:0045490	pectin catabolic process	145	BP	2.24
GO:0009060	aerobic respiration	36	BP	2.24
GO:0000786	nucleosome	114	CC	2.91
GO:0005747	mitochondrial respiratory chain complex I	53	CC	2.42
GO:0015935	small ribosomal subunit	61	CC	2.26
EC:3.1.1.11	pectinesterase	205	EC	2.39
MAP00940	phenylpropanoid biosynthesis	326	KEGG	2.31
GO:0003678	DNA helicase activity	47	MF	2.46
GO:0046982	protein heterodimerization activity	204	MF	2.44
GO:0019843	rRNA binding	129	MF	2.44
GO:0030599	pectinesterase activity	205	MF	2.40
GO:0004857	enzyme inhibitor activity	177	MF	2.34
GO:0045330	aspartyl esterase activity	123	MF	2.24
GO:0004601	peroxidase activity	256	MF	2.24
6 DAI				
GO:0009399	nitrogen fixation	29	BP	2.59
GO:0009877	nodulation	59	BP	2.34
GO:0080129	proteasome core complex assembly	114	BP	2.26

GO:0006542	glutamine biosynthetic process	16	BP	2.11
GO:0006334	nucleosome assembly	97	BP	2.11
GO:0051276	chromosome organization	75	BP	2.10
GO:0009060	aerobic respiration	36	BP	2.08
GO:0006189	de novo IMP biosynthetic process	23	BP	2.01
GO:0006511	ubiquitin-dependent protein catabolic process	264	BP	1.93
GO:0009853	photorespiration	152	BP	1.92
GO:0000786	nucleosome	114	CC	2.32
GO:0005747	mitochondrial respiratory chain complex I	53	CC	2.19
GO:0031012	extracellular matrix	30	CC	1.86
EC:6.3.1.2	glutamate--ammonia ligase	16	EC	2.10
EC:1.9.3.1	cytochrome-c oxidase	25	EC	1.99
GO:0003678	DNA helicase activity	47	MF	2.14
GO:0004356	glutamate-ammonia ligase activity	16	MF	2.05
GO:0019825	oxygen binding	15	MF	2.03
GO:0004129	cytochrome-c oxidase activity	25	MF	2.00
GO:0019843	rRNA binding	129	MF	1.89
9 DAI				
GO:0008283	cell proliferation	136	BP	2.11
GO:0006270	DNA replication initiation	67	BP	2.10
GO:0010951	negative regulation of endopeptidase activity	87	BP	2.07
GO:0007018	microtubule-based movement	173	BP	2.06
GO:0000911	cytokinesis by cell plate formation	117	BP	2.06
GO:0009399	nitrogen fixation	29	BP	2.06
GO:0045490	pectin catabolic process	145	BP	2.00
GO:0009877	nodulation	59	BP	1.94
GO:0051567	histone H3-K9 methylation	129	BP	1.93
GO:0000786	nucleosome	114	CC	2.10
GO:0005871	kinesin complex	171	CC	2.07
GO:0042555	MCM complex	15	CC	2.04

GO:0005819	spindle	45	CC	1.99
EC:1.11.1.7	peroxidase	256	EC	2.02
MAP00940	phenylpropanoid biosynthesis	326	KEGG	2.11
MAP00360	phenylalanine metabolism	364	KEGG	1.94
GO:0003678	DNA helicase activity	47	MF	2.44
GO:0003777	microtubule motor activity	171	MF	2.07
GO:0008017	microtubule binding	225	MF	2.04
GO:0004601	peroxidase activity	256	MF	2.02
12 DAI				
GO:0007018	microtubule-based movement	173	BP	2.77
GO:0000911	cytokinesis by cell plate formation	117	BP	2.75
GO:0008283	cell proliferation	136	BP	2.73
GO:0006275	regulation of DNA replication	93	BP	2.68
GO:0051567	histone H3-K9 methylation	129	BP	2.67
GO:0006270	DNA replication initiation	67	BP	2.63
GO:0006334	nucleosome assembly	97	BP	2.46
GO:0006306	DNA methylation	148	BP	2.42
GO:0007067	mitotic nuclear division	113	BP	2.40
GO:0010389	regulation of G2/M transition	42	BP	2.40
GO:0045490	pectin catabolic process	145	BP	2.32
GO:0006260	DNA replication	126	BP	2.29
GO:0016572	histone phosphorylation	47	BP	2.28
GO:0005871	kinesin complex	171	CC	2.78
GO:0000786	nucleosome	114	CC	2.67
GO:0005874	microtubule	281	CC	2.60
GO:0042555	MCM complex	15	CC	2.32
GO:0003777	microtubule motor activity	171	MF	2.76
GO:0003678	DNA helicase activity	47	MF	2.75
GO:0008017	microtubule binding	225	MF	2.67

Table 1.4. Top 20 gene sets whose expression was significantly depleted in reniform nematode-infected soybean roots at four time points after inoculation (FDR = 0.05, gene sets ranked by GSEA normalized enrichment score). On dates 9 and 12, fewer than 20 gene sets were significantly depleted.

Gene set name	Description	Total genes in set	Type	Normalized Enrichment Score
3 DAI				
GO:0043531	ADP binding	380	MF	-2.86
GO:0004012	phospholipid-translocating ATPase activity	34	MF	-2.55
GO:0045332	phospholipid translocation	34	BP	-2.52
GO:0019829	cation-transporting ATPase activity	60	MF	-2.51
EC:3.6.3.1	phospholipid-translocating ATPase	34	EC	-2.50
GO:0000956	nuclear-transcribed mRNA catabolic process	66	BP	-2.43
EC:2.4.1.34	1,3-beta-glucan synthase	30	EC	-2.43
GO:0006075	1,3-beta-D-glucan biosynthetic process	30	BP	-2.37
GO:0003843	1,3-beta-D-glucan synthase activity	30	MF	-2.37
GO:0000148	1,3-beta-D-glucan synthase complex	30	CC	-2.33
GO:0008026	ATP-dependent helicase activity	159	MF	-2.31
GO:0098655	cation transmembrane transport	108	BP	-2.30
GO:0036459	ubiquitinyl hydrolase activity	57	MF	-2.25
GO:0004386	helicase activity	181	MF	-2.25
GO:0009638	phototropism	18	BP	-2.24
GO:0010119	regulation of stomatal movement	46	BP	-2.22
GO:0006487	protein N-linked glycosylation	107	BP	-2.21
GO:0023014	signal transduction by protein phosphorylation	60	BP	-2.17
GO:0009785	blue light signaling pathway	25	BP	-2.17
EC:2.7.3	phosphotransferases with a nitrogenous group as acceptor	55	EC	-2.16

6 DAI				
GO:0009834	plant-type secondary cell wall biogenesis	46	BP	-2.52
EC:1.10.3.2	laccase	58	EC	-2.38
GO:0052716	hydroquinone:oxygen oxidoreductase activity	58	MF	-2.37
GO:0046274	lignin catabolic process	58	BP	-2.36
GO:0010417	glucuronoxylan biosynthetic process	22	BP	-2.29
GO:0010089	xylem development	81	BP	-2.29
GO:0045489	pectin biosynthetic process	26	BP	-2.19
GO:0042546	cell wall biogenesis	49	BP	-2.15
GO:0010413	glucuronoxylan metabolic process	138	BP	-2.13
GO:0009832	plant-type cell wall biogenesis	94	BP	-2.12
GO:0045492	xylan biosynthetic process	139	BP	-2.12
GO:0000139	Golgi membrane	207	CC	-2.11
GO:0018298	protein-chromophore linkage	81	BP	-2.06
GO:0071555	cell wall organization	362	BP	-2.06
EC:2.4.1.43	polygalacturonate 4-alpha-galacturonosyltransferase	28	EC	-2.06
GO:0048519	negative regulation of biological process	44	BP	-2.05
MAP00532	glycosaminoglycan biosynthesis chondroitin sulfate	27	KEGG	-2.05
GO:0008361	regulation of cell size	58	BP	-2.04
GO:0031225	anchored component of membrane	97	CC	-2.03
GO:0010051	xylem and phloem pattern formation	59	BP	-2.02
9 DAI				
GO:0043531	ADP binding	380	MF	-2.29
GO:0009785	blue light signaling pathway	25	BP	-2.20
GO:0071702	organic substance transport	20	BP	-1.98
GO:0044444	cytoplasmic part	88	CC	-1.94
GO:0009882	blue light photoreceptor activity	15	MF	-1.94

12 DAI				
GO:0043531	ADP binding	380	MF	-2.17
GO:0000956	nuclear-transcribed mRNA catabolic process	66	BP	-2.03

Figure 1.1 – Micrographs of acid fuchsin-stained soybean roots and reniform nematodes taken at 100X magnification at 3, 6, 9 and 12 days after inoculation.

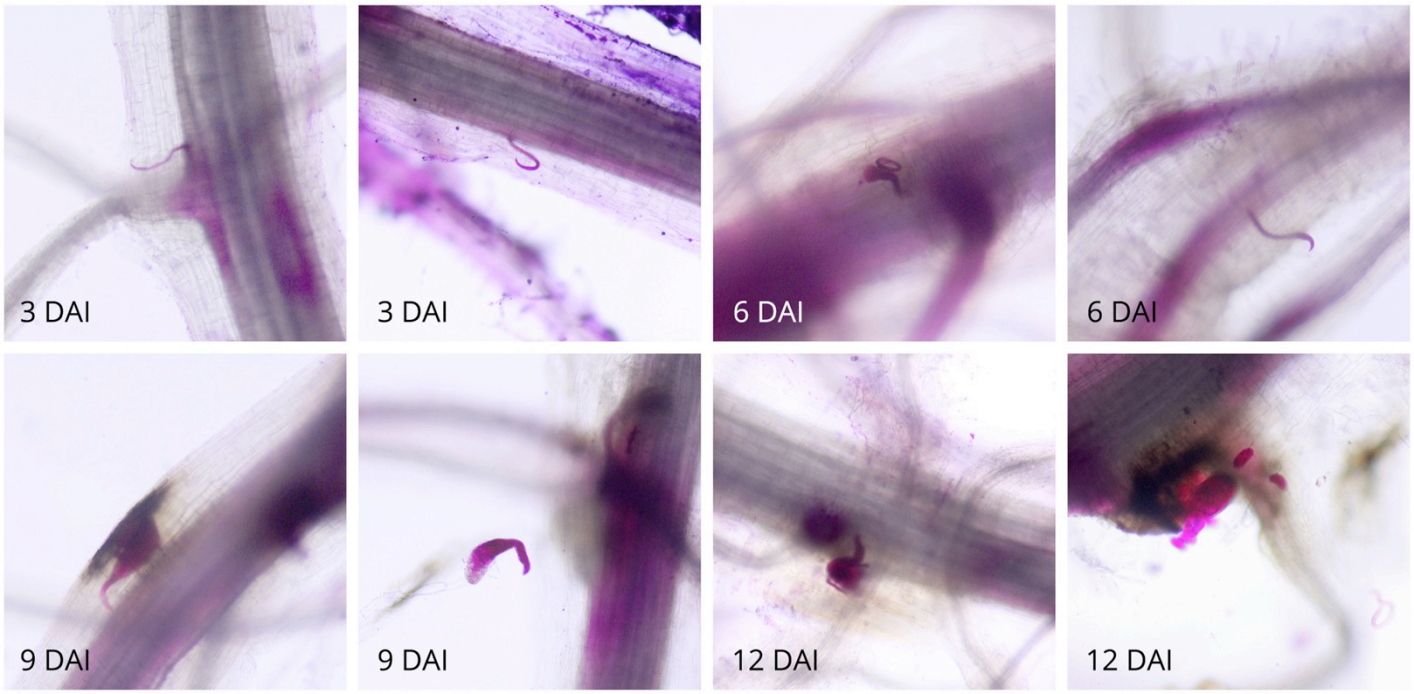

Figure 1.2 – Visualization of gene expression data using principal components analysis of rlog transformed counts for all genes in control and inoculated soybean roots at four time points after inoculation.

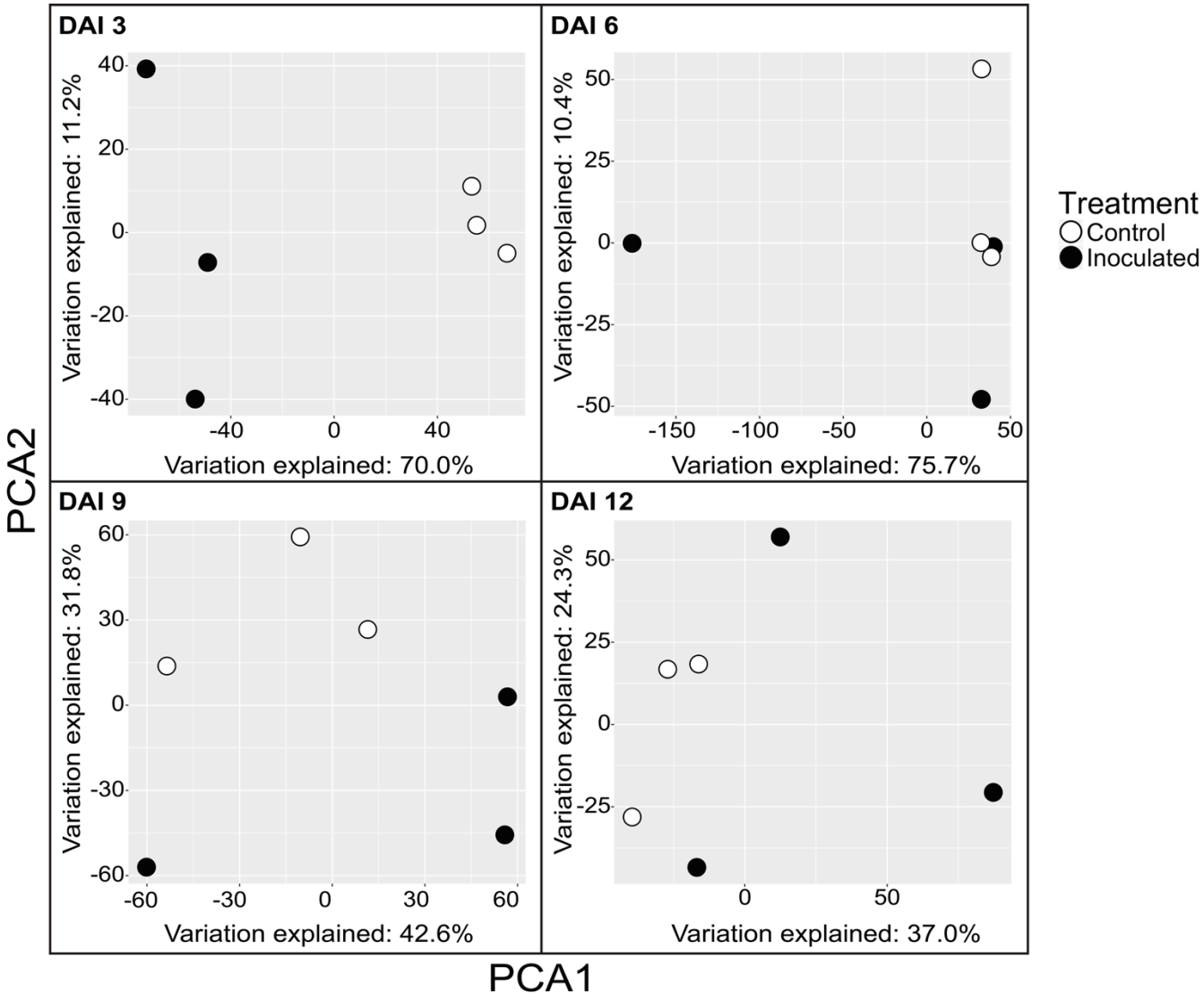

Figure 1.3 – Volcano plots of FDR adjusted *p*-values graphed against $\log_2$(fold change) estimates for all expressed genes at four time points after inoculation. Black symbols: *p-adj* > 0.01; yellow symbols: *p-adj* ≤ 0.01 and $|\log_2 FC| < 1$; red symbols: *p-adj* ≤ 0.01 and |log2FC| ≥1. Numbers in the upper-left of each panel reflect numbers of significantly up- and down-regulated genes in infected roots on each date.

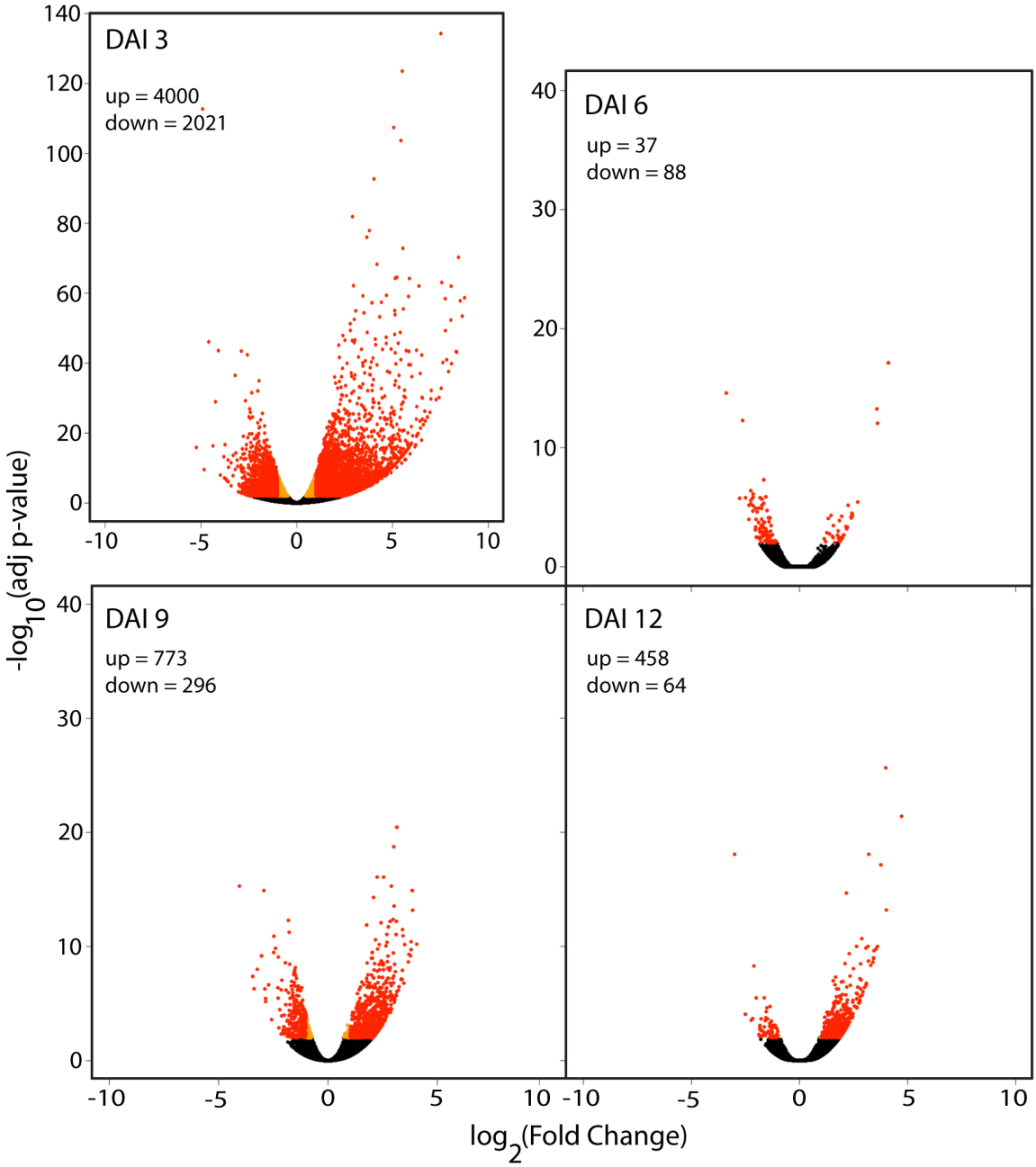

Figure 1.4 – Gene set enrichment plot for the GO:0009877 (Nodulation) gene set at 9 DAI. All expressed genes are ordered into a ranked list based on their relative expression in inoculated versus control samples. Genes at the beginning of the list (left) are up-regulated in inoculated roots; those at the end of the list (right) are down-regulated. The middle portion of the graphic shows where the 59 genes of the GO:0009877 gene set appear in the ranked list of all genes. The upper portion of the graphic illustrates the calculation of a running enrichment score for the GO:0009877 gene set. Its enrichment score peaks far to the left, indicating that genes from this set tend to be up-regulated in infected roots. The lower portion of the graph shows the value of each gene's ranking metric, a measure of its correlation with inoculation status.

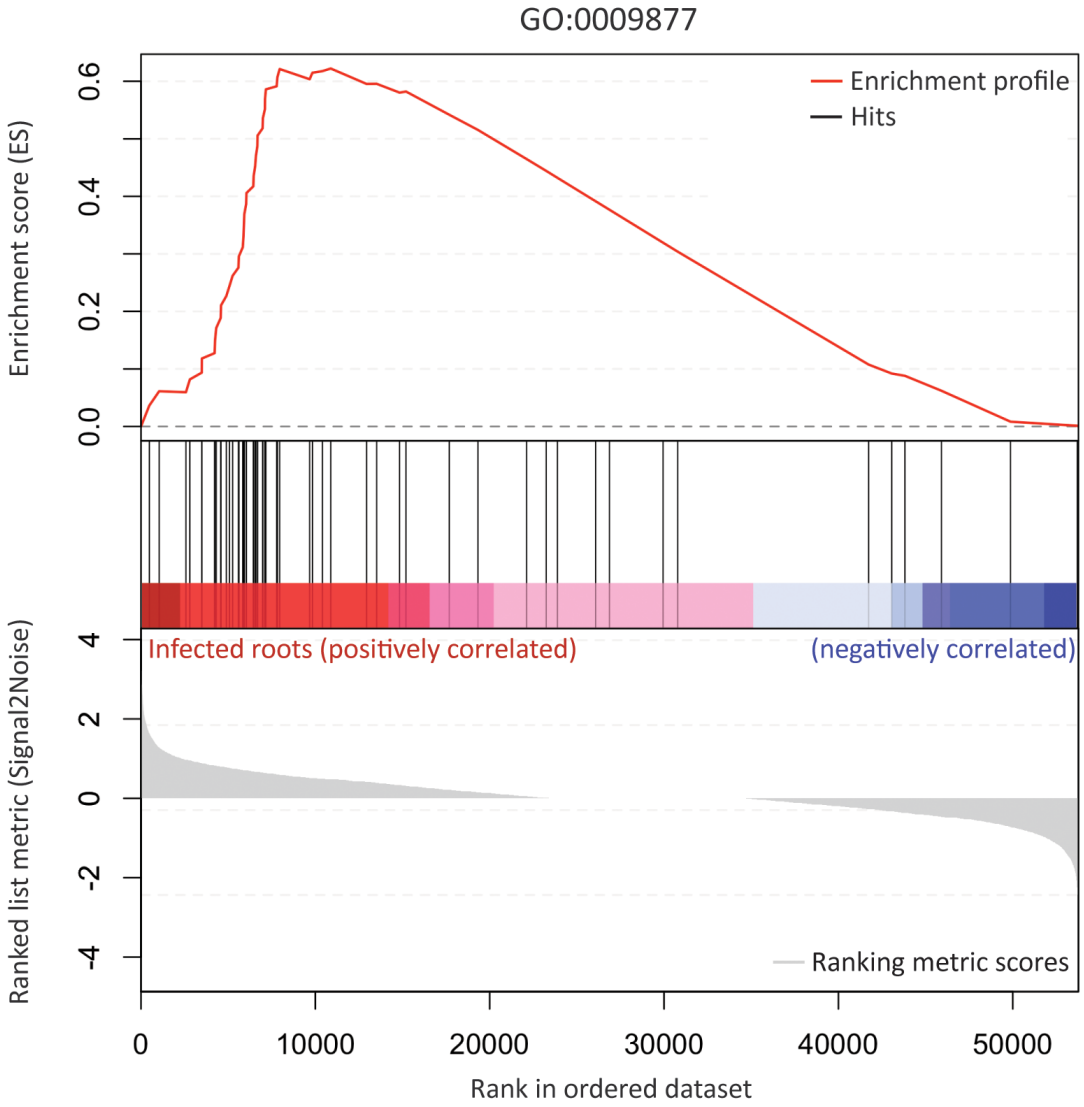
GO:0009877
Enrichment profile
Hits
Enrichment score (ES)
0.6
0.4
0.2
0.0
Infected roots (positively correlated)
(negatively correlated)
Ranked list metric (Signal2Noise)
4
2
0
-2
-4
Ranking metric scores
0
10000
20000
30000
40000
50000
Rank in ordered dataset

Figure 1.5 –Clustered heatmap of log_2FC estimates for up-regulated nodulins and nodulation-related genes in soybean roots. Red and blue indicate up- and down-regulation in infected root tissues, respectively. Asterisks indicate significant differences in expression (adjusted *p*-value ≤ 0.01 and $|log_2FC| \geq 1$). Sequence IDs for each gene in the assembled transcriptome are given in parentheses.

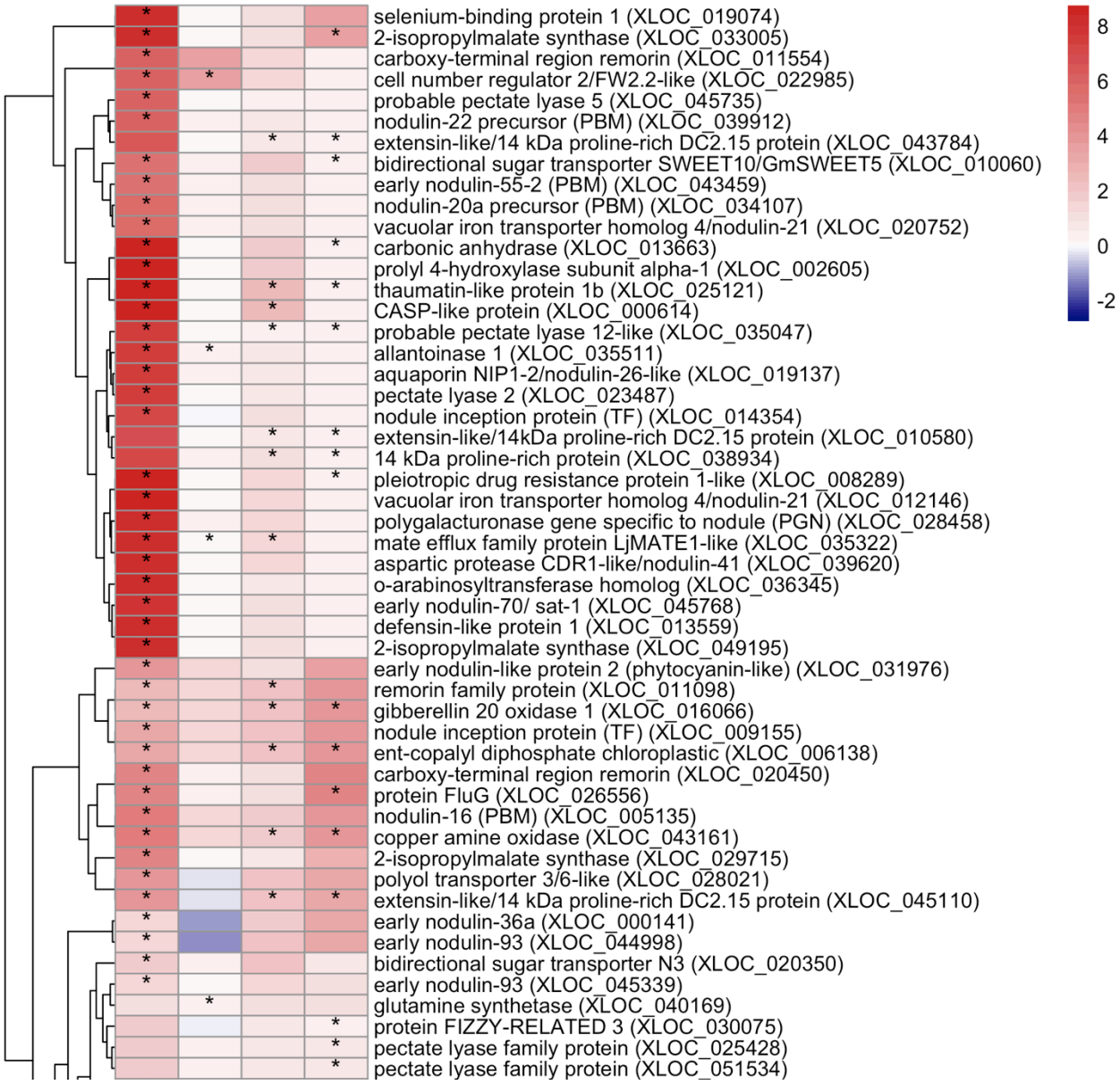

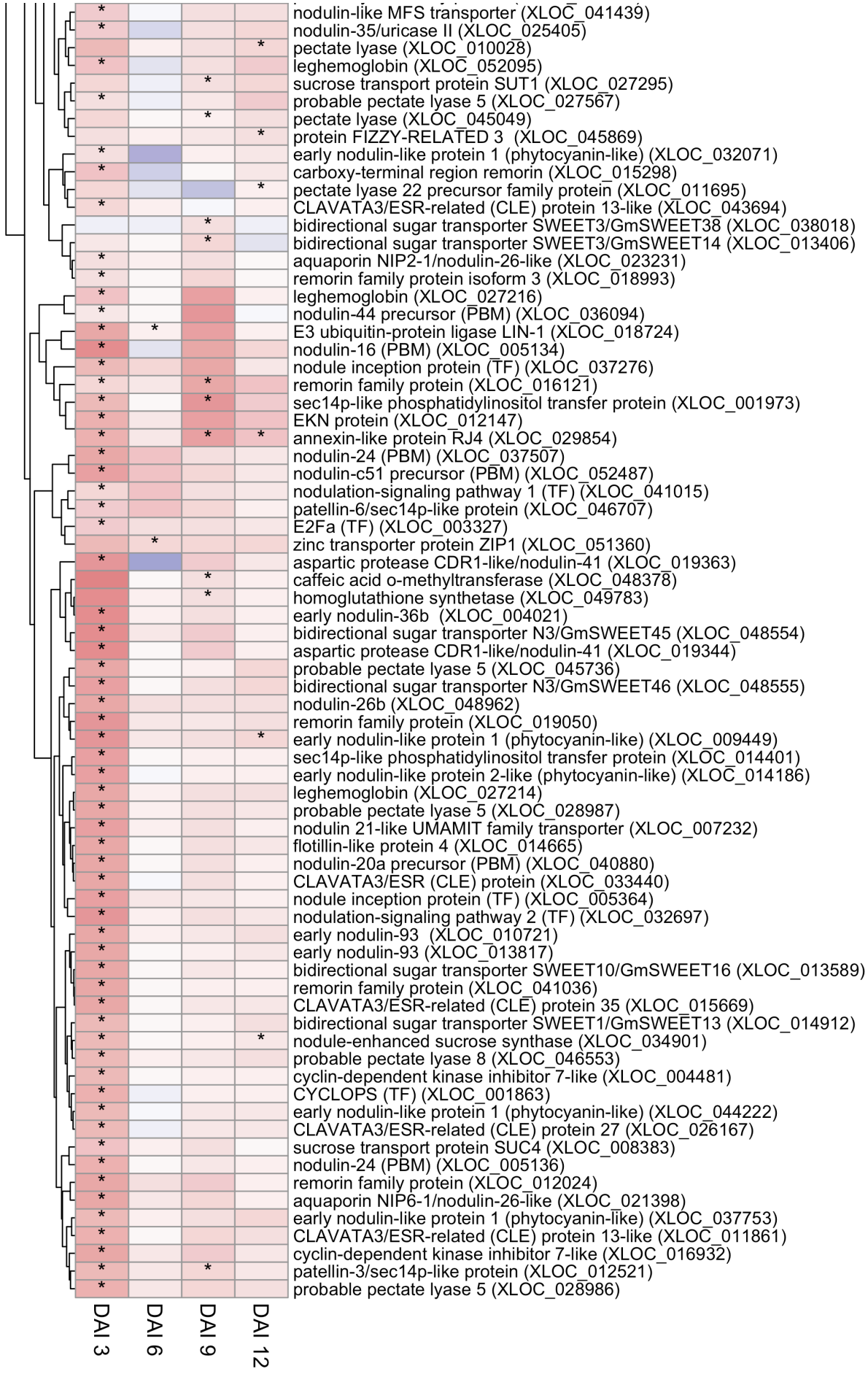
nodulin-like MFS transporter (XLOC_041439)
nodulin-35/uricase II (XLOC_025405)
pectate lyase (XLOC_010028)
leghemoglobin (XLOC_052095)
sucrose transport protein SUT1 (XLOC_027295)
probable pectate lyase 5 (XLOC_027567)
pectate lyase (XLOC_045049)
protein FIZZY-RELATED 3 (XLOC_045869)
early nodulin-like protein 1 (phytocyanin-like) (XLOC_032071)
carboxy-terminal region remorin (XLOC_015298)
pectate lyase 22 precursor family protein (XLOC_011695)
CLAVATA3/ESR-related (CLE) protein 13-like (XLOC_043694)
bidirectional sugar transporter SWEET3/GmSWEET38 (XLOC_038018)
bidirectional sugar transporter SWEET3/GmSWEET14 (XLOC_013406)
aquaporin NIP2-1/nodulin-26-like (XLOC_023231)
remorin family protein isoform 3 (XLOC_018993)
leghemoglobin (XLOC_027216)
nodulin-44 precursor (PBM) (XLOC_036094)
E3 ubiquitin-protein ligase LIN-1 (XLOC_018724)
nodulin-16 (PBM) (XLOC_005134)
nodule inception protein (TF) (XLOC_037276)
remorin family protein (XLOC_016121)
sec14p-like phosphatidylinositol transfer protein (XLOC_001973)
EKN protein (XLOC_012147)
annexin-like protein RJ4 (XLOC_029854)
nodulin-24 (PBM) (XLOC_037507)
nodulin-c51 precursor (PBM) (XLOC_052487)
nodulation-signaling pathway 1 (TF) (XLOC_041015)
patellin-6/sec14p-like protein (XLOC_046707)
E2Fa (TF) (XLOC_003327)
zinc transporter protein ZIP1 (XLOC_051360)
aspartic protease CDR1-like/nodulin-41 (XLOC_019363)
caffeic acid o-methyltransferase (XLOC_048378)
homoglutathione synthetase (XLOC_049783)
early nodulin-36b (XLOC_004021)
bidirectional sugar transporter N3/GmSWEET45 (XLOC_048554)
aspartic protease CDR1-like/nodulin-41 (XLOC_019344)
probable pectate lyase 5 (XLOC_045736)
bidirectional sugar transporter N3/GmSWEET46 (XLOC_048555)
nodulin-26b (XLOC_048962)
remorin family protein (XLOC_019050)
early nodulin-like protein 1 (phytocyanin-like) (XLOC_009449)
sec14p-like phosphatidylinositol transfer protein (XLOC_014401)
early nodulin-like protein 2-like (phytocyanin-like) (XLOC_014186)
leghemoglobin (XLOC_027214)
probable pectate lyase 5 (XLOC_028987)
nodulin 21-like UMAMIT family transporter (XLOC_007232)
flotillin-like protein 4 (XLOC_014665)
nodulin-20a precursor (PBM) (XLOC_040880)
CLAVATA3/ESR (CLE) protein (XLOC_033440)
nodule inception protein (TF) (XLOC_005364)
nodulation-signaling pathway 2 (TF) (XLOC_032697)
early nodulin-93 (XLOC_010721)
early nodulin-93 (XLOC_013817)
bidirectional sugar transporter SWEET10/GmSWEET16 (XLOC_013589)
remorin family protein (XLOC_041036)
CLAVATA3/ESR-related (CLE) protein 35 (XLOC_015669)
bidirectional sugar transporter SWEET1/GmSWEET13 (XLOC_014912)
nodule-enhanced sucrose synthase (XLOC_034901)
probable pectate lyase 8 (XLOC_046553)
cyclin-dependent kinase inhibitor 7-like (XLOC_004481)
CYCLOPS (TF) (XLOC_001863)
early nodulin-like protein 1 (phytocyanin-like) (XLOC_044222)
CLAVATA3/ESR-related (CLE) protein 27 (XLOC_026167)
sucrose transport protein SUC4 (XLOC_008383)
nodulin-24 (PBM) (XLOC_005136)
remorin family protein (XLOC_012024)
aquaporin NIP6-1/nodulin-26-like (XLOC_021398)
early nodulin-like protein 1 (phytocyanin-like) (XLOC_037753)
CLAVATA3/ESR-related (CLE) protein 13-like (XLOC_011861)
cyclin-dependent kinase inhibitor 7-like (XLOC_016932)
patellin-3/sec14p-like protein (XLOC_012521)
probable pectate lyase 5 (XLOC_028986)
DAI 3
DAI 6
DAI 9
DAI 12

Figure 1.6 – Clustered heatmap of $\log_2$FC estimates for a combination of down-regulated and non-differentially expressed nodulation-related genes in soybean roots. Red and blue indicate up- and down-regulation in infected root tissues, respectively. Asterisks indicate significant differences in expression (adjusted *p*-value ≤ 0.01 and $|\log_2 FC| \geq 1$). Genes are a combination of those significantly down-regulated on at least one sampling date and genes that did not show significant differential expression but that were identified through leading edge analysis or homology. XLOC_050155 showed mix regulation being down on DAI 3 and up on DAI 12.

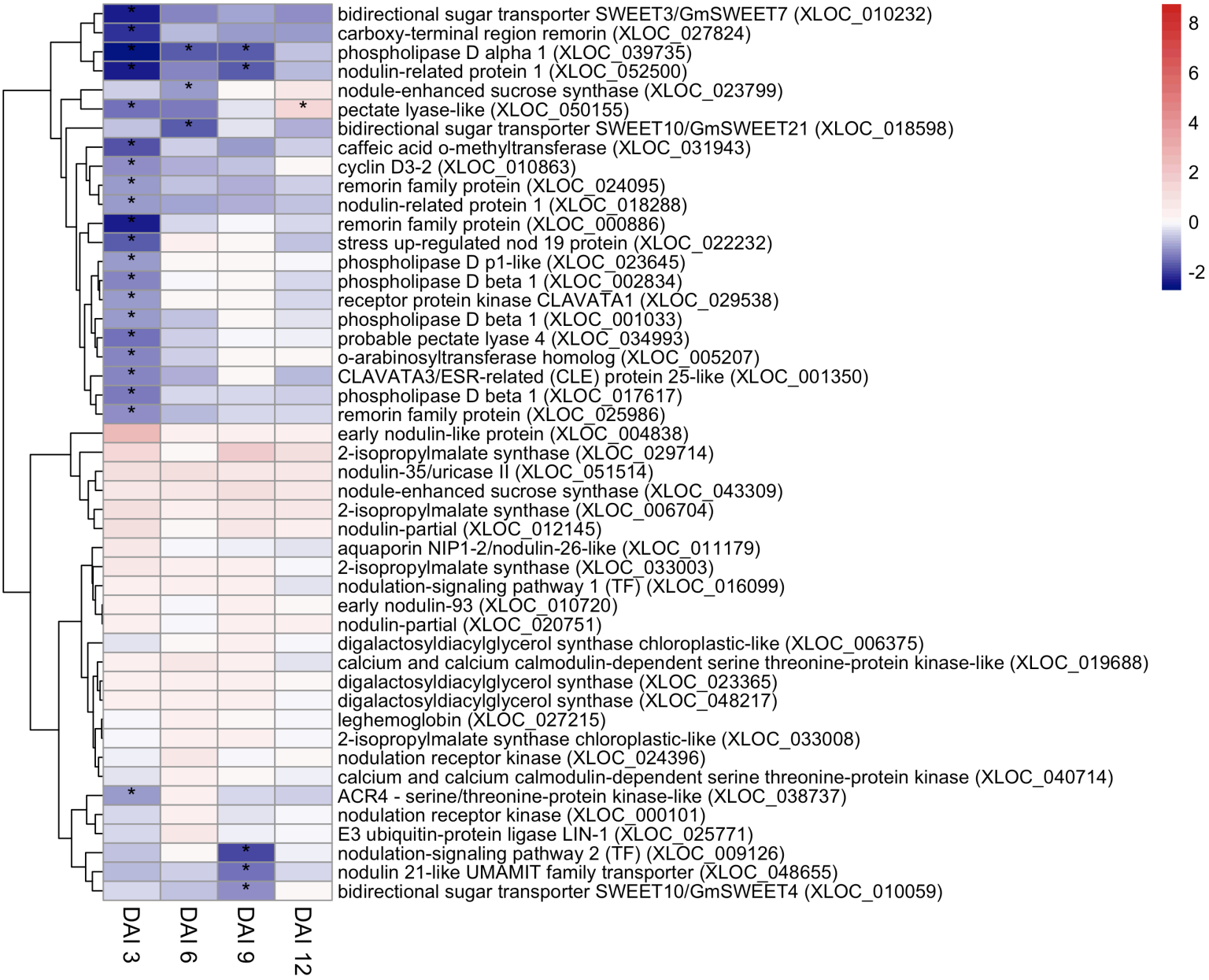
bidirectional sugar transporter SWEET3/GmSWEET7 (XLOC_010232)
carboxy-terminal region remorin (XLOC_027824)
phospholipase D alpha 1 (XLOC_039735)
nodulin-related protein 1 (XLOC_052500)
nodule-enhanced sucrose synthase (XLOC_023799)
pectate lyase-like (XLOC_050155)
bidirectional sugar transporter SWEET10/GmSWEET21 (XLOC_018598)
caffeic acid o-methyltransferase (XLOC_031943)
cyclin D3-2 (XLOC_010863)
remorin family protein (XLOC_024095)
nodulin-related protein 1 (XLOC_018288)
remorin family protein (XLOC_000886)
stress up-regulated nod 19 protein (XLOC_022232)
phospholipase D p1-like (XLOC_023645)
phospholipase D beta 1 (XLOC_002834)
receptor protein kinase CLAVATA1 (XLOC_029538)
phospholipase D beta 1 (XLOC_001033)
probable pectate lyase 4 (XLOC_034993)
o-arabinosyltransferase homolog (XLOC_005207)
CLAVATA3/ESR-related (CLE) protein 25-like (XLOC_001350)
phospholipase D beta 1 (XLOC_017617)
remorin family protein (XLOC_025986)
early nodulin-like protein (XLOC_004838)
2-isopropylmalate synthase (XLOC_029714)
nodulin-35/uricase II (XLOC_051514)
nodule-enhanced sucrose synthase (XLOC_043309)
2-isopropylmalate synthase (XLOC_006704)
nodulin-partial (XLOC_012145)
aquaporin NIP1-2/nodulin-26-like (XLOC_011179)
2-isopropylmalate synthase (XLOC_033003)
nodulation-signaling pathway 1 (TF) (XLOC_016099)
early nodulin-93 (XLOC_010720)
nodulin-partial (XLOC_020751)
digalactosyldiacylglycerol synthase chloroplastic-like (XLOC_006375)
calcium and calcium calmodulin-dependent serine threonine-protein kinase-like (XLOC_019688)
digalactosyldiacylglycerol synthase (XLOC_023365)
digalactosyldiacylglycerol synthase (XLOC_048217)
leghemoglobin (XLOC_027215)
2-isopropylmalate synthase chloroplastic-like (XLOC_033008)
nodulation receptor kinase (XLOC_024396)
calcium and calcium calmodulin-dependent serine threonine-protein kinase (XLOC_040714)
ACR4 - serine/threonine-protein kinase-like (XLOC_038737)
nodulation receptor kinase (XLOC_000101)
E3 ubiquitin-protein ligase LIN-1 (XLOC_025771)
nodulation-signaling pathway 2 (TF) (XLOC_009126)
nodulin 21-like UMAMIT family transporter (XLOC_048655)
bidirectional sugar transporter SWEET10/GmSWEET4 (XLOC_010059)
DAI 3
DAI 6
DAI 9
DAI 12
8
6
4
2
0
-2

References

Agudelo, P., Robbins, R. T., Kim, K. S., and Stewart, J. M. 2005. Histological changes in *Gossypium hirsutum* associated with reduced reproduction of *Rotylenchulus reniformis*. J. Nematol. 37(2):185-189.

Albrecht, C., Geurts, R., and Bisseling, T. 1999. Legume nodulation and mycorrhizae formation; two extremes in host specificity meet. EMBO J. 18(2):281-288.

Anders, S., Pyl, P. T., and Huber, W. 2015. HTSeq-a python framework to work with high-throughput sequencing data. Bioinformatics 31(2):166-169.

Bakhetia, M., Urwin, P. E., and Atkinson, H. J. 2007. qPCR analysis and RNAi define pharyngeal gland cell-expressed genes of *Heterodera glycines* required for initial interactions with the host. Mol. Plant-Microbe Interact. 20(3):306-312.

Bellafiore, S., Shen, Z., Rosso, M., Abad, P., Shih, P., and Briggs, S. P. 2008. Direct identification of the *Meloidogyne incognita* secretome reveals proteins with host cell reprogramming potential. Plos Pathog. 4(10):e1000192.

Benkova, E., and Bielach, A. 2010. Lateral root organogenesis - from cell to organ. Curr. Opin. Plant Biol. 13(6):677-683.

Bolger, A. M., Lohse, M., and Usadel, B. 2014. Trimmomatic: A flexible trimmer for Illumina sequence data. Bioinformatics 30(15):2114-2120.

Bybd, D., Kirkpatrick, T., and Barker, K. 1983. An improved technique for clearing and staining plant-tissues for detection for nematodes. J. Nematol. 15(1):142-143.

Cabrera, J., Díaz-Manzano, F. E., Fenoll, C., and Escobar, C. 2015. Chapter seven - Developmental pathways mediated by hormones in nematode feeding sites. Adv. Bot. Res. 73:167-188.

Catoira, R., Galera, C., de Billy, F., Penmetsa, R., Journet, E., Maillet, F., Rosenberg, C., Cook, D., Gough, C., and Denarie, J. 2000. Four genes of *Medicago truncatula* controlling components of a nod factor transduction pathway. Plant Cell 12(9):1647-1665.

Chen, L., Hou, B., Lalonde, S., Takanaga, H., Hartung, M. L., Qu, X., Guo, W., Kim, J., Underwood, W., Chaudhuri, B., Chermak, D., Antony, G., White, F. F., Somerville, S. C., Mudgett, M. B., and Frommer, W. B. 2010. Sugar transporters for intercellular exchange and nutrition of pathogens. Nature 468(7323):527-U199.

Complainville, A., Brocard, L. Roberts, I., Dax, E., Sever, N., Sauer, N., Kondorosi, A., Wolf, S., Oparka, K., and Crespi, M. 2003. Nodule initiation involves the creation of a new symplasmic field in specific root cells of *Medicago* species. Plant Cell 15:2778-2791.

Conesa, A., Gotz, S., Garcia-Gomez, J., Terol, J., Talon, M., and Robles, M. 2005. Blast2GO: A universal tool for annotation, visualization and analysis in functional genomics research. Bioinformatics 21(18):3674-3676.

Denance, N., Szurek, B., and Noel, L. D. 2014. Emerging functions of nodulin-like proteins in non-nodulating plant species. Plant Cell Physiol. 55(3):469-474.

Desbrosses, G. J., and Stougaard, J. 2011. Root nodulation: A paradigm for how plant-microbe symbiosis influences host developmental pathways. Cell Host Microbe 10(4):348-358.

Edgar, B. A., Zielke, N., and Gutierrez, C. 2014. Endocycles: A recurrent evolutionary innovation for post-mitotic cell growth. Nat. Rev. Mol. Cell Biol. 15(3):197-210.

Endre, G., Kereszt, A., Kevei, Z., Mihacea, S., Kalo, P., and Kiss, G. 2002. A receptor kinase gene regulating symbiotic nodule development. Nature 417(6892):962-966.

Engler, J. d. A., and Gheysen, G. 2013. Nematode-induced endoreduplication in plant host cells: Why and how? Mol. Plant-Microbe Interact. 26(1):17-24.

Engler, J. d. A., Vieira, P., Rodiuc, N., Grossi de Sa, M. F., and Engler, G. 2015. Chapter four - the plant cell cycle machinery: Usurped and modulated by plant-parasitic nematodes. Adv. Bot. Res. 73:91-118.

Eom, J., Chen, L., Sosso, D., Julius, B. T., Lin, I. W., Qu, X., Braun, D. M., and Frommer, W. B. 2015. SWEETs, transporters for intracellular and intercellular sugar translocation. Curr. Opin. Plant Biol. 25:53-62.

Eves-Van den Akker, S., Lilley, C. J., Yusup, H. B., Jones, J. T., and Urwin, P. E. 2016. Functional C-TERMINALLY ENCODED PEPTIDE (CEP) plant hormone domains evolved *de novo* in plant parasite *Rotylenchulus reniformis*. Mol. Plant Pathol. 17(8):1265-1275.

Favery, B., Complainville, A., Vinardell, J., Lecomte, P., Vaubert, D., Mergaert, P., Kondorosi, A., Kondorosi, E., Crespi, M., and Abad, P. 2002. The endosymbiosis-induced genes ENOD40 and CCS52a are involved in endoparasitic-nematode interactions in *Medicago truncatula*. Mol. Plant-Microbe Interact. 15(10):1008-1013.

Ferguson, B. J., Indrasumunar, A., Hayashi, S., Lin, M., Lin, Y., Reid, D. E., and Gresshoff, P. M. 2010. Molecular analysis of legume nodule development and autoregulation. J. Integr. Plant Biol. 52(1):61-76.

Flemetakis, E., Dimou, M., Cotzur, D., Efrose, R. C., Aivalakis, G. Colebatch, G., Udvardi, M., and Katinakis, P. 2003. A sucrose transporter, LjSUT4, is up-regulated during *Lotus japonicus* nodule development. J. Exp. Bot. 54(388):1789-1791.

Fu, Q., Li, S., and Yu, D. 2010. Identification of an Arabidopsis nodulin-related protein in heat stress. Mol. Cells 29(1)77-84.

Gamas, P., de Carvalho-Niebel, F., Lescure, N., and Cullimore, J. 1996. Use of a subtractive hybridization approach to identify new *Medicago truncatula* genes induced during root nodule development. Mol. Plant-Microbe Interact. 9(4):233-242.

Ghosh, R., and Bankaitis, V. A. 2011. Phosphatidylinositol transfer proteins: negotiating the regulatory interface between lipid metabolism and lipid signaling in diverse cellular processes. Biofactors 37(4):290-308.

Ghosh, R., de Campos, M. K. F., Huang, J., Huh, S. K., Orlowski, A., Yang, Y., Tripathi, A., Nile, A., Lee, H., Dynowski, M., Schaefer, H., Rog, T., Lete, M. G., Ahyayauch, H., Alonso, A., Vattulainen, I., Igumenova, T. I., Schaaf, G., and Bankaitis, V. A. 2015. Sec14-nodulin proteins and the patterning of phosphoinositide landmarks for developmental control of membrane morphogenesis. Mol. Biol. Cell 26(9):1764-1781.

Guo, X., Chronis, D., De La Torre, C. M., Smeda, J., Wang, X., and Mitchum, M. G. 2015. Enhanced resistance to soybean cyst nematode *Heterodera glycines* in transgenic soybean by silencing putative CLE receptors. Plant Biotechnol. J. 13(6):801-810.

Heald, C., and Robinson, A. 1990. Survey of current distribution of *Rotylenchulus reniformis* in the United States. J. Nematol. 22(4):695-699.

Huang, G., Allen, R., Davis, E. L., Baum, T. J., and Hussey, R. S. 2006a. Engineering broad root-knot resistance in transgenic plants by RNAi silencing of a conserved and essential root-knot nematode parasitism gene. Proc. Natl. Acad. Sci. USA 103(39):14302-14306.

Huang, G., Dong, R., Allen, R., Davis, E., Baum, T., and Hussey, R. 2006b. A root-knot nematode secretory peptide functions as a ligand for a plant transcription factor. Mol. Plant-Microbe Interact. 19(5):463-470.

Huang, P., Catinot, J., and Zimmerli, L. 2016. Ethylene response factors in Arabidopsis immunity. J. Exp. Bot. 67(5):1231-1241.

Hutangura, P., Mathesius U., Jones, M. G. K., and Rolfe B. G. 1999. Auxin induction is a trigger for root gall formation caused by root-knot nematodes in white clover and is associated with the activation of the flavonoid pathway. Aust. J. Plant Physiol. 26(3):221-231.

Langmead, B., and Salzberg, S. 2012. Fast gapped-read alignment with Bowtie 2. Nat. Methods 9(4):357-359.

Jaouannet, M., Magliano, M., Arguel, M. J., Gourgues, M., Evangelisti, E., Abad, P., and Rosso, M. N. 2013. The root-knot nematode calreticulin mi-CRT is a key effector in plant defense suppression. Mol. Plant-Microbe Interact. 26(1):97-105.

Jenkins, W. R. 1964. A rapid centrifugal-flotation technique for separating nematodes from soil. Plant Dis. Rep. 48(9):692.

Jones, M. G. K., and Dropkin, V. H. 1975. Cellular alterations induced in soybean roots by three endoparasitic nematodes. Physiol. Plant Pathol. 5(2):119-124.

Juergensen, K., Scholz-Starke, J., Sauer, N., Hess, P., van Bel, A., and Grundler, F. 2003. The companion cell-specific Arabidopsis disaccharide carrier AtSUC2 is expressed in nematode-induced syncytia. Plant Physiol. 131(1):61-69.

Kassaw, T., Bridges, W.,Jr., and Frugoli, J. 2015. Multiple autoregulation of nodulation (AON) signals identified through split root analysis of *Medicago truncatula sunn* and *rdn1* mutants. Plants-Basel 4(2):209-224.

Kennedy, M., Niblack, T., and Krishnan, H. 1999. Infection by *Heterodera glycines* elevates isoflavonoid production and influences soybean nodulation. J. Nematol. 31(3):341-347.

Lefebvre, B., Timmers, T., Mbengue, M., Moreau, S., Herve, C., Toth, K., Bittencourt-Silvestre, J., Klaus, D., Deslandes, L., Godiard, L., Murray, J. D., Udvardi, M. K., Raffaele, S., Mongrand, S., Cullimore, J., Gamas, P., Niebel, A., and Ott, T. 2010. A remorin protein interacts with symbiotic receptors and regulates bacterial infection. Proc. Natl. Acad. Sci. USA 107(5):2343-2348.

Li, R., Rashotte, A. M., Singh, N. K., Lawrence, K. S., Weaver, D. B., and Locy, R. D. 2015. Transcriptome analysis of cotton (*Gossypium hirsutum* L.) genotypes that are susceptible, resistant, and hypersensitive to reniform nematode *(Rotylenchulus reniformis*). PLoS One 10(11):e0143261.

Liu, C.W., and Murray, J. D. 2016. The role of flavonoids in nodulation host-range specificity: an update. Plants-Basel 5(33).

Lohar, D., and Bird, D. 2003. *Lotus japonicus*: A new model to study root-parasitic nematodes. Plant Cell Physiol. 44(11):1176-1184.

Lohar, D., Schaff, J., Laskey, J., Kieber, J., Bilyeu, K., and Bird, D. 2004. Cytokinins play opposite roles in lateral root formation, and nematode and rhizobial symbioses. Plant J. 38(2):203-214.

Love, M. I., Huber, W., and Anders, S. 2014. Moderated estimation of fold change and dispersion for RNA-seq data with DESeq2. Genome Biol. 15(12):550.

Madsen, E., Madsen, L., Radutoiu, S., Olbryt, M., Rakwalska, M., Szczyglowski, K., Sato, S., Kaneko, T., Tabata, S., Sandal, N., and Stougaard, J. 2003. A receptor kinase gene of the LysM type is involved in legume perception of rhizobial signals. Nature 425(6958):637-640.

Maroti, G., and Kondorosi, E. 2014. Nitrogen-fixing rhizobium-legume symbiosis: Are polyploidy and host peptide-governed symbiont differentiation general principles of endosymbiosis? Front. Microbiol. 5:326.

Mathesius, U. 2003. Conservation and divergence of signalling pathways between roots and soil microbes - the rhizobium-legume symbiosis compared to the development of lateral roots, mycorrhizal interactions and nematode-induced galls. Plant Soil 255(1):105-119.

McCarter, J. P., Mitreva, M. D., Martin, J., Dante, M., Wylie, T., Rao, U., Pape, D., Bowers, Y., Theising, B., Murphy, C. V., Kloek, A. P., Chiapelli, B. J., Clifton, S. W., Bird, D. M., and Waterston, R. H. 2003. Analysis and functional classification of transcripts from the nematode *Meloidogyne incognita*. Genome Biol. 4(4):R26.

Mitra, R., Shaw, S., and Long, S. 2004. Six nonnodulating plant mutants defective for nod factor-induced transcriptional changes associated with the legume-rhizobia symbiosis. Proc. Natl. Acad. Sci. USA 101(27):10217-10222.

Oldroyd, G., and Long, S. 2003. Identification and characterization of nodulation-signaling pathway 2, a gene of *Medicago truncatula* involved in nod factor signaling. Plant Physiol. 131(3):1027-1032.

Ott, T., van Dongen, J., Gunther, C., Krusell, L., Desbrosses, G., Vigeolas, H., Bock, V., Czechowski, T., Geigenberger, P., and Udvardi, M. 2005. Symbiotic leghemoglobins are crucial for nitrogen fixation in legume root nodules but not for general plant growth and development. Curr. Biol. 15(6):531-535.

Patel, N., Hamamouch, N., Li, C., Hussey, R., Mitchum, M., Baum, T., Wang, X., and Davis, E. L. 2008. Similarity and functional analyses of expressed parasitism genes in *Heterodera schachtii* and *Heterodera glycines*. J. Nematol. 40(4):299-310.

Peiro, A., Izquierdo-Garcia, A. C., Sanchez-Navarro, J. A., Pallas, V., Mulet, J. M., and Aparicio, F. 2014. Patellins 3 and 6, two members of the plant patellin family, interaction with the movement protein of alfalfa mosaic virus and interfere with viral movement. Mol. Plant Pathol. 15(9):881-891.

Peterman, T., Ohol, Y., McReynolds, L., and Luna, E. 2004. Patellin1, a novel Sec14-like protein, localizes to the cell plate and binds phosphoinositides. Plant Physiol. 136(2):3080-3094.

Quentin, M., Abad, P., and Favery, B. 2013. Plant parasitic nematode effectors target host defense and nuclear functions to establish feeding cells. Front. Plant Sci. 4:53.

Rebois, R. V., Madden, P. A., and Eldridge, B. J. 1975. Some ultrastructural changes induced in resistant and susceptible soybean roots following infection by *Rotylenchulus reniformis*. J. Nematol. 7(2):122-139.

Rebois, R. V. 1980. Ultrastructure of a feeding peg and tube associated with *Rotylenchulus reniformis* in cotton. Nematologica 26(4):396-405.

Reddy, P., Aggarwal, R., Ramos, M., Ladha, J., Brar, D., and Kouchi, H. 1999. Widespread occurrence of the homologues of the early nodulin (ENOD) genes in *Oryza* species and related grasses. Biochem. Biophys. Res. Commun. 258(1):148-154.

Robinson, A. F., Inserra, R. N., Caswell-Chen, E. P., Vovlas, N., and Troccoli, A. 1997. *Rotylenchulus* species: Identification, distribution, host ranges, and crop plant resistance. Nematropica 27(2):127-180.

Robinson, A. F. 2007. Reniform in US cotton: When, where, why, and some remedies. Annu. Rev. Phytopathol. 45:263-288.

Schmutz, J., Cannon, S. B., Schlueter, J., Ma, J., Mitros, T., Nelson, W., Hyten, D. L., Song, Q., Thelen, J. J., Cheng, J., Xu, D., Hellsten, U., May, G. D., Yu, Y., Sakurai, T., Umezawa, T., Bhattacharyya, M. K., Sandhu, D., Valliyodan, B., Lindquist, E., Peto, M., Grant, D., Shu, S., Goodstein, D., Barry, K., Futrell-Griggs, M., Abernathy, B., Du, J., Tian, Z., Zhu, L., Gill, N., Joshi, T., Libault, M., Sethuraman, A., Zhang, X., Shinozaki, K., Nguyen, H. T., Wing, R. A., Cregan, P., Specht, J., Grimwood, J., Rokhsar, D., Stacey, G., Shoemaker, R. C., and Jackson, S. A. 2010. Genome sequence of the palaeopolyploid soybean. Nature 463(7278):178-183.

Singh, S., Katzer, K., Lambert, J., Cerri, M., and Parniske, M. 2014. CYCLOPS, A DNA-binding transcriptional activator, orchestrates symbiotic root nodule development. Cell Host Microbe 15(2):139-152.

Smeds, L., and Kunstner, A. 2011. CONDETRI - A content dependent read trimmer for Illumina data. Plos One 6(10):e26314.

Soyano, T., Hirakawa, H., Sato, S., Hayashi, M., and Kawaguchi, M. 2014. NODULE INCEPTION creates a long-distance negative feedback loop involved in homeostatic regulation of nodule organ production. Proc. Natl. Acad. Sci. USA 111(40):14607-14612.

Stracke, S., Kistner, C., Yoshida, S., Mulder, L., Sato, S., Kaneko, T., Tabata, S., Sandal, N., Stougaard, J., Szczyglowski, K., and Parniske, M. 2002. A plant receptor-like kinase required for both bacterial and fungal symbiosis. Nature 417(6892):959-962.

Subramanian, A., Tamayo, P., Mootha, V., Mukherjee, S., Ebert, B., Gillette, M., Paulovich, A., Pomeroy, S., Golub, T., Lander, E., and Mesirov, J. 2005. Gene set enrichment analysis: A knowledge-based approach for interpreting genome-wide expression profiles. Proc. Natl. Acad. Sci. USA 102(43):15545-15550.

Suzaki, T., Yoro, E., and Kawaguchi, M. 2015. Leguminous plants: Inventors of root nodules to accommodate symbiotic bacteria. Int. Rev. Cell Mol. Biol. 316:111-158.

Trapnell, C., Roberts, A., Goff, L., Pertea, G., Kim, D., Kelley, D. R., Pimentel, H., Salzberg, S. L., Rinn, J. L., and Pachter, L. 2012. Differential gene and transcript expression analysis of RNA-seq experiments with TopHat and cufflinks. Nat. Protoc. 7(3):562-578.

Truernit, E. and Sauer, N. 1995. The promoter of the *Arabidopsis thaliana* SUC2 sucrose-H+ symporter gene directs expression of beta-glucuronidase to the phloem – Evidence for phloem loading and unloading by SUC2. Planta 196(3):564-570.

Verma, D., Fortin, M., Stanley, J., Mauro, V., Purohit, S., and Morrison, N. 1986. Nodulins and nodulin genes of *Glycine max* - a perspective. Plant Mol. Biol. 7(1):51-61.

Vieira, P., Kyndt, T., Gheysen, G., and Engler, J. d. A. 2013. An insight into critical endocycle genes for plant-parasitic nematode feeding sites establishment. Plant Signal. Behav. 8(6):e24223.

Vieira-de-Mello, G. S., dos Santos, P. B., Soares-Cavalcanti, N. d. M., and Benko-Iseppon, A. M. 2011. Identification and expression of early nodulin in sugarcane transcriptome revealed by in silico analysis. Lect. Notes Bioinform. 6685:72-85.

Vinardell, J. M., Fedorova, E., Cebolla, A., Kevei, Z., Horvath, G., Kelemen, Z., Tarayre, S., Roudier, F., Mergaert, P., Kondorosi, A., and Kondorosi, E. 2003. Endoreduplication mediated by the anaphase-promoting complex activator CCS52A is required for symbiotic cell differentiation in *Medicago truncatula* nodules. Plant Cell 15(9):2093-2105.

Wang, X., Mitchum, M., Gao, B., Li, C., Diab, H., Baum, T., Hussey, R., and Davis, E. 2005. A parasitism gene from a plant-parasitic nematode with function similar to CLAVATA3/ESR (CLE) of *Arabidopsis thaliana*. Mol. Plant Pathol. 6(2):187-191.

Wasson, A. P., Ramsay, K., Jones, M. G. K., and Mathesius, U. 2009. Differing requirements for flavonoids during the formation of lateral roots, nodules and root knot nematode galls in *Medicago truncatula*. New Phytol. 183(1):167-179.

Weerasinghe, R., Bird, D., and Allen, N. 2005. Root-knot nematodes and bacterial nod factors elicit common signal transduction events in *Lotus japonicus*. Proc. Natl. Acad. Sci. USA 102(8):3147-3152.

Weise, A., Barker, L., Kuhn, C., Lalonde, S., Buschmann, H., Frommer, W., and Ward, J. 2000. A new subfamily of sucrose transporters, SUT4, with low affinity/high capacity localized in enucleate sieve elements of plants. Plant Cell 12(8):1345-1355.

Wieczorek, K. 2015. Chapter three - cell wall alterations in nematode-infected roots. Adv. Bot. Res. 73:61-90.

Wubben, M. J., Gavilano, L., Baum, T. J., and Davis, E. L. 2015. Sequence and spatiotemporal expression analysis of CLE-motif containing genes from the reniform nematode (*Rotylenchulus reniformis* Linford & Oliveira). J. Nematol. 47(2):159-165.

Xie, F., Murray, J. D., Kim, J., Heckmann, A. B., Edwards, A., Oldroyd, G. E. D., and Downie, A. 2012. Legume pectate lyase required for root infection by rhizobia. Proc. Natl. Acad. Sci. USA 109(2):633-638.

Yano, K., Shibata, S., Chen, W., Sato, S., Kaneko, T., Jurkiewicz, A., Sandal, N., Banba, M., Imaizumi-Anraku, H., Kojima, T., Ohtomo, R., Szczyglowski, K., Stougaard, J., Tabata, S., Hayashi, M., Kouchi, H., and Umehara, Y. 2009. CERBERUS, a novel U-box protein containing WD-40 repeats, is required for formation of the infection thread and nodule development in the legume-rhizobium symbiosis. Plant J. 60(1):168-180.

Zhao, J. 2015. Phospholipase D and phosphatidic acid in plant defence response: From protein-protein and lipid-protein interactions to hormone signaling. J. Exp. Bot. 66(7):1721-1736.

CHAPTER TWO

RENIFORM NEMATODE INFECTION ALTERS ROOT ACHITECTURE AND GENE EXPRESSION IN SOYBEAN

INTRODUCTION

Reniform nematode, *Rotylenchulus reniformis* (Linford and Oliveira), is a damaging root parasite with a broad host range of over 300 different plant species (Heald and Robinson 1990; Robinson et al. 1997). During infection, female nematodes burrow into roots and establish permanent syncytia in host pericycle tissue. Syncytia are hypermetabolic feeding sites consisting of a few hundred cells that have lost their cell wall partitions and have fused to form a continuous mass of dense, organelle rich cytoplasm. While syncytial ultrastructure has been extensively characterized, reniform nematode-induced changes in root growth and morphology have not previously been investigated (Agudelo et al. 2005; Jones and Dropkin 1975; Rebois 1980; Rebois et al. 1975).

We recently examined differences in gene expression between infected and uninfected soybean roots across a multi-day time course. Results showed significant overlap between gene expression in response to reniform nematode (RN) and gene expression in response to rhizobial symbionts (Redding et al. 2018). Several differentially expressed genes also had roles in lateral root initiation, a finding consistent with the hypothesis that diverse belowground symbionts and parasites manipulate the lateral root organogenesis program to generate novel structures (Imin et al. 2013; Mathesius 2003; Ng et al. 2015; Wasson et al. 2009). We were therefore interested in

whether reniform nematode parasitism also altered lateral root initiation and, by extension, root system growth and architecture.

Several better-studied sedentary nematodes are known to cause macroscopic changes in host root morphology. Infection by root-knot nematodes (RKN; *Meloidogyne sp.*) causes the formation of swollen areas, i.e. galls, around permanent feeding sites comprised of 'giant cells.' Galls arise from asymmetrical cell divisions and vascularization around the giant cells, which disrupts normal water and nutrient flow (Bartlem et al. 2014). At sufficiently high levels of infection (above the damage threshold), root-knot nematodes can be especially destructive, reducing plant growth and yield. However, a study investigating the effects of low-levels of root-knot nematode inoculum on barley (*Hordeum vulgare*) showed that infection increased root length **(**Haase et al. 2007).

Cyst nematode (CN; *Heterodera* and *Globodera sp.*) infection produces more subtle changes in root anatomy. These nematodes induce the formation of syncytia in procambial or young vascular tissue; like reniform nematodes, their feeding sites are not surrounded by gall tissue (Jones and Dropkin 1975). Studies examining root architecture changes in clover infected by *Heterodera trifolii* showed variable results, causing both an increase in root system biomass (Bardgett et al. 1999) or no change in weight but a decrease in root length (Treonis et al. 2007). The studies' primarily focus was on the effect of nematode feeding on the rhizosphere microbial community and difference may be attributed to the methods employed in each experiment, though inoculum levels were similar.

Feeding site formation in root-knot and cyst nematodes is controlled by hormones and transcription factors that also have roles in lateral root initiation. Auxin and its transporters have been shown to regulate both RKN giant cell and CN syncytium development (Goverse et al. 2000; Grunewald et al. 2009; Karczmarek et al. 2004; Lee et al. 2011; Mazarei et al. 2003). Likewise, auxin acts through highly regulated signaling modules involving AUX/IAA and Auxin Response Factors to induce the gene expression changes that lead to the development of lateral root primoridia and ultimately root emergence (Lavenus et al. 2013). Transcription factors, including LATERAL ORGAN BOUNDARIES, auxin response factors, and WRKY genes, also play roles in both nematode infection and lateral root growth (Cabrera et al. 2014; Grunewald 2012; Hewezi et al. 2014). Given that similar suites of genes are common to both feeding site formation and lateral root initiation, we hypothesized that infection by reniform nematode would (1) induce greater lateral root production in parasitized roots and (2) alter the local expression of lateral root-related genes in parasitized roots.

Here we present root growth and architecture data from young soybean (*Glycine max*) plants infected with reniform nematode in two growth systems across a twelve-day time course. In both systems, roots exposed to reniform nematode initiated more new lateral roots per unit initial root length. We also examined lateral root-related gene expression in infected and control roots across a 12-day time course in the split-root growth system. The number of differentially expressed genes and gene expression magnitude were highest early in infection. More lateral root genes were up-regulated

than down. Among the differentially expressed genes include a large group involved in the transport, regulation, and biosynthesis of auxin. Several transcription factors and gene regulators also changed expression including LATERAL ROOT PRIMORDIUM 1, LATERAL ORGAN BOUNDARIES, SOMBRERO, SHORT-ROOT, RPT2a, and MADS-box genes.

MATERIALS AND METHODS

Split-root growth system

The effects of reniform nematode (RN) infection on root growth and architecture were assessed in two separate plant growth systems. In the split-root growth system, the root systems of individual plants were separated into two pots: one inoculated and the other uninoculated. This system allowed us to measure local effects of RN on root growth, while controlling for the effect of parasitism on overall plant size and carbon allocation. The split-root system also allowed us to identify genes that were locally up- and down-regulated in response to infection, while controlling for plant-to-plant variation in gene expression.

Seeds of the RN-susceptible soybean *Glycine max* cultivar 'Hutcheson' were surface sterilized, germinated on sterilized vermiculite, and maintained in a growth room at 28 ± 2°C, with 50% relative humidity (RH) and a 14-h/10-h (light/dark) photoperiod. Following cotyledon emergence, a horizontal cut was made at the base of each taproot to encourage primary lateral root proliferation. After one week, primary lateral roots were grouped into two equal bundles, threaded through the arms of a Y-shaped plastic tube (diameter 2.22 cm), and directed into adjacent 300 cm^3 pots filled with pasteurized fine sand. Roots were then treated with RN inoculum or a tap water control as described below. In this growth system, primary laterals (i.e. roots arising directly from the cut taproot) were exposed to inoculum and were therefore the "treated roots."

Reniform nematode inoculum was prepared from soil collected from an infested cotton field in St. Matthews, SC. Sugar centrifugal flotation was used to extract vermiform nematodes, which were rinsed and collected in a 500μm mesh sieve (Jenkins 1964). Following inspection and quantification, nematodes were suspended in tap water at a concentration of 1500 individuals/ml. One side of each split-root system was selected at random and inoculated with 2ml of the nematode suspension (~3000 nematodes); the other side received an equivalent volume of tap water as a negative control. Plants were grown for up to 12 days after inoculation. Their location within the growth room was randomized daily. Five replicates of each system were harvested at 3, 6, 9, and 12 days after inoculation (DAI) as described below.

Individual pot growth system

In the individual pot growth system, plants were grown intact in plastic pots and their whole root systems were treated with either a reniform nematode suspension or tap water. This growth system required no disturbance of the taproot and eliminated any potential effects of taproot pruning on subsequent root growth and architecture. However, it was not possible to control for the effects of parasitism on whole-plant growth and carbon allocation.

Surface sterilized seeds of *G. max* cv. 'Hutcheson' were germinated on moist paper towels under the conditions described above. After four days, radicals had emerged and taproots had begun to lengthen. Sixty uniform seedlings were selected and planted in 1000 cm^3 plastic pots filled with pasteurized fine sand. The taproots of

inoculated plants received 2ml of the nematode suspension described above (~3000 nematodes); those of control plants received an equal volume of tap water. In this growth system, the taproots were exposed to inoculum and were therefore the "treated roots."

Plants were grown for up to 12 days after inoculation in a growth room at 28 ± 2°C, with 50% relative humidity (RH) and a 14-h/10-h (light/dark) photoperiod. Their location within the growth room was randomized daily. Fifteen replicates of each treatment were harvested at 6 and 12 DAI.

Root architecture analysis

Root systems from the split-root trial were harvested at 3, 6, 9, and 12 DAI for a total of 40 samples (2 infection statuses x 4 dates x 5 biological replicates). Root systems from the individual pot trial were harvested at 6 and 12 DAI for a total of 60 samples (2 infection statuses x 2 dates x 15 biological replicates). Root fresh weights (g) were collected prior to storage in a 50% (V/V) ethanol solution at 4°C. Shoot lengths (cm) were measured for all plants, and, in the individual pot trial, shoot fresh weights (g) were also recorded.

Root architecture data were obtained from digital images using the WinRHIZO Pro system (Regent Instruments Canada Inc.). Each root sample was carefully positioned on a clear tray containing a thin layer of tap water and imaged using an Epson Perfection V800 Photo scanner. Images were processed in WinRHIZO Pro 2016a software with the 'interpolation,' and 'root morphology' measurement options. A rough edge removal filter with the 'HIGH' option was used to remove distortions caused by residual sand, and a

debris removal filter was used to exclude objects smaller than 0.008cm^2. Measured parameters included total root length (cm), average root diameter, and number of root tips. The total root number was estimated as the number of root tips minus double the number of broken root fragments in the image. The lengths of the original "treated" roots (taproots in the individual pot trial; primary lateral roots in the split-root trial) were measured by hand-tracing in ImageJ v1.47 (Schneider et al. 2012). The number of new daughter roots that had arisen directly from each original root were counted by hand. These data were used to calculate the number of new roots produced per unit of original root length following inoculation or mock inoculation.

Statistical analysis of root growth and architectural parameters was performed with the REML method for ANOVA models in JMP® Pro v13.2 (SAS Institute Inc.). Split-root and individual pot trials were analyzed separately using the variables DATE, TREATMENT, and their interaction as fixed effects. For split-root plants, two separate root samples (infected and control) were harvested from five individual plants on each of four sampling dates (20 plants and 40 samples total). The effect of the individual plant nested within date and the interaction of this effect with treatment were treated as random effects. In the individual pot trial, 15 independent plants were harvested from each treatment on two sampling dates (60 plants total). Only fixed effects were included in the model.

Transcriptome Assembly and Gene Expression Analysis

A soybean root transcriptome was assembled from inoculated and control roots grown in a separate split-root trial conducted as above. Approximately 500 mg fresh weight (FW) of infected and control root tissue was harvested from each of three replicate plants at 3, 6, 9, and 12 DAI, for a total of 24 samples (2 infection statuses x 4 dates x 3 biological replicates). Tissue was stored in RNA*later*® Stabilization Reagent (Ambion, Austin, TX) and sent to the University of Arizona Genetics Core (Tucson, AZ). RNA was extracted using the Qiagen RNAeasy Mini Kit, and RNA quality was assessed with the Agilent 2100 Bioanalyzer prior to 100-bp paired-end library preparation with the Illumina TruSeq 2 RNA kit. Samples were sequenced across two lanes of the Illumina HiSeq 2000 platform (Illumina, San Diego, CA).

A total of 619 million paired-end 100-bp reads were generated across the experiment, with an average of 25.8 million reads per sample. Read quality was assessed with FastQC v0.10.1, sequencing adaptors were trimmed with Trimmomatic v0.32 (Bolger et al. 2014), and low-quality bases were removed using the default settings of ConDeTri v2.2 (Smeds and Kunstner 2011). The average per-read PHRED quality score after trimming was 36.7, and the minimum per-read score was 36.02. All raw reads were uploaded to the NCBI Sequence Read Archive under accession number SRP091708.

Trimmed reads from each sample were mapped to the Wm82.a1.v1 build of the soybean reference genome using Bowtie2 v2.1.0 and TopHat v2.0.11 with default parameters (Trapnell et al. 2012). Transcripts were assembled separately for each sample using Cufflinks v2.2.1, and then merged with the Glyma1.0 reference annotation to generate a soybean root transcriptome (Trapnell et al. 2012). The new reference

transcriptome was annotated in Blast2GO Pro v3.0, which performs a BLASTx search against the NCBI nr protein database and assigns sequence descriptions, gene ontology (GO) terms, Interpro IDs, enzyme codes (EC), and KEGG pathways to transcripts with significant blast hits ($E < 10^{-6}$) (Conesa et al. 2005).

To examine the expression of genes specifically related to lateral root initiation and development, differential expression analysis was performed on a subset of 440 pre-selected genes. Testing expression of a pre-selected target gene set gave us greater statistical power to detect differences than testing expression of all assembled genes. Genes were chosen *a priori* based on two criteria: (1) annotation with a gene ontology term pertaining to lateral root development, and/or (2) annotation with a sequence description containing the word "root." Genes specifically related to root hair development were excluded. Several additional genes were included based on differential expression of their cotton homologs in response to RN (unpublished data). The full set of lateral root-related GO terms used for gene selection is provided in Supplementary File 2.1, and annotation information for all 440 pre-selected genes is provided in Supplementary File 2.2.

Reads from all splice forms of a given gene were pooled, and count data were imported to DESeq2 for differential expression analysis using default parameters (Anders et al. 2015; Love et al. 2014). Data were analyzed separately by date to identify genes differentially expressed between inoculated and non-inoculated roots, while controlling for the effect of individual plants (FDR = 0.01). Data from all assembled genes were initially included to generate accurate dispersion estimates in DESeq2. Differential

expression of the 440 root-related genes was then assessed by subsetting the DESeq2 results object and recalculating the FDR-adjusted *p*-values. Genes differentially expressed between inoculated and non-inoculated roots were identified using an FDR-adjusted *p*-value ≤ 0.05. Log_2FC estimates were calculated in DESeq2, implementing empirical Bayes shrinkage to permit accurate comparison of effect sizes across all genes (Love et al. 2014).

RESULTS

Split root trial: root growth and architecture

In the split-root trial, greater root length was present on the inoculated sides of the split-root systems (Figure 1; treatment main effect $p = 0.0096$). Differences in root length were greater at later sampling dates: on 9 and 12 DAI, the average root length in inoculated sides was 46% and 27% greater than in controls.

There were no significant differences in root weight between inoculated and control sides, suggesting that inoculated roots had smaller diameters, lower tissue densities, or both (Figure 1A). The latter possibility appears more likely, as there were no differences in average root diameter between inoculated and control sides (data not shown). That inoculated roots weighed less than control roots was also suggested by higher numbers of lateral roots per gram in inoculated sides (Figure 1C; treatment main effect $p = 0.0245$). Finally, the number of new roots produced per cm of original treated root length was significantly higher in the inoculated sides (Fig 1D; treatment main effect $p = 0.0291$).

Individual pot trial: root growth and architecture

In the individual pot trial, infection resulted in smaller plants with significantly lower root and shoot fresh weights (Figure 2A; Table 2). At 12 DAI, average shoot and root fresh weights of infected plants were 11% and 23% lower than those of control plants. Smaller infected plants also had shorter root systems: mean root length at 12 DAI

was 764.8 ± 45.9 cm in infected plants and 868.1 ± 41.2 cm in controls (Figure 2B; treatment main effect $p = 0.0269$).

RN parasitism of whole root systems reduced whole plant growth in the individual pot trial. Nonetheless, several effects of RN on root growth and morphology were similar to those in the split-root trial. First, the number of roots per unit fresh weight was higher in inoculated plants (Figure 2C; treatment main effect $p = 0.0209$). Second, the number of new lateral roots produced per cm of original root length was significantly higher in the inoculated pots (Fig 2D; treatment main effect $p = 0.0491$). For example, at 6 DAI inoculated pots had 4.9 new roots per cm of original root length versus 3.9 new roots/cm in control pots.

Taken together, root measurements from two growth systems suggested that RN infection stimulated new lateral root formation in the inoculated roots of young soybean plants, an effect that was partially masked in intact root systems by the overall negative effect of parasitism on plant growth.

Root-related gene expression

We used the split-root system to examine local differences in the expression of pre-selected target genes that had documented roles in lateral root initiation and development. Of the 440 target genes examined, 131 were differentially expressed (DE) between inoculated and control roots on at least one sampling date. Annotation and expression data for all significantly DE target genes are provided in Supplementary File 2.2.

More lateral root-related genes were up-regulated than down-regulated in infected roots, and the greatest number of DE genes occurred early in infection at 3 DAI. The magnitude of differential expression was also highest at 3 DAI, when log2(fold change) (L2FC) estimates for individual DE genes ranged from -2.6 to 4.7. The L2FC ranges of DE genes were smaller at later dates: -1.2 to 1.8 at 6 DAI, -1.4 to 2.8 at 9 DAI, and -0.9 to 2.6 at 12 DAI. Previous work in our lab has shown that syncytia are not yet established at 3 DAI, but that females have begun to penetrate the root cortex and select initial syncytial cells (Redding et al. 2018). The greatest differential gene expression was therefore occurring in the earliest stages of infection, prior to syncytium formation.

Up-regulated auxin-related genes

Up to twenty DE genes with the greatest positive and negative L2FC estimates on each date are provided in Tables 3 and 4. Among the top up-regulated genes, half encoded proteins related to auxin signaling, and nearly a third dealt specifically with auxin transport. Most up-regulated transporters were auxin efflux carriers, including two PIN1Cs, two PIN2s, two ABCB19s, one ABCB15, and an auxin efflux carrier family protein. One ABCB19 homolog was differentially expressed on three sampling dates, and three PINs were differentially expressed on two sampling dates (Table 3).

A number of auxin influx transporters were also up-regulated: a LAX3-like protein was up-regulated 10-fold at 3 DAI, and three other LAX genes were also DE on this date (Table 3, Supplementary File 2.2). In addition to direct auxin transporters, three auxin canalization proteins were up-regulated at 3 DAI, one of which was up-regulated

on two subsequent sampling dates. Homologs of ROOT PHOTOTROPISM 3, which controls PIN2 re-localization in the plasma membrane, and TORNADO2, which participates in basipetal auxin transport, were also more highly expressed in infected roots.

In addition to auxin transporter genes, auxin biosynthetic genes were up-regulated throughout the infection process. These included multiple YUCCA family flavin monooxygenases that convert indole-3-pyruvate to indole-3-acetic acid (Stepanova et al. 2008; Won et al. 2011; Zhao et al. 2001). A YUCCA8 homolog had the highest fold change estimate of any gene at 3 DAI and remained up-regulated on two subsequent dates. Two additional YUCCA genes were also up-regulated at 3 DAI but were not among the top twenty genes, as was an earlier enzyme in the auxin biosynthetic pathway, tryptophan aminotransferase-related protein 2 (TAR2; Supplementary File 2.2).

Two homologs of the auxin-inducible transcription factor Lateral Root Primordium 1 (LRP1) showed higher expression in infected roots at 3 and 9 DAI; LRP1 is expressed during the early stages of lateral root primordium development and serves as a molecular marker for lateral root initiation (Krichevsky et al. 2009; Smith and Federoff 1995). Also up-regulated during infection were three genes encoding TRANSPORT INHIBITOR RESPONSE 1 (TIR1) auxin receptors, which mediate the release of pericycle cells from G2 arrest during lateral root initiation (Dharmasiri et al. 2005).

Additional up-regulated genes

Two homologs of the SOMBRERO transcription factor that controls cellular maturation in the Arabidopsis root cap were up-regulated at 3 DAI (Table 3, Supplemental File 2.2), while an ANR1-like transcription factor was up-regulated at 9 DAI. Members of the ANR1 MADS-box family have been shown to control lateral root growth in response to nutrients and are largely root-expressed in Arabidopsis (Zhang and Forde 2000). Additional transcription factors up-regulated at 3 DAI but not on the top twenty list included three genes for SHORT-ROOT-like (SHR-like) proteins whose Arabidopsis homologs control longitudinal patterning of the developing root (Koizumi et al. 2012).

Finally, up to four genes annotated as root cap/late embryogenesis abundant (LEA)-like proteins were among the top twenty up-regulated genes at 3, 9 and 12 DAI (Table 3). Their predicted proteins contain a ~60 residue conserved region that has been previously described in root cap proteins (pfam06830). The function(s) of proteins with this domain remain uncharacterized, and it has been suggested that their annotation as LEA proteins may reflect an early annotation error in Arabidopsis (Hundertmark and Hincha 2008).

Down-regulated auxin-related genes

Auxin-associated genes were also among the top down-regulated root-related genes across multiple sampling dates, although they were fewer in number. In several cases, down-regulated genes were members of the same auxin transporter and biosynthetic gene families whose members were also up-regulated in infected roots

(Table 4). A PIN3-like efflux carrier and an auxin efflux carrier protein were among the top down-regulated genes at 3 and 9 DAI, respectively, and a LAX2-like influx transporter was significantly down-regulated at both 3 and 6 DAI (Table 4). Likewise a YUCCA flavin monooxygenase was strongly down-regulated at 3 DAI.

Other auxin-associated genes on the top down-regulated list included two auxin response factor 5 (ARF5) homologs, several root dependent phototropism 2 homologs, a LON2 protease associated with indole-3-butyric acid (IBA) conversion to IAA and multiple auxin-induced in root cultures (AIR12)-like genes (Laskowski et al. 2006; Preger 2009). Also down-regulated were several shaggy-related protein kinase etas, whose homologous Arabidopsis proteins regulate cross-talk between the brassinosteroid and auxin signaling pathways (Charrier et al. 2002; Li and Nam 2002).

Other down-regulated genes

The most strongly down-regulated gene at 3 DAI was a Lateral Organ Boundaries-like transcription factor (Table 4). The LOB transcription factor family is unique to plants, and some members of the family have been shown to function downstream of auxin influx carriers and auxin response factors to control lateral root initiation and development (Lee et al. 2015). A number of receptors were down-regulated on multiple sampling dates: HSL1-like LRR receptor kinases, a plastid adenylate kinase, and two STRUBBELIG-receptor kinases from a family whose proteins control cell proliferation, morphogenesis, and planes of division (Chevalier et al. 2005).

A type-3 metallothionein was the only gene to show significantly lower expression in infected roots on three out of four sampling dates. Metallothioneins are best know for their role in metal homeostasis and stress response, although some have also been linked to root formation in rice (Guo et al. 2003; Jin et al. 2017; Xue et al. 2009; Yuan et al. 2008).

DISCUSSION

Root growth and architecture changes

Studies of reniform nematode effects on host roots have focused primary on the cellular changes that lead to feeding site formation (Agudelo et al. 2005; Jones and Dropkin 1975; Rebois 1980; Rebois et al. 1975). The process begins when an immature female nematode penetrates the root epidermis and moves through the cortex to reach an endodermal cell, where she secretes effectors (Eves-Van den Akker et al. 2016; Wubben et al. 2015). Cell wall lysis spreads from the initial cell, ultimately incorporating 100 to 200 pericycle cells into a multinucleate syncytium with a dense, continuous cytoplasm. In addition to well-documented histological changes, reniform nematode infection of soybean is also associated with dramatic changes in gene expression, including the expression of genes normally associated with rhizobial symbiosis (Redding et al. 2018). Overlap has also been observed between the interactions of mutalistic and parasitic symbionts and lateral root development, suggesting that these processes may involve common signaling pathways (Imin et al. 2013; Mathesius 2003; Ng et al. 2015; Wasson et al. 2009). Infection by other sedentary plant-parasitic nematodes has been linked to changes in host root growth and architecture, but the molecular mechanisms underlying these changes are unknown (Bardgett et al. 1999; Haase et al. 2007; Treonis et al. 2007).

In this study, reniform nematode infection increased root length and/or new root initiation by young soybean plants, particularly when the effect of parasitism on whole-plant carbon status was controlled. In the split-root system, greater root length was produced in the inoculated pots, and the original treated roots gave rise to more lateral

roots per unit length. The latter result was also seen in the individual pot trial, despite the fact that inoculated plants had smaller root systems overall. A similar pattern has been reported in clover infected by the cyst nematode *Heterodera trifolii.* Infected clover root systems had more secondary lateral roots per millimeter of primary root (Treonis et al. 2007).

Root length on the infected sides of split-root plants was greater that on the control sides, but root weight did not differ between inoculated and control sides. This result indicates a decrease in root diameter and/or tissue density in infected roots. Likewise, in both the split-root and individual pot trials, there were more roots per unit root weight in inoculated root systems. A similar result was reported in barley plants exposed to low-levels of root-knot nematode (*Meloidogyne incognita*): infected barley root systems had increased length but showed no difference in biomass compared to controls (Haase et al. 2007).

Whether the root growth changes reported here and in previous studies have functional significance for whole plant physiology or successful nematode parasitism is unclear. They may be a transient side effect of the nematode's manipulation of host root hormonal and developmental pathways. Both syncytia and lateral roots arise from the same cell layer, i.e. the pericyle, a meristematic cylinder of cells that surrounds the stele and whose relatively undifferentiated state may make it amenable to parasite manipulation.

Changes in root-related gene expression

Gene expression changes in pre-selected root development genes were most numerous and of a higher magnitude early in infection. More root-related genes were up-regulated than down-regulated during infection on every date except 6 DAI, when only four genes were significantly differentially expressed (two up- and two down-regulated). The majority of differentially expressed genes were connected with auxin biosynthesis, transport, or signaling and response. The role of auxin in lateral root development has been thoroughly examined (Benkova and Bielach 2010; Du and Scheres 2018; Lavenus et al. 2013; Peret et al. 2009). PIN auxin efflux carriers move auxin from the root apex to the basal region of the meristem in an oscillating fashion. Auxin response modules facilitate the conversion of xylem pole pericycle cells to primed founder cells when auxin levels reach a certain threshold. Additional auxin input via auxin transporters causes founder cells to begin lateral root initiation through the expression of specific transcription factors. Ultimately, cell division leads to the formation of a lateral root primordium, which grows out through the endodermis and cortex. Emergence is further regulated by auxin transporters PIN3 and LAX3, which increase the auxin gradient ahead of the growing tip, thus stimulating cell wall modifiers to act in and around these cortical cells (Vilches-Barro and Maizel 2015).

Of the 60 unique genes that showed the highest differential expression magnitude across the time course (Table 3 and 4), five were YUCCA family genes, involved in the final reaction of the tryptophan-dependent auxin biosynthetic pathway (Stepanova et al. 2008; Won et al. 2011; Zhao et al. 2001). All but one of these highly expressed genes was up-regulated. Two additional YUCCAs were differentially expressed 3 DAI but at

lower expression magnitudes (one up- and one down-regulated) and another enzyme in the biosynthesis pathway, TAR2, was also up-regulated. In addition to YUCCA driven production of IAA, auxin can also be produced through peroxisome mediated conversion of IBA (Schlicht et al. 2013). A LON2 protease associated with peroxisomal function and IBA-induced lateral root formation was down-regulated early in infection (Goto-Yamada 2014; Lingard et al. 2009), suggesting that this pathway of auxin biosynthesis may have been curtailed in infected roots.

Twelve of the highest expressed genes were involved in direct auxin transport and six had putative roles in auxin transporter relocalization. Seven additional transporters were differentially expressed 3 DAI at lower expression magnitudes, as were three transport regulators. PINs and ABCBs are auxin efflux carriers that maintain the movement of auxin in root tissue necessary for lateral root formation (Benkova et al. 2003; Wu et al. 2007; Yang and Murphy 2009; Zazimalova 2010). Four LAX family proteins were up-regulated and one was down-regulated. Two of the up-regulated genes were homologs of LAX3, an influx transporter known to positively regulate lateral root emergence (Peret et al. 2013).

Three auxin canalization proteins were up-regulated and two auxin transport protein BIGs were down-regulated. Proteins with an auxin canalization domain are thought to aid in auxin flux by recruiting transporters to the plasma membrane (Hou et al. 2010). BIGs play a part in PIN localization and pericycle cell activation (Gil et al. 2001; Lopez-Bucio 2005). TRN2 and ROOT PHOTOTROPISM 3-like (NPH3-like) were up-regulated, and two ROOT PHOTOTROPISM 2s were down-regulated. TRN2 in linked

with proper root patterning and has been implicated in auxin homeostasis in floral development (Cnops et al. 2000; Yamaguchi 2017). In Arbidopsis, AtNPH3 regulates PIN2 relocalization within the plasma membrane, and ROOT PHOTOTROPISM 2 may also have relocalization activity (Sakai and Haga 2012; Wan et al. 2012). Finally an AXR4 that regulates AUX1 transporter localization was slightly down-regulated (Dharmasiri et al. 2006).

Taken together, these results indicate that normal auxin production and distribution is altered early in the process of reniform nematode infection. Indeed, the importance of auxin transporters in cyst nematode (CN) infection has previously been demonstrated. *H. schachtii* formed fewer cysts when infecting Arabidopsis PIN mutants, while tomato plants treated with PIN inhibitors developed abnormal syncytia (Goverse et al. 2000; Grunewald et al. 2009). LAX3 gene expression has been reported in cells of developing CN syncytia, the CN effector Hs19C07 interacts with the AtLAX3 protein, and AtLAX3 ectopic expression increases the rate of lateral root emergence (Lee et al. 2011).

Up-regulation of several highly expressed transcription factors singly or in conjunction with other genes may explain the increased number of lateral roots in infected root systems. Two Lateral Root Primordium 1 genes were among the strongest up-regulated genes at 3 DAI and were also significantly expressed 9 DAI, while a third LRP1 was down-regulated at 3 DAI. All three share homology to AtLRP1, a SHI family protein expressed during the early stages of lateral root primordium development (Kuusk et al. 2006; Smith and Fedoroff 1995). Other SHI proteins have been hypothesized to

play a role in auxin production through YUCCA regulation, and overexpression of AtLRP1 results in root elongation (Baylis et al. 2013; Krichevsky et al. 2009).

Two SOMBRERO-like genes, three SHORT-ROOT-like (SHR-like) transcription factors, and two 26s proteasome regulatory subunit 4 homolog A (RPT2a) genes were overexpressed in infected roots at 3 DAI. These genes regulate processes at the root tip. SOMBREROs regulate proper root cap development (Bennett et al. 2010), SHR-like genes are involved in root patterning and specification of cells in the quiescent center (Helariutta et al. 2000; Petricka et al. 2012), and RPT2a is involved in root meristem maintenance (Ueda et al. 2011). Two MADS-box transcription factors, an ANR1 homolog and an AGL12 homolog, also changed expression, one highly up-regulated and the other down-regulated. MADS-box genes have been studies most extensively for their role in floral development, but members of the ANR1 family function in lateral root development (Zhang and Forde 2000). AGL12 is associated with root meristem function and maintenance, and it was down-regulated during infection (Tapia-Lopez et al. 2008; Yu et al. 2014).

Conclusion

RN induced changes in lateral root initiation and the concomitant up-regulation of multiple genes associated with lateral root production and auxin dynamics suggests that there is mechanistic overlap between the feeding sites organogenesis and the initiation of lateral roots. Both reniform nematode syncytia and lateral roots develop from pericycle cells, and the processes might therefore be expected to interfere or promote one another.

Similar increases in new root initiation have been documented in previous studies of cyst and root-knot nematodes.

Increased production of lateral roots may result from the manipulation of plant hormones by reniform nematodes during formation of their feedings sites, i.e. it may be an unintended consequence of parasitism. Alternately, increased lateral root initiation may provide some benefit to the nematodes themselves, perhaps by increasing nearby sites available for parasitism by their offspring. If lateral root genes are indeed a direct target of reniform nematode effectors, this would support the hypothesis that parasites and symbionts have co-opted normal root developmental programs to construct novel belowground organs (Mathesius 2003).

Table 2.1. Fix effects test for split-root system

Parameter	Source	Nparm	DF	DFDen	F Ratio	P-value > F
Root fresh weight (g)	TREATMENT	1	1	16	0.86	0.3687
	DATE	3	3	16	3.99	**0.0268**
	TREATMENT*DATE	3	3	16	1.13	0.3651
Root length (cm)	TREATMENT	1	1	16	8.66	**0.0096**
	DATE	3	3	16	14.69	**<0.0001**
	TREATMENT*DATE	3	3	16	2.90	0.0673
Lateral roots/root weight (g)	TREATMENT	1	1	16	6.16	**0.0245**
	DATE	3	3	16	15.45	**<0.0001**
	TREATMENT*DATE	3	3	16	2.09	0.1425
New roots/ Original root length (cm)	TREATMENT	1	1	16	5.75	**0.0291**
	DATE	3	3	16	0.25	0.8619
	TREATMENT*DATE	3	3	16	4.48	**0.0183**

Table 2.2. Fix effects test for individual pot system

Parameter	Source	Nparm	DF	Sum of Squares	F Ratio	P-value > F
Shoot fresh weight (g)	TREATMENT	1	1	0.504	4.44	**0.0397**
	DATE	1	1	32.12	282.58	**<0.0001**
	TREATMENT*DATE	1	1	0.14	1.23	0.2715
Root fresh weight (g)	TREATMENT	1	1	5.22	18.47	**<0.0001**
	DATE	1	1	86.64	306.46	**<0.0001**
	TREATMENT*DATE	1	1	0.89	3.14	0.0818
Root length (cm)	TREATMENT	1	1	92097.10	5.17	**0.0269**
	DATE	1	1	6397074.90	358.91	**<0.0001**
	TREATMENT*DATE	1	1	9321.40	0.52	0.4726
Lateral roots/root weight (g)	TREATMENT	1	1	11489.46	5.65	**0.0209**
	DATE	1	1	40813.25	20.07	**<0.0001**
	TREATMENT*DATE	1	1	363.86	0.18	0.6739
New roots/ Original root length (cm)	TREATMENT	1	1	6.46	4.05	**0.0491**
	DATE	1	1	0.46	0.29	0.5951
	TREATMENT*DATE	1	1	1.87	1.17	0.2844

Table 2.3. Mean normalized read counts, log2(fold change) estimates, and FDR-adjusted *P*-values associated with genes whose expression was significantly higher in inoculated than control roots at 3, 6, 9, and 12 days after inoculation (DAI). For 3 DAI, the top twenty up-regulated genes are shown, ranked by log2(fold change) estimate. For other dates, all up-regulated genes are shown.

Gene ID	Description	Mean Normalized Counts			
		Inoculated	Control	log2FC estimate	FDR-adjusted P-value
3 DAI					
XLOC_049446	indole-3-pyruvate monooxygenase YUCCA8-like	302	8	4.67	0.000
XLOC_026556	protein FluG/nodulin-61	2781	7	4.59	0.000
XLOC_030634	root cap/late embryogenesis-like protein	414	3	3.98	0.000
XLOC_028585	root cap/late embryogenesis-like protein	583	18	3.59	0.000
XLOC_026890	indole-3-pyruvate monooxygenase YUCCA3-like	25	0	3.51	0.000
XLOC_015523	root cap/late embryogenesis-like protein	379	30	3.50	0.000
XLOC_044764	auxin canalization protein	265	21	3.38	0.000
XLOC_032612	auxin efflux carrier component 2 (PIN2)	169	11	3.32	0.000
XLOC_052706	indole-3-pyruvate monooxygenase YUCCA3-like	22	0	3.24	0.000
XLOC_045445	omega-hydroxypalmitate O-feruloyl transferase	21	0	3.23	0.000
XLOC_013316	auxin transporter-like protein 3-like (LAX3-like)	250	22	3.09	0.000
XLOC_006213	indole-3-pyruvate monooxygenase YUCCA8-like	178	19	3.00	0.000
XLOC_028584	root cap/late embryogenesis-like protein	386	5	2.96	0.001
XLOC_047158	Ole e 1 allergen	28	2	2.87	0.000
XLOC_014221	auxin efflux carrier family protein	56	3	2.72	0.001
XLOC_039651	protein SOMBRERO-like	52	5	2.71	0.000
XLOC_033495	protein LATERAL ROOT PRIMORDIUM 1-like (LRP1-like)	247	27	2.67	0.000
XLOC_034540	ABC transporter B family member 19 (ABCB19)	708	75	2.54	0.001
XLOC_043383	auxin efflux carrier component 2 (PIN2)	154	4	2.49	0.006

XLOC_034400	auxin canalization protein	212	35	2.47	0.000
6 DAI					
XLOC_049982	ABC transporter B family member 15 (ABCB15)	232	11	1.83	0.009
XLOC_049446	indole-3-pyruvate monooxygenase YUCCA8-like	148	6	1.59	0.025
9 DAI					
XLOC_049446	indole-3-pyruvate monooxygenase YUCCA8-like	106	8	2.75	0.000
XLOC_030634	root cap/late embryogenesis-like protein	42	2	2.19	0.002
XLOC_044601	DNA replication licensing factor MCM2	104	16	2.12	0.000
XLOC_040767	protein LATERAL ROOT PRIMORDIUM 1-like (LRP1-like)	36	1	2.10	0.004
XLOC_028585	root cap/late embryogenesis-like protein	60	5	2.08	0.002
XLOC_017064	DNA replication licensing factor MCM2	128	20	1.80	0.002
XLOC_028584	root cap/late embryogenesis-like protein	37	4	1.80	0.022
XLOC_034540	ABC transporter B family member 19 (ABCB19)	157	28	1.73	0.002
XLOC_033495	protein LATERAL ROOT PRIMORDIUM 1-like (LRP1-like)	152	24	1.62	0.029
XLOC_036086	root phototropism protein 3-like/NPH3 family protein	73	15	1.60	0.025
XLOC_015523	root cap/late embryogenesis-like protein	100	18	1.55	0.028
XLOC_044764	auxin canalization protein	51	10	1.52	0.034
XLOC_049627	protein TRANSPORT INHIBITOR RESPONSE 1 (TIR1)	122	41	1.41	0.002
XLOC_006004	auxin efflux carrier component 1c (PIN1C)	219	79	1.27	0.002
XLOC_035579	ANR1-like MADS-box transcription factor	356	147	1.06	0.022
XLOC_006291	triosephosphate isomerase, chloroplastic	1152	493	1.06	0.034
XLOC_003104	protein TRANSPORT INHIBITOR RESPONSE 1 (TIR1)	254	133	0.87	0.042
XLOC_047513	fasciclin-like arabinogalactan protein 1	508	283	0.77	0.034
12 DAI					
XLOC_032612	auxin efflux carrier component 2 (PIN2)	54	0	2.59	0.000
XLOC_044764	auxin canalization protein	60	7	2.03	0.001
XLOC_050007	ABC transporter B family member 19 (ABCB19)	280	63	1.61	0.002
XLOC_044601	DNA replication licensing factor MCM2	175	45	1.57	0.003

XLOC_015523	root cap/late embryogenesis-like protein	80	8	1.50	0.043
XLOC_034540	ABC transporter B family member 19 (ABCB19)	105	21	1.47	0.035
XLOC_025882	auxin down-regulated protein	8222	2261	1.47	0.001
XLOC_017064	DNA replication licensing factor MCM2	211	59	1.45	0.006
XLOC_049236	auxin efflux carrier component 1c (PIN1C)	153	58	1.19	0.022
XLOC_013477	LRR family receptor-like protein kinase	259	99	1.17	0.023
XLOC_024408	protein TORNADO 2 (TRN2)	213	90	1.08	0.033

Table 2.4. Mean normalized read counts, log2(fold change) estimates, and FDR-adjusted *P*-values associated with genes whose expression was significantly lower in inoculated than control roots at 3, 6, 9, and 12 days after inoculation (DAI). For 3 DAI, the top twenty down-regulated genes are shown, ranked by log2(fold change) estimate. For other dates, all down-regulated genes are shown.

Gene ID	Description	Mean Normalized Counts			
		Inoculated	Control	log2FC estimate	FDR-adjusted P-value
3 DAI					
XLOC_011675	LOB domain protein	3	34	-2.56	0.001
XLOC_031029	metallothionein 3	893	4768	-2.43	0.000
XLOC_037896	indole-3-pyruvate monooxygenase YUCCA6-like	47	159	-1.68	0.000
XLOC_035765	receptor-like protein kinase HSL1	343	1066	-1.60	0.000
XLOC_003797	mTERF family protein	9	30	-1.48	0.035
XLOC_019118	shaggy-related protein kinase eta	11	36	-1.46	0.041
XLOC_052443	auxin efflux carrier component 3-like (PIN3-like)	109	294	-1.38	0.000
XLOC_040020	protein STRUBBELIG-receptor family 3 (SRF3)	83	214	-1.33	0.000
XLOC_037260	auxin response factor 5 (ARF5)	34	89	-1.26	0.007
XLOC_011221	protein ROOT PRIMORDIUM DEFECTIVE 1-like (RPD1-like)	33	85	-1.26	0.006
XLOC_001698	auxin transporter-like protein 2 (LAX2)	102	253	-1.23	0.001
XLOC_045928	root phototropism protein 2 (RPT2)	62	149	-1.21	0.003
XLOC_033716	protein STRUBBELIG-receptor family 3 (SRF3)	73	176	-1.20	0.001
XLOC_038079	pectin methyltransferase QUA2	703	1607	-1.18	0.000
XLOC_023645	phospholipase D P1-like (PLDZETA1)	149	319	-1.09	0.002
XLOC_015667	shaggy-related protein kinase eta	214	461	-1.09	0.001
XLOC_045617	auxin response factor 5 (ARF5)	87	190	-1.08	0.006
XLOC_002132	LON protease 2	259	554	-1.07	0.000

XLOC_038217	root phototropism protein 2 (RPT2)	1715	3589	-1.06	0.000
XLOC_042192	ATP-dependent helicase BRM	1032	2181	-1.06	0.000
6 DAI					
XLOC_001698	auxin transporter-like protein 2 (LAX2)	112	278	-1.17	0.010
XLOC_031029	metallothionein 3	614	1316	-0.99	0.010
9 DAI					
XLOC_001895	auxin efflux carrier family protein	69	191	-1.35	0.001
XLOC_031029	metallothionein 3	1001	2539	-1.29	0.000
XLOC_045928	root phototropism protein 2 (RPT2)	63	159	-1.18	0.024
XLOC_035001	adenylate kinase chloroplastic-like	208	432	-1.01	0.003
XLOC_008441	protein ROOT PRIMORDIUM DEFECTIVE 1-like (RPD1-like)	144	259	-0.80	0.042
XLOC_042422	auxin-induced in root cultures protein 12 (AIR12)	14925	22496	-0.58	0.039
12 DAI					
XLOC_035765	receptor-like protein kinase HSL1	382	844	-0.94	0.037

Figure 2.1 – Bar graphs representing mean measurements and standard errors of seven root architecture parameters from control and infected sides of split-root plants across four dates. P-values are given in the top left corner of each graph for fixed effects of the REML method analysis: TREATMENT, DATE, and their interaction. Letters that differ above bars denote a significant difference in means within date (means comparison LSMean Student's t-test; $p \leq 0.05$).

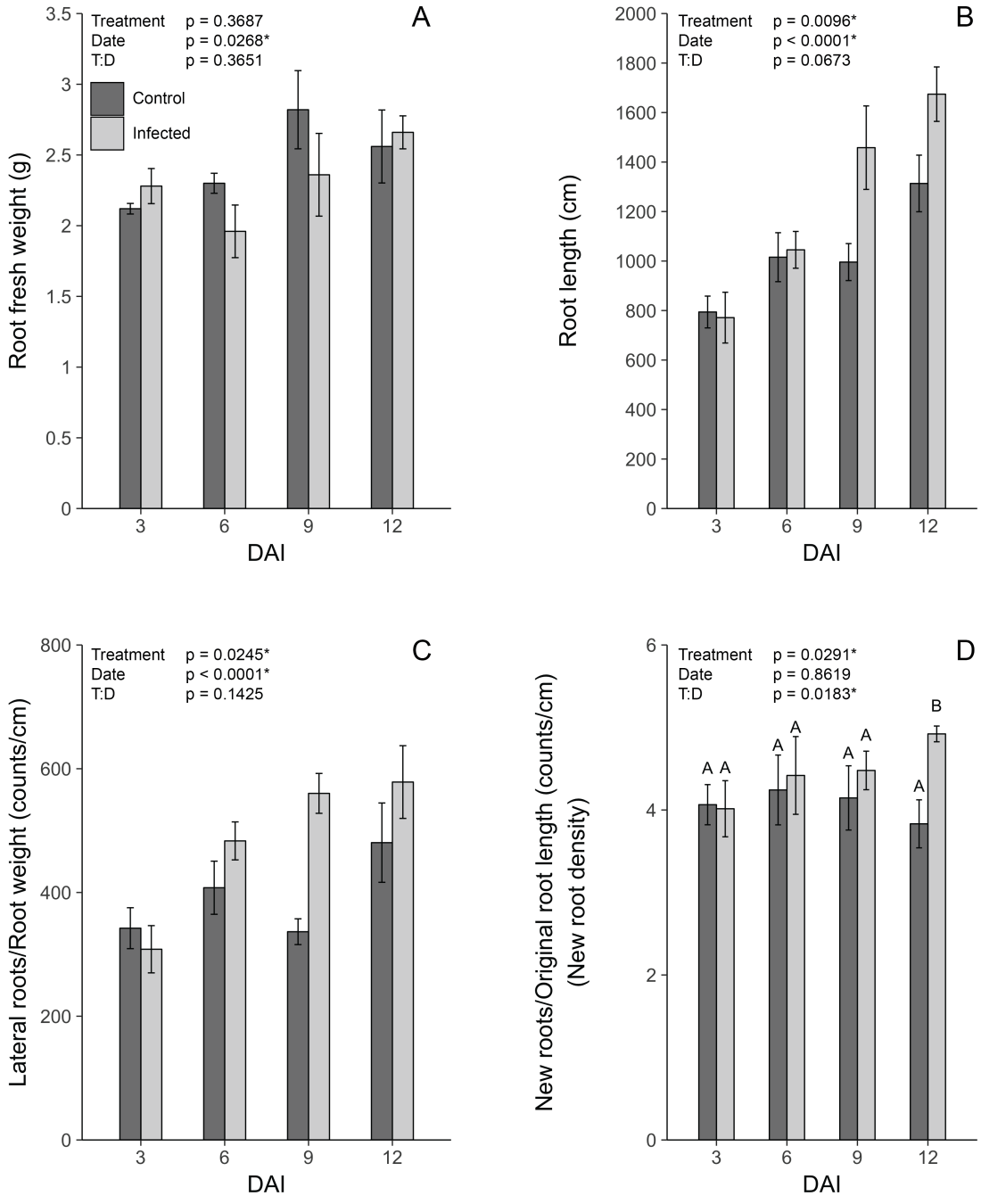

Figure 2.2 - Bar graphs representing mean measurements and standard errors of eight root architecture parameters from control and infected root systems of individual plants across four dates. P-values are given in the top left corner of each graph for fixed effects of the REML method analysis: TREATMENT, DATE, and their interaction.

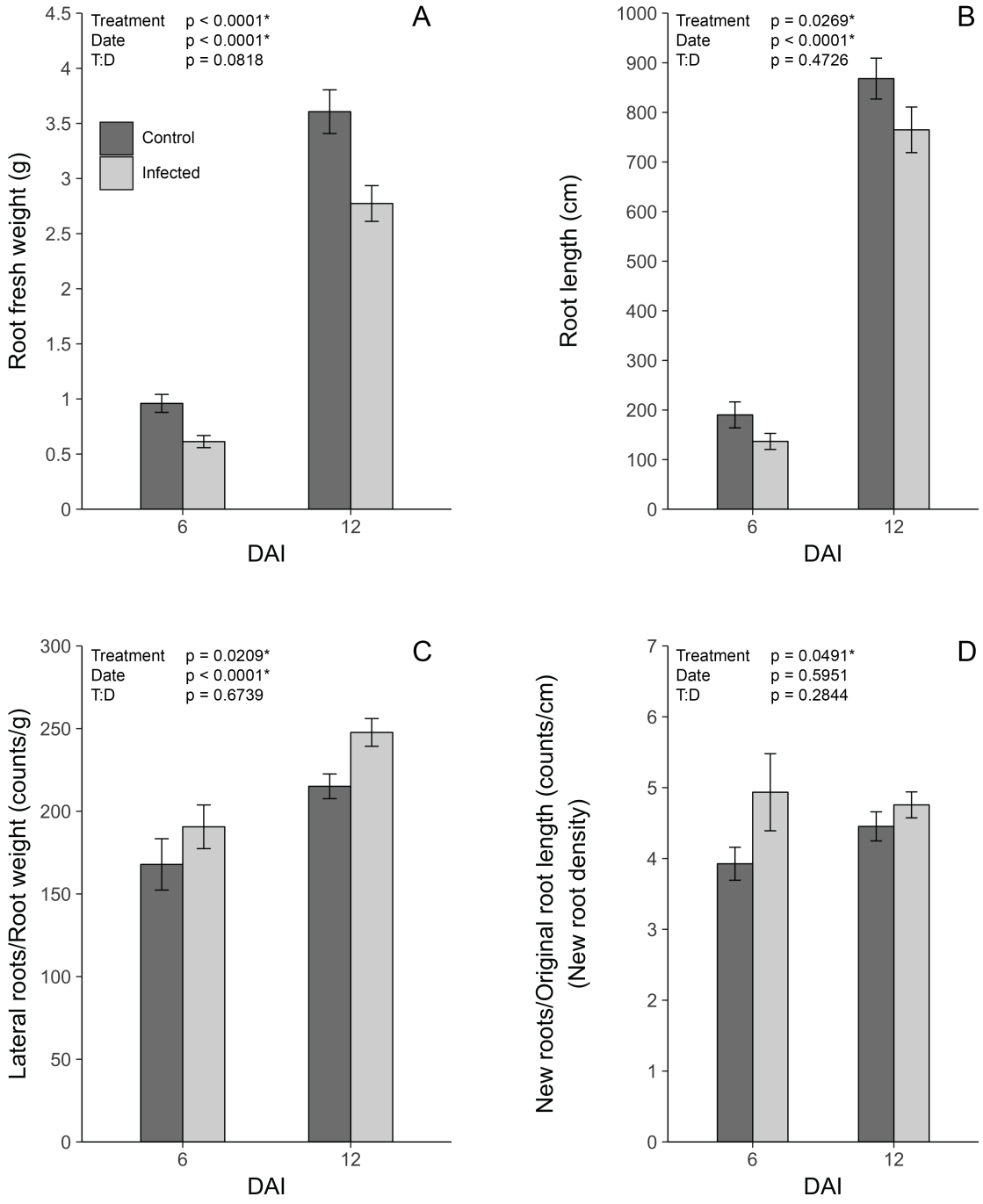

References

Agudelo, P., Robbins, R. T., Kim, K. S., and Stewart, J. M. 2005. Histological changes in *Gossypium hirsutum* associated with reduced reproduction of *Rotylenchulus reniformis*. J. Nematol. 37(2):185-189.

Anders, S., Pyl, P. T., and Huber, W. 2015. HTSeq-a python framework to work with high-throughput sequencing data. Bioinformatics 31(2):166-169.

Bardgett, R., Denton, C., and Cook, R. 1999. Below-ground herbivory promotes soil nutrient transfer and root growth in grassland. Ecol. Lett. 2(6):357-360.

Bartlem, D. G., Jones, M. G. K., and Hammes, U. Z. 2014. Vascularization and nutrient delivery at root-knot nematode feeding sites in host roots. J. Exp. Bot. 65(7):1789-1798.

Baylis, T., Cierlik, I., Sundberg, E., and Mattsson, J. 2013. SHORT INTERNODES/STYLISH genes, regulators of auxin biosynthesis, are involved in leaf vein development in *Arabidopsis thaliana*. New Phytol 197(3):737-50.

Benkova, E., Michniewicz, M., Sauer, M., Teichmann, T., Seifertova, D., Jurgens, G., and Friml, J. 2003. Local, efflux-dependent auxin gradients as a common module for plant organ formation. Cell 115(5):591-602.

Benkova, E., and Bielach, A. 2010. Lateral root organogenesis - from cell to organ. Curr. Opin. Plant Biol. 13(6):677-683.

Bennett, T., van den Toorn, A., Sanchez-Perez, G. F., Campilho, A., Willemsen, V., Snel, B., and Scheres, B. 2010. SOMBRERO, BEARSKIN1, and BEARSKIN2 regulate root cap maturation in Arabidopsis. Plant Cell 22(3):640-654.

Bolger, A. M., Lohse, M., and Usadel, B. 2014. Trimmomatic: A flexible trimmer for Illumina sequence data. Bioinformatics 30(15):2114-2120.

Cabrera, J., Diaz-Manzano, F. E., Sanchez, M., Rosso, M., Melillo, T., Goh, T., Fukaki, H., Cabello, S., Hofmann, J., Fenoll, C., and Escobar, C. 2014. A role for LATERAL ORGAN BOUNDARIES-DOMAIN 16 during the interaction *Arabidopsis-Meloidogyne spp.* provides a molecular link between lateral root and root-knot nematode feeding site development. New Phytol. 203(2):632-645.

Charrier, B., Champion, A., Henry, Y., and Kreis, M. 2002. Expression profiling of the whole *Arabidopsis* Shaggy-like kinase multigene family by real-time reverse transcriptase-polymerase chain reaction. Plant Physiol. 130(2):577-590.

Chevalier, D., Batoux, M., Fulton, L., Pfister, K., Yadav, R. K., Schellenberg, M., and Schneitz, K. 2005. *STRUBBELIG* defines a receptor kinase-mediated signaling pathway regulating organ development in Arabidopsis. PNAS 102(25):9074-9079.

Cnops, G., Wang, X., Linstead, P., Van Montagu, M., Van Lijsebettens, M., and Dolan, L. 2000. TORNADO1 and TORNADO2 are required for the specification of radial and circumferential pattern in the Arabidopsis root. Development 127(15):3385-3394.

Conesa, A., Gotz, S., Garcia-Gomez, J., Terol, J., Talon, M., and Robles, M. 2005. Blast2GO: A universal tool for annotation, visualization and analysis in functional genomics research. Bioinformatics 21(18):3674-3676.

Dharmasiri, N., Dharmasiri, S., and Estelle, M. 2005. The F-box protein TIR1 is an auxin receptor. Nature 435(7041):441-445.

Dharmasiri, S., Swarup, R., Mockaitis, K., Dharmasiri, N., Singh, S., Kowalchyk, M., Marchant, A., Mills, S., Sandberg, G., Bennett, M., and Estelle, M. 2006. AXR4 is required for localization of the auxin influx facilitator AUX1. Science 312(5777):1218-1220.

Du, Y., and Scheres, B. 2018. Lateral root formation and the multiple roles of auxin. J. Exp. Bot. 69(2):155-167.

Eves-Van den Akker, S., Lilley, C. J., Yusup, H. B., Jones, J. T., and Urwin, P. E. 2016. Functional C-TERMINALLY ENCODED PEPTIDE (CEP) plant hormone domains evolved *de novo* in plant parasite *Rotylenchulus reniformis*. Mol. Plant Pathol. 17(8):1265-1275.

Gil, P., Dewey, E., Friml, J., Zhao, Y., Snowden, K., Putterill, J., Palme, K., Estelle, M., and Chory, J. 2001. BIG: A calossin-like protein required for polar auxin transport in Arabidopsis. Genes Dev. 15(15):1985-1997.

Goto-Yamada, S., Mano, S., Nakamori, C., Kondo, M., Yamawaki, R., Kato, A., and Nishimura, M. 2014. Chaperone and protease functions of LON protease 2 modulate the peroxisomal transition and degradation with autophagy. Plant and Cell Physiol. 55(3):482-96.

Goverse, A., Overmars, H., Engelbertink, J., Schots, A., Bakker, J., and Helder, J. 2000. Both induction and morphogenesis of cyst nematode feeding cells are mediated by auxin. Mol. Plant-Microbe Interact. 13(10):1121-1129.

Grunewald, W., Cannoot, B., Friml, J., and Gheysen, G. 2009. Parasitic nematodes modulate PIN-mediated auxin transport to facilitate infection. Plos Pathogens 5(1):e1000266.

Grunewald, W., Cannoot, B., Friml, J., and Gheysen, G. 2009. Parasitic nematodes modulate PIN-mediated auxin transport to facilitate infection. Plos Pathog. 5(1):e1000266.

Grunewald, W., De Smet, I., Lewis, D. R., Loefke, C., Jansen, L., Goeminne, G., Bossche, R. V., Karimi, M., De Rybel, B., Vanholme, B., Teichmann, T., Boerjan, W., Van Montagu, M. C. E., Gheysen, G., Muday, G. K., Friml, J., and Beeckman, T. 2012. Transcription factor WRKY23 assists auxin distribution patterns during Arabidopsis root development through local control on flavonol biosynthesis. Proc. Natl. Acad. Sci. USA 109(5):1554-1559.

Guo, W., Bundithya, W., and Goldsbrough, P. 2003. Characterization of the Arabidopsis metallothionein gene family: Tissue-specific expression and induction during senescence and in response to copper. New Phytol. 159(2):369-381.

Haase, S., Ruess, L., Neumann, G., Marhan, S., and Kandeler, E. 2007. Low-level herbivory by root-knot nematodes (*Meloidogyne incognita*) modifies root hair morphology and rhizodeposition in host plants (*Hordeum vulgare*). Plant Soil 301(1-2):151-164.

Heald, C., and Robinson, A. 1990. Survey of current distribution of *Rotylenchulus reniformis* in the United States. J. Nematol. 22(4):695-699.

Helariutta, Y., Fukaki, H., Wysocka-Diller, J., Nakajima, K., Jung, J., Sena, G., Hauser, M., and Benfey, P. 2000. The SHORT-ROOT gene controls radial patterning of the Arabidopsis root through radial signaling. Cell 101(5):555-67.

Hewezi, T., Piya, S., Richard, G., and Rice, J. H. 2014. Spatial and temporal expression patterns of auxin response transcription factors in the syncytium induced by the beet cyst nematode *Heterodera schachtii* in Arabidopsis. Mol. Plant Pathol. 15(7):730-736.

Hou, H., Erickson, J., Meservy, J., and Schultz, E. A. 2010. FORKED1 encodes a PH domain protein that is required for PIN1 localization in developing leaf veins. Plant J. 63(6):960-973.

Hundertmark, M., and Hincha, D. K. 2008. LEA (late embryogenesis abundant) proteins and their encoding genes in *Arabidopsis thaliana*. BMC Genomics 9:118.

Imin, N., Mohd-Radzman, N. A., Ogilvie, H. A., and Djordjevic, M. A. 2013. The peptide-encoding CEP1 gene modulates lateral root and nodule numbers in *Medicago truncatula*. J. Exp. Bot. 64(17):5395-5409.

Jenkins, W. R. 1964. A rapid centrifugal-flotation technique for separating nematodes from soil. Plant Dis. Rep. 48(9):692.

Jin, S., Xu, C., Li, G., Sun, D., Li, Y., Wang, X., and Liu, S. 2017. Functional characterization of a type 2 metallothionein gene, SsMT2, from alkaline-tolerant *Suaeda salsa*. Sci. Rep. 7:17914.

Jones, M. G. K., and Dropkin, V. H. 1975. Cellular alterations induced in soybean roots by three endoparasitic nematodes. Physiol. Plant Pathol. 5(2):119-124.

Karczmarek, A., Overmars, H., Helder, J., and Goverse, A. 2004. Feeding cell development by cyst and root-knot nematodes involves a similar early, local and transient activation of a specific auxin-inducible promoter element. Mol. Plant Pathol. 5(4):343-346.

Koizumi, K., Hayashi, T., Wu, S., and Gallagher, K. L. 2012. The SHORT-ROOT protein acts as a mobile, dose-dependent signal in patterning the ground tissue. Proc. Natl. Acad. Sci. USA 109(32): 13010-13015.

Krichevsky, A., Zaltsman, A., Kozlovsky, S. V., Tian, G., and Citovsky, V. 2009. Regulation of root elongation by histone acetylation in Arabidopsis. J. Mol. Biol. 385(1):45-50.

Kuusk, S., Sohlberg, J. J., Eklund, D. M., and Sundberg, E. 2006. Functionally redundant SHI family genes regulate Arabidopsis gynoecium development in a dose-dependent manner. Plant J. 47(1):99-111.

Laskowski, M., Biller, S., Stanley, K., Kajstura, T., and Prusty, R. 2006. Expression profiling of auxin-treated Arabidopsis roots: Toward a molecular analysis of lateral root emergence. Plant and Cell Physiol. 47(6):788-792.

Lavenus, J., Goh, T., Roberts, I., Guyomarc'h, S., Lucas, M., De Smet, I., Fukaki, H., Beeckman, T., Bennett, M., and Laplaze, L. 2013. Lateral root development in Arabidopsis: Fifty shades of auxin. Trends Plant Sci. 18(8):455-463.

Lee, C., Chronis, D., Kenning, C., Peret, B., Hewezi, T., Davis, E. L., Baum, T. J., Hussey, R., Bennett, M., and Mitchum, M. G. 2011. The novel cyst nematode effector protein 19C07 interacts with the Arabidopsis auxin influx transporter LAX3 to control feeding site development. Plant Physiol. 155(2):866-880.

Lee, H. W., Cho, C., and Kim, J. 2015. Lateral organ boundaries Domain16 and 18 act downstream of the AUXIN1 and LIKE-AUXIN3 auxin influx carriers to control lateral root development in Arabidopsis. Plant Physiol. 168(4):1792-U1177.

Li, J., and Nam, K. H. 2002. Regulation of brassinosteroid signaling by a GSK3/SHAGGY-like kinase. Science 295(5558):1299-1301.

Lingard, M. J., and Bartel, B. 2009. Arabidopsis LON2 is necessary for peroxisomal function and sustained matrix protein import. Plant Physiol. 151(3):1354-1365.

Lopez-Bucio, J., Hernandez-Abreu, E., Sanchez-Calderon, L., Perez-Torres, A., Rampey, R., Bartel, B., and Herrera-Estrella, L. 2005. An auxin transport independent pathway is involved in phosphate stress-induced root architectural alterations in Arabidopsis. Identification of BIG as a mediator of auxin in pericycle cell activation. Plant Physiol. 137(2):681-691.

Love, M. I., Huber, W., and Anders, S. 2014. Moderated estimation of fold change and dispersion for RNA-seq data with DESeq2. Genome Biol. 15(12):550.

Mathesius, U. 2003. Conservation and divergence of signalling pathways between roots and soil microbes - the rhizobium-legume symbiosis compared to the development of lateral roots, mycorrhizal interactions and nematode-induced galls. Plant Soil 255(1):105-119.

Mazarei, M., Lennon, K., Puthoff, D., Rodermel, S., and Baum, T. 2003. Expression of an Arabidopsis phosphoglycerate mutase homologue is localized to apical meristems, regulated by hormones, and induced by sedentary plant-parasitic nematodes. Plant Mol. Biol. 53(4):513-530.

Ng, J. L. P., Perrine-Walker, F., Wasson, A. P., and Mathesius, U. 2015. The control of auxin transport in parasitic and symbiotic root–microbe interactions. Plants 4(3):606-643.

Peret, B., De Rybel, B., Casimiro, I., Benkova, E., Swarup, R., Laplaze, L., Beeckman, T., and Bennett, M. J. 2009. Arabidopsis lateral root development: An emerging story. Trends Plant Sci 14(7):399-408.

Peret, B., Middleton, A. M., French, A. P., Larrieu, A., Bishopp, A., Njo, M., Wells, D. M., Porco, S., Mellor, N., Band, L. R., Casimiro, I., Kleine-Vehn, J., Vanneste, S., Sairanen, I., Mallet, R., Sandberg, G., Ljung, K., Beeckman, T., Benkova, E., Friml, J., Kramer, E., King, J. R., De Smet, I., Pridmore, T., Owen, M., and Bennett, M. J. 2013. Sequential induction of auxin efflux and influx carriers regulates lateral root emergence. Mol. Syst. Biol. 9:699.

Petricka, J. J., Winter, C. M., and Benfey, P. N. 2012. Control of Arabidopsis root development. Annu. Rev. of Plant Biol. 63:563-590.

Preger, V., Tango, N., Marchand, C., Lemaire, S. D., Carbonera, D., Di Valentin, M., Costa, A., Pupillo, P., and Trost, P. 2009. Auxin-responsive genes AIR12 code for a new family of plasma membrane b-type cytochromes specific to flowering plants. Plant Physiol. 150(2):606-620.

Rebois, R. V., Madden, P. A., and Eldridge, B. J. 1975. Some ultrastructural changes induced in resistant and susceptible soybean roots following infection by *Rotylenchulus reniformis*. J. Nematol. 7(2):122-139.

Rebois, R. V. 1980. Ultrastructure of a feeding peg and tube associated with *Rotylenchulus reniformis* in cotton. Nematologica 26(4):396-405.

Redding, N. W., Agudelo, P., and Wells, C. E. 2018. Multiple nodulation genes are up-regulated during establishment of reniform nematode feeding sites in soybean. Phytopathology 108(2):275-291.

Robinson, A. F., Inserra, R. N., Caswell-Chen, E. P., Vovlas, N., and Troccoli, A. 1997. *Rotylenchulus* species: Identification, distribution, host ranges, and crop plant resistance. Nematropica 27(2):127-180.

Sakai, T., and Haga, K. 2012. Molecular genetic analysis of phototropism in Arabidopsis. Plant and Cell Physiol. 53(9):1517-34.

Schlicht, M., Ludwig-Mueller, J., Burbach, C., Volkmann, D., and Baluska, F. 2013. Indole-3-butyric acid induces lateral root formation via peroxisome-derived indole-3-acetic acid and nitric oxide. New Phytol. 200(2):473-482.

Schneider, C. A., Rasband, W. S., and Eliceiri, K. W. 2012. NIH image to ImageJ: 25 years of image analysis. Nat. Methods 9(7):671-675.

Smeds, L., and Kunstner, A. 2011. CONDETRI - A content dependent read trimmer for Illumina data. Plos One 6(10):e26314.

Smith, D., and Fedoroff, N. 1995. LRP1, a gene expressed in lateral and adventitious root primordia of Arabidopsis. Plant Cell 7(6):735-745.

Stepanova, A. N., Robertson-Hoyt, J., Yun, J., Benavente, L. M., Xie, D., Dolezal, K., Schlereth, A., Juergens, G., and Alonso, J. M. 2008. TAA1-mediated auxin biosynthesis is essential for hormone crosstalk and plant development. Cell 133(1):177-191.

Tapia-Lopez, R., Garcia-Ponce, B., Dubrovsky, J. G., Garay-Arroyo, A., Perez-Ruiz, R. V., Kim, S., Acevedo, F., Pelaz, S., and Alvarez-Buylla, E. R. 2008. An AGAMOUS-related MADS-box gene, XAL1 (AGL12), regulates root meristem cell proliferation and flowering transition in Arabidopsis. Plant Physiol. 146(3):1182-1192.

Trapnell, C., Roberts, A., Goff, L., Pertea, G., Kim, D., Kelley, D. R., Pimentel, H., Salzberg, S. L., Rinn, J. L., and Pachter, L. 2012. Differential gene and transcript expression analysis of RNA-seq experiments with TopHat and cufflinks. Nat. Protoc. 7(3):562-578.

Treonis, A. M., Cook, R., Dawson, L., Grayston, S. J., and Mizen, T. 2007. Effects of a plant parasitic nematode (*Heterodera trifolii*) on clover roots and soil microbial communities. Biol Fertility Soils 43(5):541-548.

Ueda, M., Matsui, K., Ishiguro, S., Kato, T., Tabata, S., Kobayashi, M., Seki, M., Shinozaki, K., and Okada, K. 2011. Arabidopsis RPT2a encoding the 26S proteasome subunit is required for various aspects of root meristem maintenance, and regulates gametogenesis redundantly with its homolog, RPT2b. Plant and Cell Physiol. 52(9):1628-1640.

Vilches-Barro, A., and Maizel, A. 2015. Talking through walls: Mechanisms of lateral root emergence in *Arabidopsis thaliana*. Curr. Opin. Plant Biol. 23:31-38.

Wan, Y., Jasik, J., Wang, L., Hao, H., Volkmann, D., Menzel, D., Mancuso, S., Baluska, F., and Lin, J. 2012. The signal transducer NPH3 integrates the Phototropin1 photosensor with PIN2-based polar auxin transport in Arabidopsis root phototropism. Plant Cell 24(2):551-565.

Wasson, A. P., Ramsay, K., Jones, M. G. K., and Mathesius, U. 2009. Differing requirements for flavonoids during the formation of lateral roots, nodules and root knot nematode galls in *Medicago truncatula*. New Phytol. 183(1):167-179.

Won, C., Shen, X., Mashiguchi, K., Zheng, Z., Dai, X., Cheng, Y., Kasahara, H., Kamiya, Y., Chory, J., and Zhao, Y. 2011. Conversion of tryptophan to indole-3-acetic acid by TRYPTOPHAN AMINOTRANSFERASES OF ARABIDOPSIS and YUCCAs in Arabidopsis. Proc. Natl. Acad. Sci. USA 108(45):18518-18523.

Wu, G., Lewis, D. R., and Spalding, E. P. 2007. Mutations in Arabidopsis multidrug resistance-like ABC transporters separate the roles of acropetal and basipetal auxin transport in lateral root development. Plant Cell 19(6):1826-1837.

Wubben, M. J., Gavilano, L., Baum, T. J., and Davis, E. L. 2015. Sequence and spatiotemporal expression analysis of CLE-motif containing genes from the reniform nematode (*Rotylenchulus reniformis* Linford & Oliveira). J. Nematol. 47(2):159-165.

Xue, T., Li, X., Zhu, W., Wu, C., Yang, G., and Zheng, C. 2009. Cotton metallothionein GhMT3a, a reactive oxygen species scavenger, increased tolerance against abiotic stress in transgenic tobacco and yeast. J. Exp. Bot. 60(1):339-349.

Yamaguchi, N., Huang, J., Xu, Y., Tanoi, K., and Ito, T. 2017. Fine-tuning of auxin homeostasis governs the transition from floral stem cell maintenance to gynoecium formation. Nat. Commun. 8:1125.

Yang, H., and Murphy, A. S. 2009. Functional expression and characterization of Arabidopsis ABCB, AUX 1 and PIN auxin transporters in *Schizosaccharomyces pombe*. Plant J. 59(1):179-191.

Yu, L., Miao, Z., Qi, G., Wu, J., Cai, X., Mao, J., and Xiang, C. 2014. MADS-box transcription factor AGL21 regulates lateral root development and responds to multiple external and physiological signals. Mol. Plant 7(11):1653-1669.

Yuan, J., Chen, D., Ren, Y., Zhang, X., and Zhao, J. 2008. Characteristic and expression analysis of a metallothionein gene, OsMT2b, down-regulated by cytokinin suggests functions in root development and seed embryo germination of rice. Plant Physiol. 146(4):1637-1650.

Zazimalova, E., Murphy, A. S., Yang, H., Hoyerova, K., and Hosek, P. 2010. Auxin transporters - Why so many? Cold Spring Harb. Perspect. Biol. 2(3):a001552.

Zhang, H., and Forde, B. G. 2000. Regulation of Arabidopsis root development by nitrate availability. J. Exp. Bot. 51(342):51-59.

Zhao, Y., Christensen, S., Fankhauser, C., Cashman, J., Cohen, J., Weigel, D., and Chory, J. 2001. A role for flavin monooxygenase-like enzymes in auxin biosynthesis. Science 291(5502):306-309.

CHAPTER THREE

IDENTIFICATION OF PUTATIVE EFFECTORS FROM RENIFORM NEMATODE IN SOYBEAN AND COTTON

INTRODUCTION

Reniform nematode, *Rotylenchulus reniformis* (Linford and Oliveira), is a sedentary semi-endoparasite that infects a broad range of host species from 77 different plant families. *R. reniformis* is found in tropical, subtropical, and warm-temperate regions, worldwide. In the United States, it infects economically important plants including soybean (*Glycine max*), upland cotton (*Gossypium hirsutum*), pineapple (*Ananas comosus*), and sweet potato (*Ipomoea batatas*) (Heald and Robinson 1990; Robinson et al. 1997). Yield losses to upland cotton in the southeastern US are especially dramatic, costing more than $100 million dollars annually (Blasingame and Patel 2012; Robinson 2007).

During infection, the female reniform nematode (RN) establishes a permanent feeding structure called a syncytium, the ultrastructure of which has been well characterized (Agudelo et al. 2005; Jones and Dropkin 1975; Rebois 1980; Rebois et al. 1975). Following penetration of the root by the nematode, cells of the pericycle undergo dissolution of cell wall partitions and fuse together, forming a network of continuous cytoplasm. Within the mass, central vacuoles of individual cells are disassembled, endoplasmic reticula increase in surface area, nuclei become enlarged, and ribosomes, mitochondria, plastids, and small vacuoles increase in number. Taken together, the morphological changes reflect high metabolic activity and correspond with dramatic

changes in local gene expression in the host (Agudelo et al. 2005; Rebois et al. 1975; Redding et al. 2018).

Despite the thoroughly documented morphological changes induced by reniform nematode infection, there remains much to learn regarding the molecular mechanisms by which the parasite initiates and maintains its feeding site. Work on better-studied plant-parasitic nematodes has revealed that a wide variety of nematode-derived proteins play a role in feeding site formation (Mitchum et al. 2013). The majority have been identified from nematode esophageal glands where these "effectors" are produced before being secreted from the feeding stylet into the host cell or apoplasm (Davis et al. 2008; Gheysen and Mitchum 2011).

The first plant parasitic effectors identified were cellulases produced by the potato cyst nematode (*Globodera rostochiensis*) (Smant et al. 1998). Since that time, pectate lyases, expansins, hemicellulases, and xylanases have been identified as effectors in several cyst and root-knot nematode species, where they are thought to aid in migration through root tissue (Wieczorek 2015). In addition, both groups produce effectors that mimic plant-derived CLE (CLAVATA3/ESR) signaling peptides, and root-knot nematodes have also been shown to produce C-terminally encoded peptides (CEPs) (Bird et al. 2015; Mitchum et al. 2012; Ohyama et al. 2008). Still other effectors are believed to suppress plant defenses (Mantelin et al. 2015).

Initial work on reniform nematode effectors has focused on expressed sequence tag (EST) data from sedentary female nematodes on cotton roots. Early studies revealed significant sequence homology between reniform nematode and cyst nematode effectors

and led to the identification of a reniform nematode cellulase, numerous C-type lectins (CTLs), and three CLE peptides (Ganji et al. 2014; Wubben et al. 2015; Wubben et al. 2010a; Wubben et al. 2010b). Additionally, an RNAseq study of reniform nematodes on cotton found that a family of reniform nematode CEP transcripts may act as plant peptide mimics (Eves-Van den Akker et al. 2016). With this exception, no RNAseq work has been published on reniform nematode.

Here we report the isolation of reniform nematode transcripts from *de novo* transcriptome assemblies of infected soybean and cotton root tissue. We highlight reniform nematode genes that are highly expressed in parasitized root tissue across a twelve-day time course, and we identify putative effector proteins based on sequence homology to known effectors. Results show a dramatic shift in effector gene expression late in infection that corresponds with reproduction. We also identify homologs of many parasitism genes that are known from cyst and root-knot nematodes, including cell wall modify enzymes, immune suppressors, ROS detoxifying agents, and signaling molecules.

MATERIALS AND METHODS

Split-root growth system and nematode inoculation

Cotton and soybean experiments were run sequentially using the following growth conditions. Seeds of reniform nematode-susceptible soybean (*Glycine max* cv. 'Hutcheson') or upland cotton (*Gossypium hirsutum* cv. 'Deltapine 50') were surface sterilized and germinated in a growth room at 28 ± 2°C and 50% relative humidity (RH) with a 14-h/10-h (light/dark) photoperiod (Redding et al. 2018). After cotyledon emergence, a horizontal cut was made at the base of the primary root on each plant to promote lateral root proliferation. After one week, primary lateral roots were grouped into two equal bundles, inserted through the arms of a Y-shaped plastic tube, and directed into adjacent 300 cm^3 pots filled with pasteurized fine sand. Plants were grown for one week, and twelve uniform seedlings were selected for use in the experiment.

Reniform nematode inoculum was prepared from soil collected at an infested cotton field in St. Matthews, SC. Vermiform nematodes were extracted by sugar centrifugal flotation, rinsed, and collected in a 500μm mesh sieve (Jenkins 1964). Following inspection and quantification, nematodes were suspended in tap water at a concentration of 1500 individuals/ml. One side in each split-root system was selected at random and inoculated with 2ml of the nematode suspension (3,000 individuals); the other side received an equivalent volume of tap water as a negative control.

Plants were grown for up to 12 days after inoculation. Three replicates of each system were harvested at 3, 6, 9, and 12 days after inoculation (DAI) as described below.

Transcriptome sequencing

Approximately 500 mg fresh weight (FW) of infected and control root tissue was harvested from each of three replicate soybean and cotton plants at 3, 6, 9, and 12 days after reniform nematode inoculation (DAI), for a total of 48 samples: 2 hosts x 2 infection statuses x 4 dates x 3 biological replicates (Redding et al. 2018). Tissue was stored in RNA*later*® Stabilization Reagent (Ambion, Austin, TX) and sequenced at the University of Arizona Genetics Core (Tucson, AZ). RNA was extracted using the Qiagen RNAeasy Mini Kit, and RNA quality was assessed with the Agilent 2100 Bioanalyzer prior to 100-bp paired-end library preparation with the Illumina TruSeq 2 RNA kit. Samples were sequenced on the Illumina HiSeq 2000 platform (Illumina, San Diego, CA), soybean samples across two lanes and cotton across three.

Over 619 million paired-end 100-bp reads were generated from soybean roots (average of 25.8 million reads per sample). Over 593 million paired-end reads were generated from cotton roots (average of 24.7 million reads per sample). Read quality was assessed with FastQC v0.10.1, sequencing adaptors were trimmed with Trimmomatic v0.32 (Bolger et al. 2014), and low-quality bases were removed using the default settings of ConDeTri v2.2 (Smeds and Kunstner 2011). Average per-read PHRED quality score after trimming was 36.84 (minimum 36.02) for soybean-derived reads and 36.44 (minimum 36.14) for cotton-derived reads. Raw soybean and cotton reads were uploaded to the NCBI Sequence Read Archive under accession numbers SRP091708 and SRP050874, respectively.

Transcriptome Assembly and Annotation

Trimmed reads were used to create *de novo* transcriptome assemblies from soybean and cotton roots via the Trinity v2.4.0 pipeline with default parameters (Haas et al. 2013). Assembled transcripts were filtered based on the size and presence of a predicted open reading frame (ORF) using TransDecoder; transcripts with no ORFs or with ORFs shorter than 100 amino acids were removed. Transcripts were annotated in Blast2GO Pro v3.0, which performed a BLASTx search against the NCBI nr protein database and assigned sequence descriptions, top BLAST hit species, gene ontology (GO) terms, Interpro IDs, enzyme codes (EC), and KEGG pathways to transcripts with significant BLAST hits ($E < 10^{-6}$) (Conesa et al. 2005). Gene expression was quantified by mapping reads from individual samples back to their associated transcriptome using RSEM 1.3.0 with default parameters (Li and Dewey 2011). For genes with multiple isoforms, read counts for all isoforms were pooled for expression quantification. Genes were filtered by expression level, removing those with fewer than 10 FPKM when summed across all 24 samples.

The complete transcriptomes contained both plant-derived and nematode-derived transcripts. Nematode genes were identified and separated from host plant transcripts based on two criteria: (1) their top BLASTx hit was a nematode, and (2) they were consistently present in infected samples and absent in uninfected samples. These genes were considered to represent the nematode protein-coding transcriptome.

Identification of Putative Effectors

Amino acid sequences of root-knot and cyst nematode effectors, as well as published sequences for a small number of previously-identified reniform nematode effectors, were downloaded from NCBI (Ganji et al. 2014; Gardner et al. 2015; Truong et al. 2015; Wubben et al. 2015; Wubben et al. 2010b). The resulting protein sequence files were used to perform a tBLASTn search against custom BLAST databases constructed from the soybean and cotton nematode transcriptomes ($E < 10^{-6}$ cut-off). Hits from each host were compared to identify effector genes common to both transcriptomes. The presence of a signal peptide in each putative effector was assessed with SignalP v4.1 using the sensitive cut-off setting (Nielsen 2017).

RESULTS

Transcriptome assembly and identification of nematode genes

Forty-eight RNA samples (24 per host) from infected and control root systems of soybean and cotton plants were sequenced, generating over 619 and 593 million 100-bp reads, respectively. Trimmed and quality-filtered reads were combined from all soybean or cotton root samples to create two *de novo* protein-coding transcriptomes as described above. Assembled transcripts were filtered based on the size and presence of a predicted open reading frame (ORF) using TransDecoder. The soybean-derived transcriptome that resulted was comprised of 86,419 genes and 116,269 alternative splice forms of these genes, with an average transcript length of 1,467 bp and an N50 of 2,014 bp. The full cotton-derived assembly contained 170,138 genes and 299,779 alternative splice forms of these genes, with an average transcript length of 1,152 bp and an N50 of 1,749 bp.

The assembled transcriptomes contained genes from both host plants and reniform nematodes, as well as genes from associated components of the rhizosphere such as bacteria and fungi. Nematode genes were identified based on their top BLAST hits and their absence in uninoculated samples. After filtering low expressed-genes, a total of 3,485 reniform nematode (RN) protein-coding genes were identified from soybean roots, with 3,689 alternate splice forms, an average length of 1,254 bp, and an N50 of 1,515 bp. Likewise, a total of 4,852 RN protein-coding genes were identified in cotton roots, with 4,424 alternate splice forms, an average length of 720 bp, and an N50 of 810 bp. The FASTA sequences of all assembled nematode transcripts from both hosts are provided as Supplementary Files 3.1 and 3.2.

Characterization of assembled nematode genes

Most assembled RN genes had a gene from a parasitic nematode as their top BLAST hit (Fig. 1). While majority of top BLAST hits were to extensively-studied animal parasites, 116 genes from RN on soybean and 316 from RN on cotton had a plant-parasitic nematode as their top BLAST hit. The soybean cyst nematode (*Heterodera glycines*) was among the top plant-parasitic nematode BLAST hits for RN on both hosts. Several genes also had top BLAST hits to free-living nematodes, including 90 genes (soybean) and 123 genes (cotton) whose top blast hit was a *Caenorhabditis elegans* protein.

Ninety-three percent and 94% of RN genes from soybean and cotton received at least one GO term in the annotation pipeline. Among the most common GO terms were those involving nematode development and reproduction: "embryo development ending in birth or egg hatching," "nematode larval development," "P granule," and "germ plasm." Many additional GO annotations related to transcription and translation: nucleoside and nucleotide metabolism, DNA template transcription, RNA biosynthesis and modification, translation, and peptide biosynthesis. Common Cellular Component GOs were associated with ribosomes, the cytoskeleton, musculature, and vesicles, while common Biological Processes GOs were associated with protein modification and phosphorylation. The full Blast2GO transcriptome annotations are provided in Supplementary Files 3.3 and 3.4.

Tables 1 and 2 show the top twenty assembled nematode genes on each sampling date from each host species, ranked by expression level (fragments per kilobase of exon

model, FPKM). The magnitude of RN gene expression broadly increased with time, likely reflecting the growth and reproduction of nematodes in their host roots. The composition of the top expressed gene sets also changed over time. In soybean, ribosomal proteins constituted 75% of the most highly expressed nematode genes at 3 DAI and more than half of the most highly expressed genes at 6 DAI. Genes for nematode cuticular collagen proteins were also abundant on these dates. Later infection was dominated by the expression of genes encoding vitellogenin, a nematode yolk protein whose expression was likely associated with egg development in the maturing female nematodes. Similar trends were observed in RN genes from cotton. Genes for ribosomal proteins and translation elongation factors comprised half of the top expressed genes at 3 DAI, and genes involved in cuticle formation were also prevalent. Numerous vitellogenins were highly expressed at 9 and 12 DAI.

Putative effector identification

A set of published effector sequences from cyst, root-knot, and reniform nematodes was blasted against the assembled reniform transcriptomes to identify putative RN effectors. Results of both blast searches are provided in Supplementary file 3.5. One hundred two putative effectors were identified, including 11 that were common to both the soybean- and cotton-derived transcriptomes. Of the putative effectors, 46% had the highest homology to a cyst nematode effector, 34% to a root-knot nematode effector, and 20% to a previously-described reniform nematode effector.

Among these putative effectors were cell wall modifying enzymes, signaling molecules, and host defense suppressors, as well as secreted nematode proteins of unknown or poorly-characterized function (Fig. 4 - 6). In general, the expression of putative effectors was highest later in infection, particularly at 9 DAI. Notable exceptions included cell wall modifiers and a fatty acid and retinol binding protein (FAR), which were most highly expressed at 3 DAI. Overall, the most highly expressed putative effector was a C-type lectin (CTL), expressed at 1723 FPKM on 9 DAI.

Protein analysis via SignalP v4.1 revealed the 37% of the putative effectors had recognized signal peptide cleavage sites, supporting their role in nematode secretion (Suppl 3.5 and 3.6). Among these included many putative secretory proteins of unknown or poorly understood function, CLEs, CTLs, FARs, VAPs, and a few cell wall modifiers.

Genes previously identified in reniform nematodes

Previous studies have characterized a handful of RN genes, including three CLEs and a number of C-type lectins (Ganji et al. 2014; Wubben et al. 2015). CLE-like peptides are thought to promote feeding site formation by mimicking plant peptide hormones. We assembled four CLE-like peptides, two from RNs on soybean and two from RNs on cotton, all of which contained a signal peptide cleavage site (Figure 4; Suppl 3.5 and 3.6). While they were clearly homologous to known RN CLEs, they were not identical, suggesting that RN possesses a suite of CLE peptides. We also assembled eight RN CTL genes, all of which were expressed at very high levels relative to other putative effectors. CTLs are part of the innate immune response in many organisms

(Weis et al. 1998). Their exact function in plant parasitic nematode is still being uncovered. Evidence from different nematodes indicates that CTLs may act as potential effectors or play a role in nematode defense (Ganji et al. 2014; Haegeman 2013). It is possible that different classes of CTLs carry out these varying functions.

Cell wall modifiers

Multiple RN genes were homologous to previously-identified cell wall modifiers from other parasitic nematodes, including cellulases, pectate lyases, expansins, and expansin-like proteins; interestingly, these genes were only assembled in cotton roots (Fig. 5). The cell wall modifying genes generally exhibited their highest expression at 3 DAI, in contrast to other putative effectors whose expression was highest at 9 and 12 DAI.

Defense suppressors

A variety of defense suppressors have been described in other nematode pathosystems: some disrupt the plant's innate immune response, while others allow the pathogen to detoxify plant-derived reactive oxygen species (ROS). Calreticulins (CRT), FARs, SP1a and Ryanodine receptors (SPRY), ubiquitin extension proteins (UBI), and venom allergen-like (VAP) genes have all been shown to act as immune suppressors in other plant parasitic nematode systems (Chronis et al. 2013; Iberkleid et al. 2013; Jaouannet et al. 2013; Lozano-Torres 2012; Sacco et al. 2009). Three calreticulins, eight FARs, one SPRY19, one UBI-1 and seven VAP1 proteins were represented among the

putative RN effectors, and most were highly expressed only in the later stages of parasitism (Fig. 6).

Detoxification proteins include free radical scavengers like glutathione S-transferase, glutathione peroxidases, and peroxiredoxins. Nine glutathione S-transferases, six glutathione peroxidases, and a peroxiredoxin were identified among the putative RN effector genes (Fig. 6). Other genes, such as the five assembled RN annexins, may indirectly regulate detoxification. Multiple detoxification genes were expressed at high levels at 3 DAI, suggesting that detoxification and free radical scavenging is required throughout the infection process.

DISCUSSION

During the reniform nematode life cycle, first stage juveniles (J1s) develop inside eggs where they undergo one molt before emerging into the soil as J2s. Vermiform juveniles molt three times before developing into immature males and females (Robinson et al 1997). The immature female is the infective stage. She forcibly penetrates the host root before establishing a permanent syncytium composed predominantly of pericycle cells (Agudelo et al. 2005, Rebios et al. 1975). Once the feeding site is established, the nematode becomes sedentary and begins to mature and enlarge, taking on a kidney or reniform shape. Following fertilization, each female produces 60 to 200 highly nutritive eggs in a gelatinous matrix (Sivakumar and Seshadri 1971). Only the female nematodes of the species feed. Male and juvenile nematodes retain enough nutrients from the egg to sustain them throughout their lifespan (Robinson et al. 1997).

Overall trends in gene expression during infection

Previous histological work in our lab showed that feeding site formation begins by 2 to 3 DAI and that syncytia are well established by 6 to 9 DAI (Redding et al. 2018). By 9 DAI, female nematodes have grown dramatically and assumed a reniform shape; by 12 DAI, the first eggs can be observed in egg masses (Redding et al. 2018). This timeline is corroborated by numerous studies (Agudelo et al. 2005; Jones and Dropkin 1975; Rebois 1980; Rebois et al. 1975) and provides context for observed patterns in gene expression.

The lowest levels of reniform nematode gene expression in soybean were detected at 3 DAI, when the most highly expressed gene (encoding a collagen) was present at only 7.54 FPKM. Gene expression levels increased on subsequent dates, peaking at 9 DAI. RN genes from cotton showed a similar pattern, although the lowest expression occurred at 6 DAI rather than 3 DAI.

Top expressed genes changed markedly between early infection (3 and 6 DAI) and late infection (9 and 12 DAI). In both soybean and cotton roots, RN genes encoding ribosomal proteins and cuticular collagen genes were highly expressed early in infection. Collagens are an integral part of the nematode cuticle, giving it structure and providing protection from the environment (Davies and Curtis 2011). They have also been proposed to function in host/parasite interactions. Recent work in root-knot nematode infection of transgenic tomato plants has shown that knockdown of MiCOL-1 through RNAi leads to a reduction in the number of adult females, egg masses, and the number of eggs within egg masses (Banerjee et al. 2018). These results suggest MiCOL-1 is vital to the maturation and egg laying of female root-knot nematodes. One constitutively expressed collagen gene identified in soybean roots shared homology with MiCOL-1.

A set of potential defense and stress response nematode genes were also identified and were particularly highly expressed in the cotton root samples. A saposin type B domain gene was among the top twenty expressed genes at 3 and 6 DAI. Saposin-like proteins have been described in *Caenorhabditis elegans*, where they have been shown to act as antimicrobial agents that permeablize the cytoplasmic membrane of bacteria (Hoeckendorf and Leippe 2012; Roeder et al. 2010). Saposins have also been

documented in entomopathogenic nematodes and root-knot nematodes, but their role in pathogenicity and parasitism is unknown (Hao et al 2010; Hoeckendorf and Leippe 2012; Nguyen et al. 2018).

Late infection is dominated by the expression of multiple vitellogenin genes and the continued expression of collagen genes. Vitellogenin proteins are transported to oocytes and converted into yolk granules to provide energy and nutrients for developing embryos and juveniles (Almenara et al. 2013; Grant and Hirsh 1999; Schneider 1996). The high and continued expression of many vitellogenins highlights the magnitude of nutrient reallocation that occurs as resources are taken from the host plant and diverted to nematode reproduction. In both soybean- and cotton-derived nematode transcripts, the same sets of vitellogenins were consistently highly expressed at 9 and 12 DAI.

In nematodes from both hosts, chondroitin proteoglycan 3 (CPG-3) genes were expressed late in infection and may have functioned in embryo development. Knockdown of chondroitin proteoglycan family members CPG-1 and -2 in *C. elegans* prevented embryo cell division (Olson et al. 2006), while a CPG in *Toxocara canis* showed high expression in the oviducts (Ma et al. 2018). Major sperm protein (MSP) genes were also expressed in the later stages of RN infection. MSP has well-characterized roles in nematode spermatozoa movement and in egg development; it may also play a role in neural development and other cytoskeletal processes (Kosinski 2005; Kuwabara 2003; Rodriguez et al. 2014).

Expression of putative parasitism genes: Cell wall modifiers

Reniform nematode infection begins when the female nematode forcibly enters the root at an angle perpendicular to the epidermis, then forces her way through cortical cell layers to reach the endodermis (Rebois et al. 1975). Due to the strength of the polysaccharides that compose them, plant cell walls provide a mechanical defense against parasitism. The better-studied root-knot and cyst nematodes have been shown to employ a combination of mechanical damage and enzymatic cell wall modification (via cellulases, polygalacturonases, pectin lyases, expansins, cell wall binding proteins, etc.) to migrate through host tissue (Wieczorek 2015).

Comparing known nematode cell wall modifiers with our assembled RN transcripts revealed several homologs, including a number of highly expressed beta-1,4-endoglucanases and pectate lyases. Beta-1,4-endoglucanases are cellulases that catalyze the hydrolysis of glycosidic bonds (Boraston et al. 2004), weakening the network of cellulose fibers and making it easier for nematodes to migrate through the root. This chemical process may be vital for parasitism, as RNAi silencing of a beta-1,4-endoglucanases in *G. rostochiensis* caused fewer nematodes to successfully penetrate host roots (Chen 2005).

A single beta-1,4-endoglucanase (RrENG-1) has been previously identified in reniform nematode (Abad et al. 2008; Gao et all. 2004; Ledger et al. 2006; Wubben et al. 2010b). Of the eleven beta-1,4-endoglucanases identified in this study, eight showed significant homology to RrENG-1 gene with E-values ranging from 6.63E-118 to 1.26E-21. These genes were not identical to the known RrENG-1, providing the possibility that

other reniform nematode ENGs exist. The three remaining genes match the *H. glycines* cellulases ENG-5 and putative gland protein G26D05.

In addition to cellulases, pectate lyases are produced by nematodes to soften the pectin-rich middle lamella and ease penetration (de Boer et al. 2002a; Doyle et al. 2002); eight pectate lyases were identified in the RN transcriptome. Much like cellulase, these genes play an important role in infection, as demonstrated by decreased *H. schachtii* infection following their knockdown through RNAi (Vanholme et al. 2007).

Expansins promote cell wall loosening by interfering with the non-covalent bonds between cellulose and hemicellulose (Cosgrove et al. 2000). Cyst nematodes produce expansins which appear to function in both cell wall modification and host defense suppression (Ali et al. 2015; Qin et al. 2004). Here, four expansin homologs were identified, two of which also showed homology to *M. incognita* avirulence proteins (Semblat et al. 2001).

Unlike most putative effectors that showed higher expression later in infection, multiple cell wall modifiers showed high expression at 3 DAI, particularly the cellulases and pectate lyases. This is consistent with early RN infection relying on host root penetration and therefore requiring expression of cell wall modifiers.

CLEs

Following penetration, the nematode establishes a new feeding site from existing pericycle cells. A growing body of evidence suggests that nematode-derived plant hormone mimics are vital to this process in a range of sedentary feeders. CLE peptide

mimics have been identified in cyst, root-knot, and recently reniform nematodes (Bakhetia et al. 2007; Guo et al. 2015; Patel et al. 2008; Wang et al. 2005; Wubben et al. 2015). Their role as plant hormone mimics has been demonstrated as overexpression of nematode-derived CLEs can alter shoot, root, and floral meristem formation (Lu et al. 2009; Wang, et al. 2010; Wang et al. 2005). Four RN CLE genes were identified in the present work, although none were identical to the three known CLEs from earlier work. Interestingly, the CLEs expressed in soybean were not the same as those expressed in cotton, raising the intriguing possibility that different host species may elicit different parasite effectors.

Defense suppressors

A successful parasite must have mechanisms in place to evade and protect itself from the host immune system and plant parasitic nematodes are no different. Several homologs of glutathione S-transferase-1 and glutathione peroxidase were identified. Glutathione S-transferase-1 (GST1) is thought to play a role in detoxifying ROS during root-knot nematode infection. It was detected in *M. incognita* stylet secretions and is highly expressed in *M. incognita* J3s. GST1 may be involved in reproduction because suppression through RNAi resulted in fewer eggs (Dubreuil et al. 2007). Two glutathione peroxidases have been identified in the cyst nematode *G. rostochiensis* (Jones et al. 2004). One is predicted to be intracellular and shows activity in highly metabolic tissue, including reproductive tissue. The second is expressed in the hypodermis and is thought to protect the nematode for ROS. Both show homology to reniform nematode

genes. Annexin homologs are also present among the reniform nematode genes indicating that the nematode might protect itself from plant ROS indirectly by coopting plant processes. An annexin 4C10 homolog from *H. schachtii* was shown to interact with an Arabidopsis oxidoreductase using yeast-two hybrid screens (Patel et al. 2010). Further, suppression of the annexin through RNAi led to a decrease in the number of mature females.

CTLs showed extremely high expression throughout the time course. Their role as effector genes has been proposed based on evidence of CTL expression in the subventral glands of *M. graminicola* and *M. chitwoodi* (Haegeman 2013; Roze et al. 2008). In cyst nematode, CTL expression has been documented in the hypodermis and a recent study suggests a class of reniform nematode CTLs are also expressed in this region (de Boer et al. 2002b; Ganji et al. 2014). The CTLs identified in this study share homology to the known reniform nematode CTLs.

Fatty acid and retinol binding proteins (FARs) were also among the highest expressed genes on multiple days. Five of the eight assembled had signal peptide cleavage site (Suppl 3.5 and 3.6). The reniform nematode genes share homology with the *M. javanica* MjFAR1, which induces host susceptibility in tomato (Iberkleid et al. 2013). Knockdown studies of MjFAR1 reduced infection, while overexpression of MjFAR1 in transgenic tomatoes resulted in increased susceptibility characterized by accelerated gall growth, larger giant cells, and a higher percentage of nematodes developing into females. High levels of MjFAR1 also corresponded to decreased expression of jasmonic acid response genes (Iberkleid et al. 2013).

Several reniform nematode genes share homology with VAP1 from *G. rostochiensis* and most contained a signal peptide cleavage site (Suppl 3.5 and 3.6). GrVAP1 is secreted in the apoplast were it interacts with an RCR3 protease, blocking its activity. In some resistant plant varieties, the presence of the immune receptor Cf-2 protects RCR3 leading to effector triggered immunity and programed cell death (Lozano-Torres et al. 2012).

Conclusion

R. reniformis is a generalist parasite that causes damage to a wide range of host species. Despite its importance, there remains relatively little information on the molecular biology of the species. Our work contributes to reniform nematode biology by identifying many putative effectors, including pectate lyases, annexins, calreticulins, VAPs, FARs, ROS detoxifying agents, and homologs of several cyst and root-knot nematode effectors. The time course provided insight into highly expressed genes that may be necessary for the nematode to mature and reproduce. Taken together, the nematode genes we have identified will enable future studies to characterize these putative effector genes for their role in parasitism.

Table 3.1 - The top twenty nematode genes assembled from soybean roots on four sampling dates, ranked by expression level (mapped Fragments per kilobase of exon model, FPKM)

Gene ID	Description	Mean FPKM	SD
3 DAI			
SB_DN45651_c0_g1	nematode cuticle collagen protein COL5A1	7.54	12.84
SB_DN47363_c0_g1	C-type lectin	5.66	8.52
SB_DN48292_c0_g1	cuticular collagen	5.21	9.02
SB_DN52878_c1_g1	nematode cuticle collagen protein COL-1	2.83	4.58
SB_DN44349_c0_g1	40s ribosomal protein s8	2.43	4.04
SB_DN39925_c0_g1	60s ribosomal protein L21	1.76	3.05
SB_DN40299_c0_g1	fatty acid and retinol binding protein	1.74	1.84
SB_DN5239_c0_g1	60s ribosomal protein L44	1.72	2.57
SB_DN38244_c0_g1	60s ribosomal protein L30	1.69	2.93
SB_DN44348_c0_g1	60s ribosomal protein L17	1.54	2.67
SB_DN35199_c1_g1	60s ribosomal protein L14	1.50	2.24
SB_DN35056_c0_g1	60s ribosomal protein L32	1.46	2.53
SB_DN40060_c0_g1	60s acidic ribosomal P0	1.44	2.50
SB_DN41002_c0_g1	60s acidic ribosomal P2	1.41	2.44
SB_DN37486_c0_g1	40s ribosomal protein S24	1.23	2.12
SB_DN37790_c0_g1	ribosomal protein L35Ae	1.21	2.10
SB_DN46401_c0_g1	40s ribosomal protein S13	1.20	2.08
SB_DN26577_c0_g1	ribosomal protein	1.20	2.08
SB_DN41534_c0_g1	40s ribosomal protein S4	1.18	1.69
SB_DN44943_c0_g1	40s ribosomal protein S6	1.14	1.79
6 DAI			
SB_DN45651_c0_g1	nematode cuticle collagen protein COL5A1	170.07	181.14

SB_DN47363_c0_g1	C-type lectin	97.23	113.72
SB_DN52878_c1_g1	nematode cuticle collagen protein COL-1	60.15	64.73
SB_DN51004_c0_g1	cuticular collagen	59.03	63.31
SB_DN40299_c0_g1	fatty acid and retinol binding protein	45.50	60.97
SB_DN48292_c0_g1	cuticular collagen	40.38	45.17
SB_DN51004_c0_g2	nematode cuticle collagen domain protein	36.66	37.69
SB_DN51004_c0_g3	cuticular collagen	23.40	26.61
SB_DN5239_c0_g1	60s ribosomal protein L44	19.39	21.82
SB_DN41002_c0_g1	60s acidic ribosomal protein P2	19.04	24.33
SB_DN40047_c0_g1	40s ribosomal protein S18	18.18	19.34
SB_DN40060_c0_g1	60s acidic ribosomal protein P0	17.79	20.04
SB_DN37486_c0_g1	40s ribosomal protein S24	17.75	17.18
SB_DN44941_c0_g1	60s ribosomal protein l13a	17.55	19.80
SB_DN7186_c0_g1	small subunit ribosomal protein 14	17.55	20.93
SB_DN38244_c0_g1	60s ribosomal protein L30	17.50	22.27
SB_DN65056_c0_g1	eukaryotic translation initiation factor 5A-2	16.62	19.64
SB_DN37790_c0_g1	ribosomal protein L35Ae	16.54	17.93
SB_DN26971_c0_g1	40s ribosomal protein S23	16.34	19.28
SB_DN93115_c0_g1	large subunit ribosomal protein 23	16.28	21.32
9 DAI			
SB_DN47363_c0_g1	C-type lectin	1722.99	1492.90
SB_DN42402_c0_g1	vitellogenin-6	1587.22	1420.94
SB_DN40299_c0_g1	fatty acid and retinol binding	1304.62	1135.80
SB_DN45651_c0_g1	nematode cuticle collagen protein COL5A1	1178.80	1165.97
SB_DN47550_c0_g1	vitellogenin-6	903.73	943.13
SB_DN54179_c10_g3	vitellogenin-6	810.03	739.46
SB_DN54179_c10_g1	vitellogenin-6	716.22	624.02
SB_DN37025_c0_g1	chondroitin proteoglycan 3	686.66	603.80

SB_DN51004_c0_g1	cuticular collagen	554.40	558.38
SB_DN51004_c0_g3	cuticular collagen	450.85	441.08
SB_DN47649_c0_g1	fatty acid-binding-like protein 5	443.70	383.77
SB_DN52878_c1_g1	nematode cuticle collagen protein COL-1	418.54	435.25
SB_DN44437_c0_g1	CRE-VIT-5 protein	399.34	400.61
SB_DN42402_c0_g2	vitellogenin-6	347.00	319.29
SB_DN54179_c11_g2	vitellogenin-1	343.66	348.32
SB_DN36838_c0_g2	vitellogenin-6	276.22	244.29
SB_DN48879_c1_g1	vitellogenin-6	266.77	291.35
SB_DN38324_c0_g1	chondroitin proteoglycan 3	237.28	208.30
SB_DN42924_c0_g1	glyceraldehyde-3-phosphate dehydrogenase 1	229.07	198.33
SB_DN46153_c0_g1	cytosolic fatty-acid binding domain/calycin-like domain protein	205.16	177.80
12 DAI			
SB_DN42402_c0_g1	vitellogenin-6	886.17	1435.92
SB_DN47363_c0_g1	C-type lectin	665.97	949.76
SB_DN40299_c0_g1	fatty acid and retinol binding protein	525.98	762.14
SB_DN37025_c0_g1	chondroitin proteoglycan 3	382.79	564.36
SB_DN54179_c10_g1	vitellogenin-6	364.17	566.42
SB_DN45651_c0_g1	nematode cuticle collagen protein COL5A1	363.59	488.51
SB_DN47550_c0_g1	vitellogenin-6	348.75	564.40
SB_DN54179_c10_g3	vitellogenin-6	330.20	536.17
SB_DN47649_c0_g1	fatty acid-binding-like protein 5	241.25	361.57
SB_DN42402_c0_g2	vitellogenin-6	195.45	314.57
SB_DN51004_c0_g1	cuticular collagen	175.78	223.62
SB_DN44437_c0_g1	CRE-VIT-5 protein	164.38	268.54
SB_DN51004_c0_g3	cuticular collagen	162.20	216.50
SB_DN54179_c11_g2	vitellogenin-1	148.37	245.67

SB_DN36838_c0_g2	vitellogenin-6	139.52	220.45
SB_DN38324_c0_g1	chondroitin proteoglycan 3	125.61	187.54
SB_DN52878_c1_g1	nematode cuticle collagen protein COL-1	121.92	167.60
SB_DN48879_c1_g1	vitellogenin-6	112.89	183.82
SB_DN46153_c0_g1	cytosolic fatty-acid binding domain and calycin-like domain family protein	95.34	143.94
SB_DN42924_c0_g1	glyceraldehyde-3-phosphate dehydrogenase 1	91.93	127.34

Table 3.2 - The top twenty nematode genes assembled from cotton roots on four sampling dates, ranked by expression level (mapped Fragments per kilobase of exon model, FPKM)

Gene ID	Description	Mean FPKM	SD
3 DAI			
CT_DN119052_c1_g1	fatty acid and retinol binding protein	77.04	60.85
CT_DN119049_c2_g1	eukaryotic translation elongation factor 1A protein (EF1A)	72.26	58.90
CT_DN118186_c3_g1	eukaryotic translation elongation factor 1A protein (EF1A)	66.13	45.06
CT_DN95726_c0_g1	saposin B domain-containing protein	52.95	61.47
CT_DN108054_c1_g2	40s ribosomal protein	51.27	41.78
CT_DN113040_c8_g1	collagen alpha-5(IV) chain	50.59	33.12
CT_DN108879_c0_g1	acidic ribosomal protein P1	50.30	38.16
CT_DN117980_c0_g6	small subunit ribosomal protein 1	49.44	40.29
CT_DN121565_c2_g1	ADP/ATP translocase 4	47.99	31.95
CT_DN117499_c1_g1	cuticle collagen 6	47.11	21.55
CT_DN120934_c0_g1	60s ribosomal protein L7a	45.22	37.84
CT_DN122901_c1_g1	vitellogenin-6	43.56	52.73
CT_DN119410_c1_g1	nematode cuticle collagen domain protein	41.95	23.67
CT_DN119808_c1_g2	tropomyosin	41.69	45.55
CT_DN117968_c0_g1	60s ribosomal protein L26	40.65	40.22
CT_DN113477_c0_g1	60s ribosomal protein L21	40.42	31.45
CT_DN123173_c2_g1	cuticlin protein	40.13	34.16
CT_DN110017_c0_g1	60s ribosomal protein L32	39.60	31.16
CT_DN112472_c0_g1	ribosomal protein S4	39.51	27.47
CT_DN116635_c1_g1	EF hand family protein	39.41	29.61
6 DAI			

CT_DN108694_c1_g1	60s ribosomal protein L12	21.07	27.59
CT_DN98757_c0_g1	cytochrome c oxidase subunit 2, mitochondrial	16.35	17.04
CT_DN114701_c4_g1	translation elongation factor EF-1, subunit alpha (EF1A)	15.25	18.31
CT_DN104216_c0_g1	nematode cuticle collagen domain protein	11.88	15.94
CT_DN118917_c5_g2	cuticle collagen 12	10.29	14.99
CT_DN103336_c0_g1	nematode cuticle collagen domain protein	8.86	14.91
CT_DN68815_c0_g1	zona pellucida-like domain protein	7.88	13.65
CT_DN111473_c5_g1	nematode cuticle collagen domain protein	7.71	13.19
CT_DN99289_c0_g1	saposin type B domain containing protein	7.35	11.24
CT_DN76640_c0_g1	inorganic pyrophosphatase	7.29	12.62
CT_DN102844_c0_g1	nematode cuticle collagen domain protein sqt-1	7.28	12.20
CT_DN121565_c2_g1	ADP/ATP translocase 4	6.84	1.77
CT_DN119049_c2_g1	eukaryotic translation elongation factor 1A protein (EF1A)	6.76	3.16
CT_DN88881_c0_g1	inorganic pyrophosphatase	6.00	10.40
CT_DN114861_c1_g2	actin	5.90	2.25
CT_DN81162_c0_g1	metalloproteinase inhibitor	5.60	9.69
CT_DN118186_c3_g1	eukaryotic translation elongation factor 1A protein (EF1A)	5.60	3.13
CT_DN95087_c0_g2	destabilase	5.48	8.72
CT_DN116635_c1_g1	EF hand family protein	5.45	1.07
CT_DN117358_c2_g6	heat shock 70 Kda protein F	5.13	5.88
9 DAI			
CT_DN84557_c0_g1	vitellogenin-6	500.16	866.30
CT_DN94617_c0_g1	C-type lectin	400.97	694.50
CT_DN121047_c0_g2	vitellogenin-6	385.01	666.86
CT_DN101880_c0_g1	fatty acid and retinol binding protein	277.15	478.58
CT_DN109069_c0_g2	vitellogenin-6	243.56	421.85
CT_DN102101_c0_g1	FACT complex subunit SSRP1	238.80	345.35

CT_DN123016_c0_g4	vitellogenin-6	202.03	349.93
CT_DN123016_c0_g3	vitellogenin-6	190.47	329.90
CT_DN123488_c13_g1	vitellogenin-6	148.11	256.53
CT_DN119746_c1_g1	nematode cuticle collagen protein COL-1	143.09	247.84
CT_DN107234_c1_g1	vitellogenin-6	108.48	187.89
CT_DN117242_c0_g1	vitellogenin-6	107.84	186.78
CT_DN122508_c0_g1	linker histone H1/H5 domain containing protein	104.17	146.74
CT_DN112976_c0_g1	fatty acid-binding-like protein 5	86.43	149.71
CT_DN113251_c0_g1	histone H1.6	85.10	127.20
CT_DN109069_c0_g1	vitellogenin-6	82.77	143.37
CT_DN116935_c0_g1	major sperm protein	82.16	123.67
CT_DN114701_c3_g1	eukaryotic translation elongation factor 1A protein (EF1A)	73.15	125.51
CT_DN106674_c0_g1	Chondroitin proteoglycan 3	63.52	110.03
CT_DN121047_c0_g3	vitellogenin-6	61.30	106.17
12 DAI			
CT_DN118759_c3_g3	major sperm protein	184.42	317.26
CT_DN84557_c0_g1	vitellogenin-6	166.14	287.76
CT_DN94617_c0_g1	C-type lectin	96.29	166.78
CT_DN121047_c0_g2	vitellogenin-6	89.11	154.35
CT_DN123016_c0_g3	vitellogenin-6	54.55	94.48
CT_DN109069_c0_g2	vitellogenin-6	53.37	91.79
CT_DN123016_c0_g4	vitellogenin-6	46.89	81.22
CT_DN101880_c0_g1	fatty acid and retinol binding protein	46.24	79.86
CT_DN108694_c1_g1	60s ribosomal protein L12	42.31	33.06
CT_DN102101_c0_g1	FACT complex subunit SSRP1	37.55	28.03
CT_DN116935_c0_g1	major sperm protein	36.52	45.39
CT_DN104216_c0_g1	nematode cuticle collagen domain protein	31.38	28.17
CT_DN117242_c0_g1	vitellogenin-6	31.27	53.97

CT_DN106674_c0_g1	chondroitin proteoglycan 3	31.05	53.78
CT_DN123488_c13_g1	vitellogenin-6	29.65	51.36
CT_DN112374_c0_g3	major sperm protein	29.10	50.40
CT_DN99084_c0_g2	trypsin	24.54	10.38
CT_DN114701_c4_g1	translation elongation factor EF-1, subunit alpha (EF1A)	24.02	17.13
CT_DN95244_c0_g1	N-acylethanolamine-hydrolyzing acid amidase (NAAA)	23.74	41.12
CT_DN50021_c0_g1	nematode cuticle collagen domain protein	23.63	40.92

Figure 3.1 – distribution of nematode genes per top blast hit species from soybean and cotton transcriptomes. Species with >30 genes were included. Colors denote feeding behavior of the nematode.

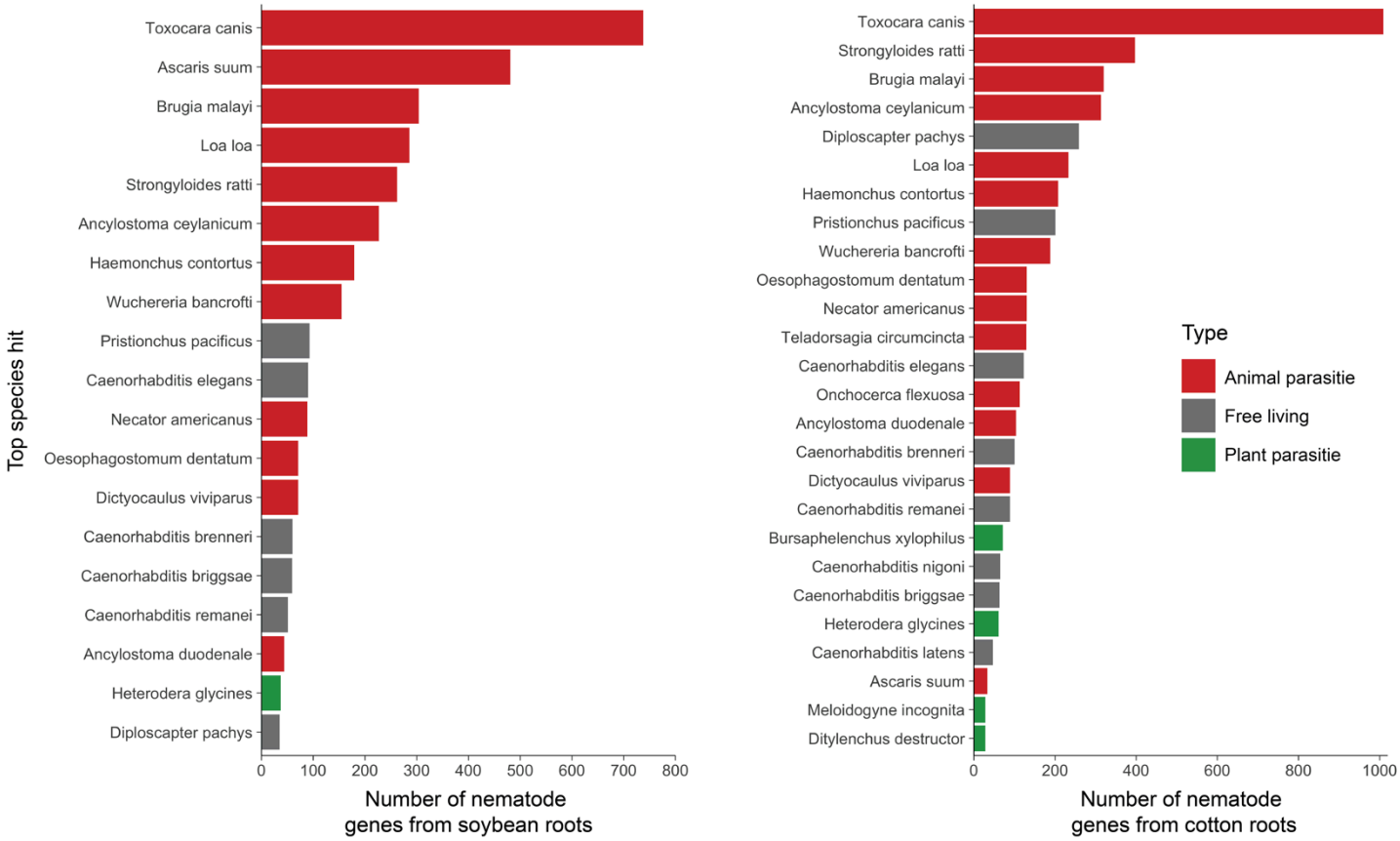

Figure 3.2 – distribution of nematode genes for the top twenty biological process gene ontology (GO) terms from soybean and cotton transcriptomes. Terms from level six in GO hierarchy were used for comparison.

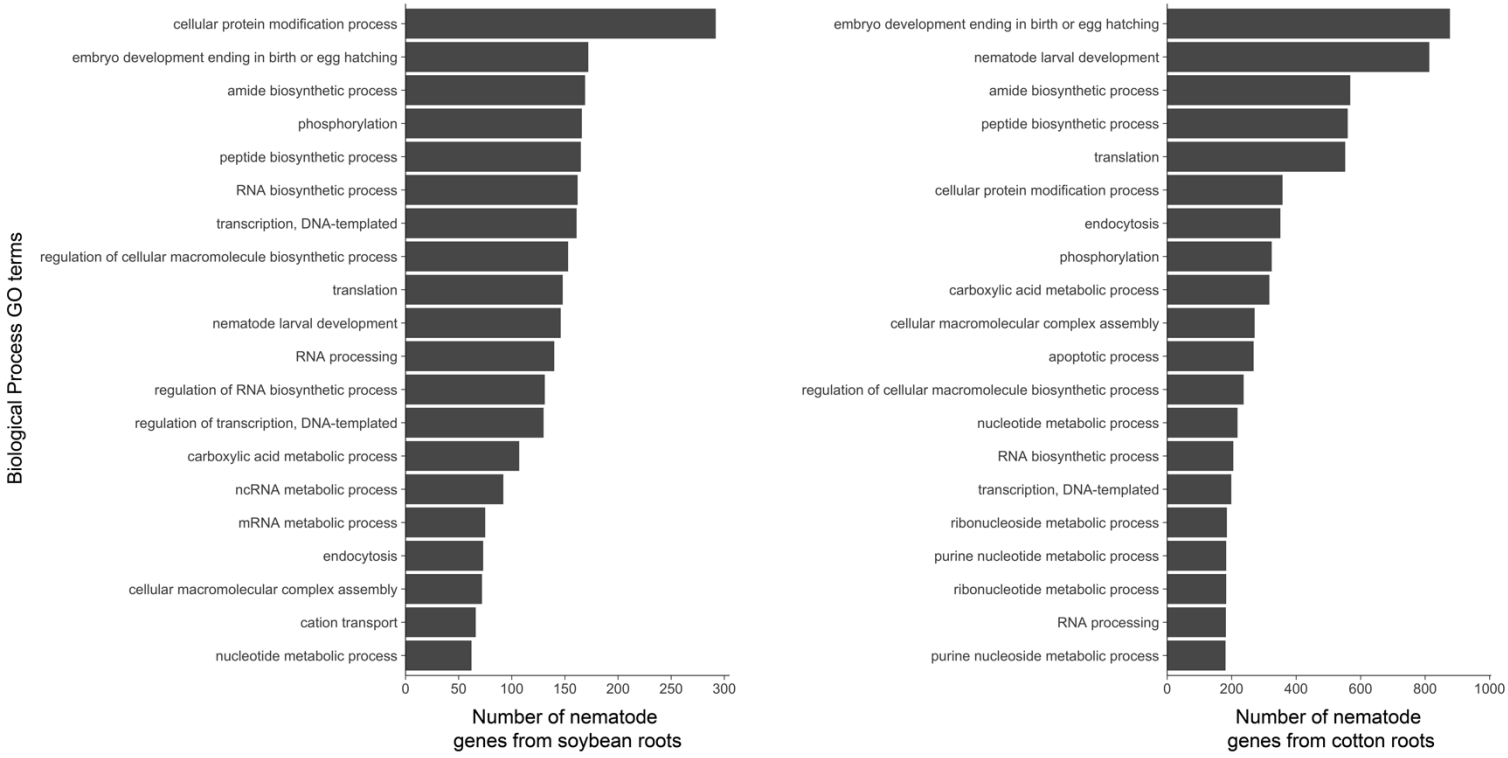

Figure 3.3 – distribution of nematode genes for the top twenty cellular component gene ontology (GO) terms from soybean and cotton transcriptomes. Terms from level six in GO hierarchy were used for comparison.

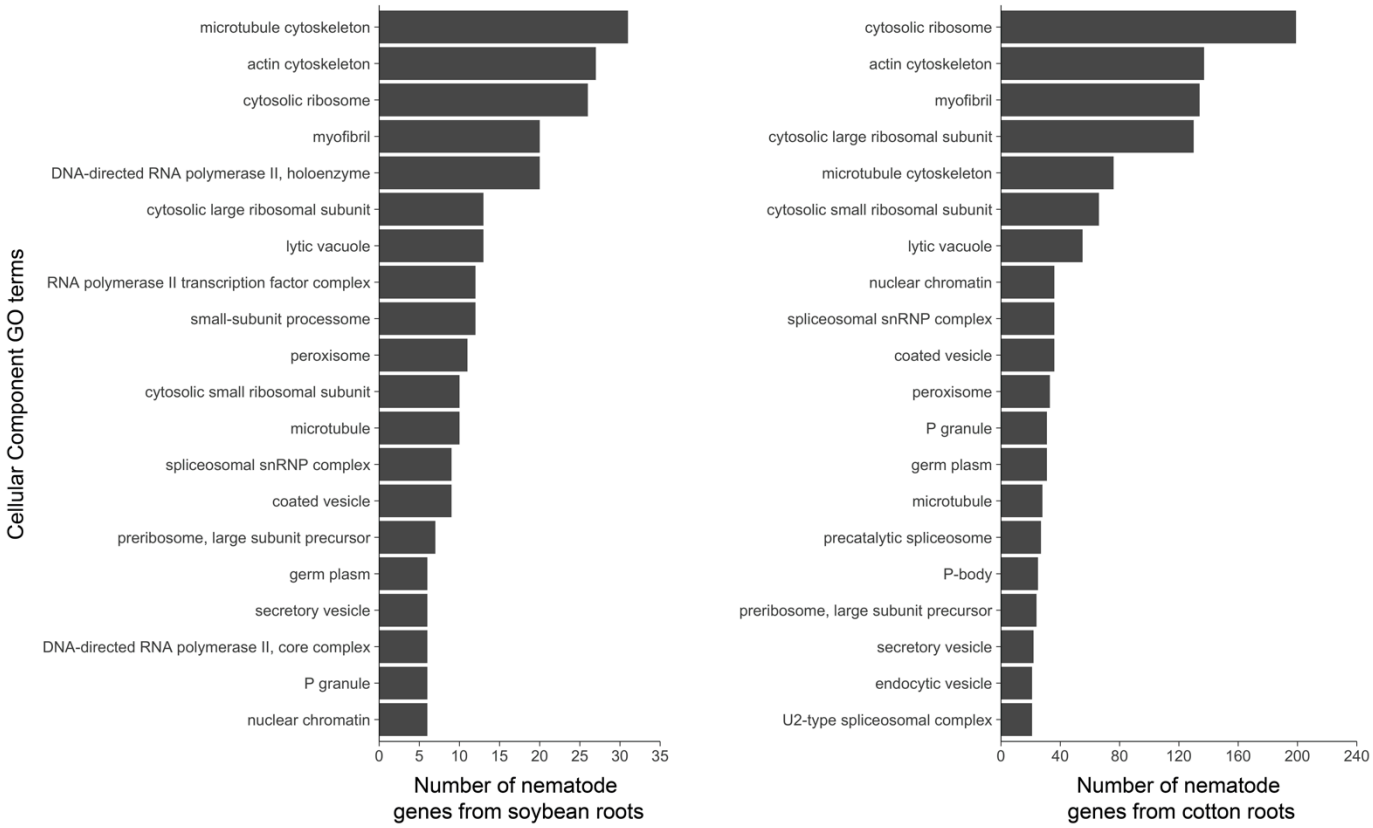

Figure 3.4 - Clustered heatmap of FPKM estimates for putative reniform nematode plant signal mimics, C-type lectins, and gland protein homologs. Red indicates high mean expression. Descriptions for each gene are given in parentheses. Gene IDs with shared superscripts are homologs (Suppl 3.5 and 3.6).

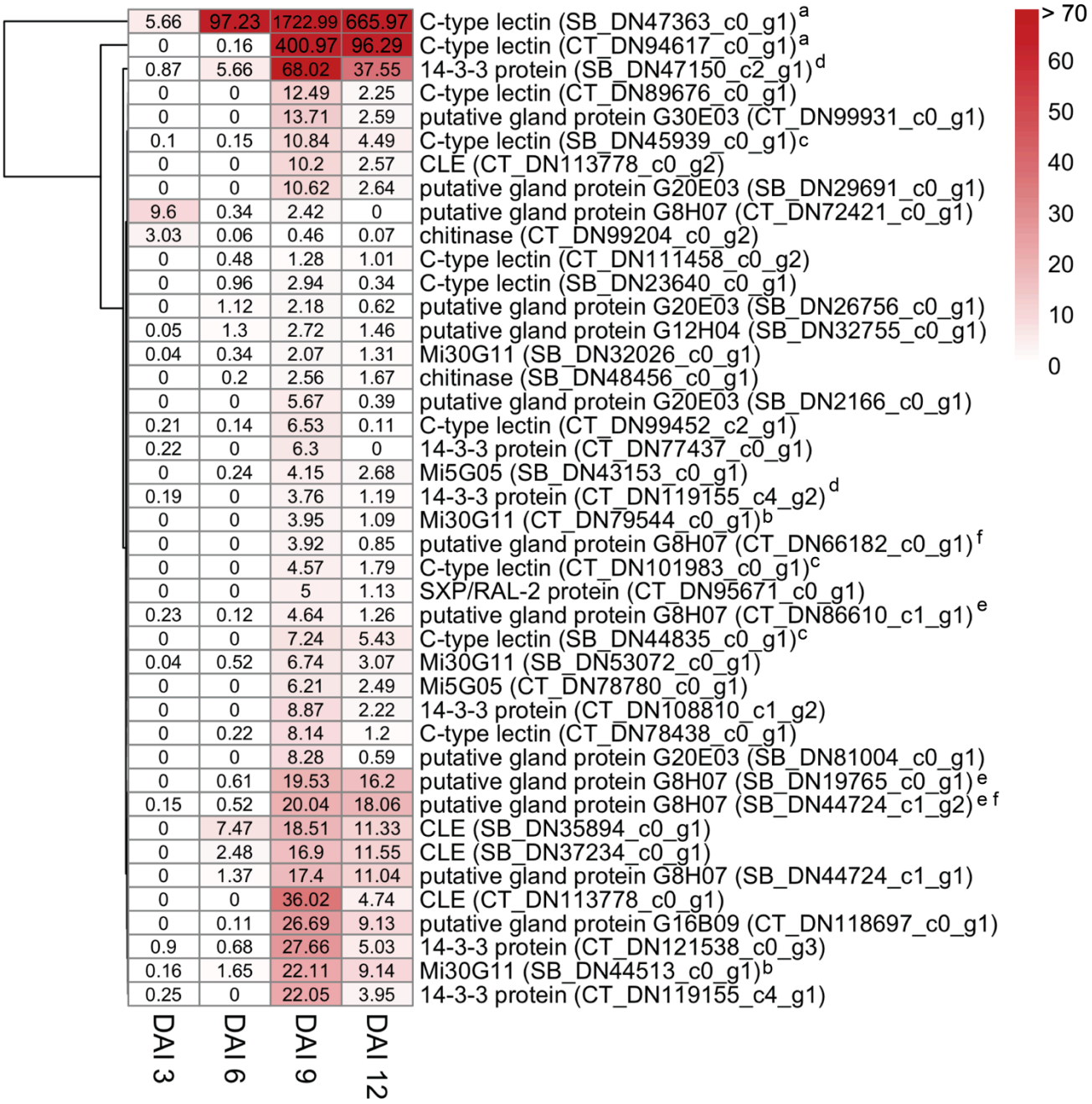

Figure 3.5 – Clustered heatmap of FPKM estimates for putative reniform nematode plant cell wall modifying genes. Red indicates high mean expression. Descriptions for each gene are given in parentheses.

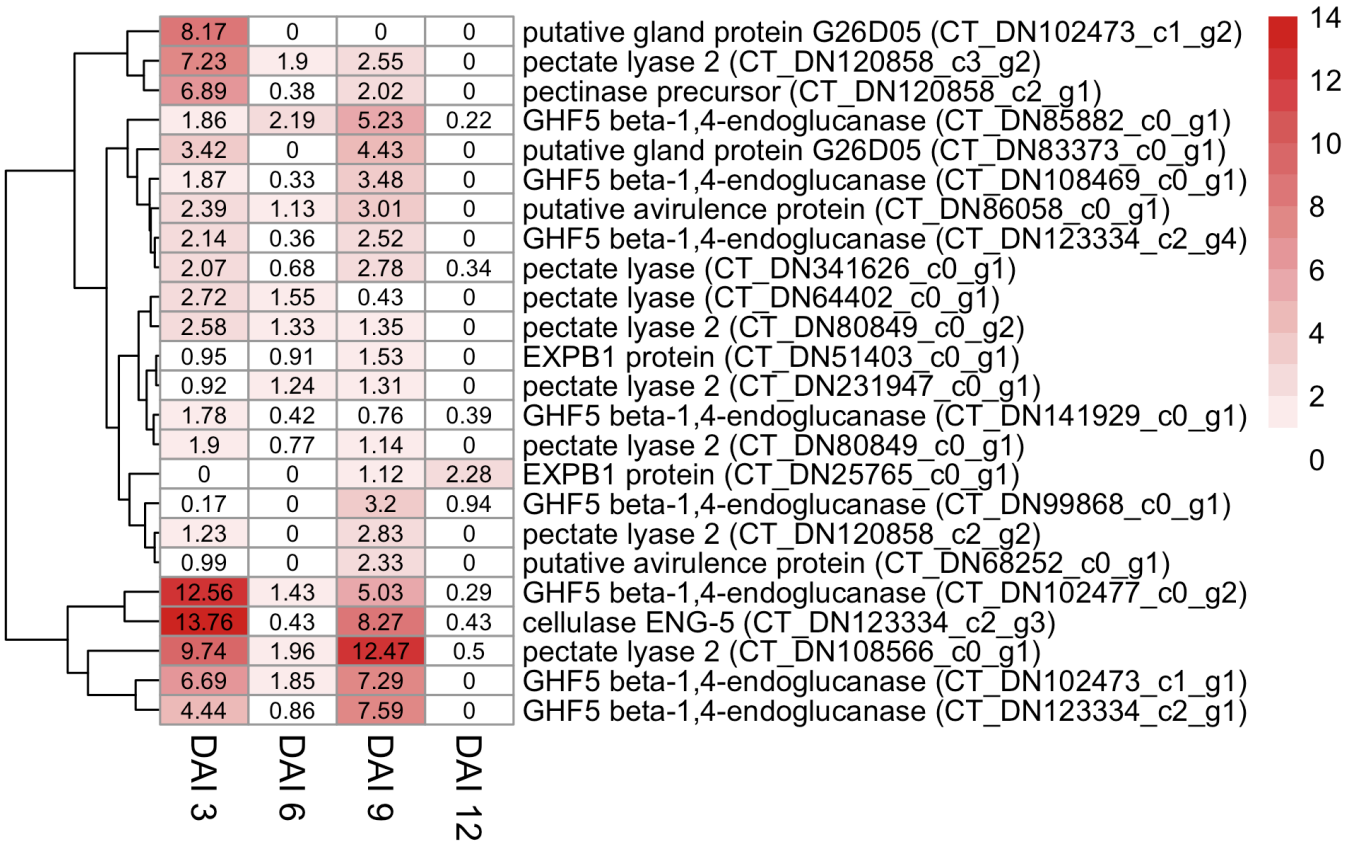

Figure 3.6 - Clustered heatmap of FPKM estimates for putative reniform nematode plant defense repressors. Red indicates high mean expression. Descriptions for each gene are given in parentheses. Gene IDs with shared superscripts are homologs (Suppl 3.5 and 3.6).

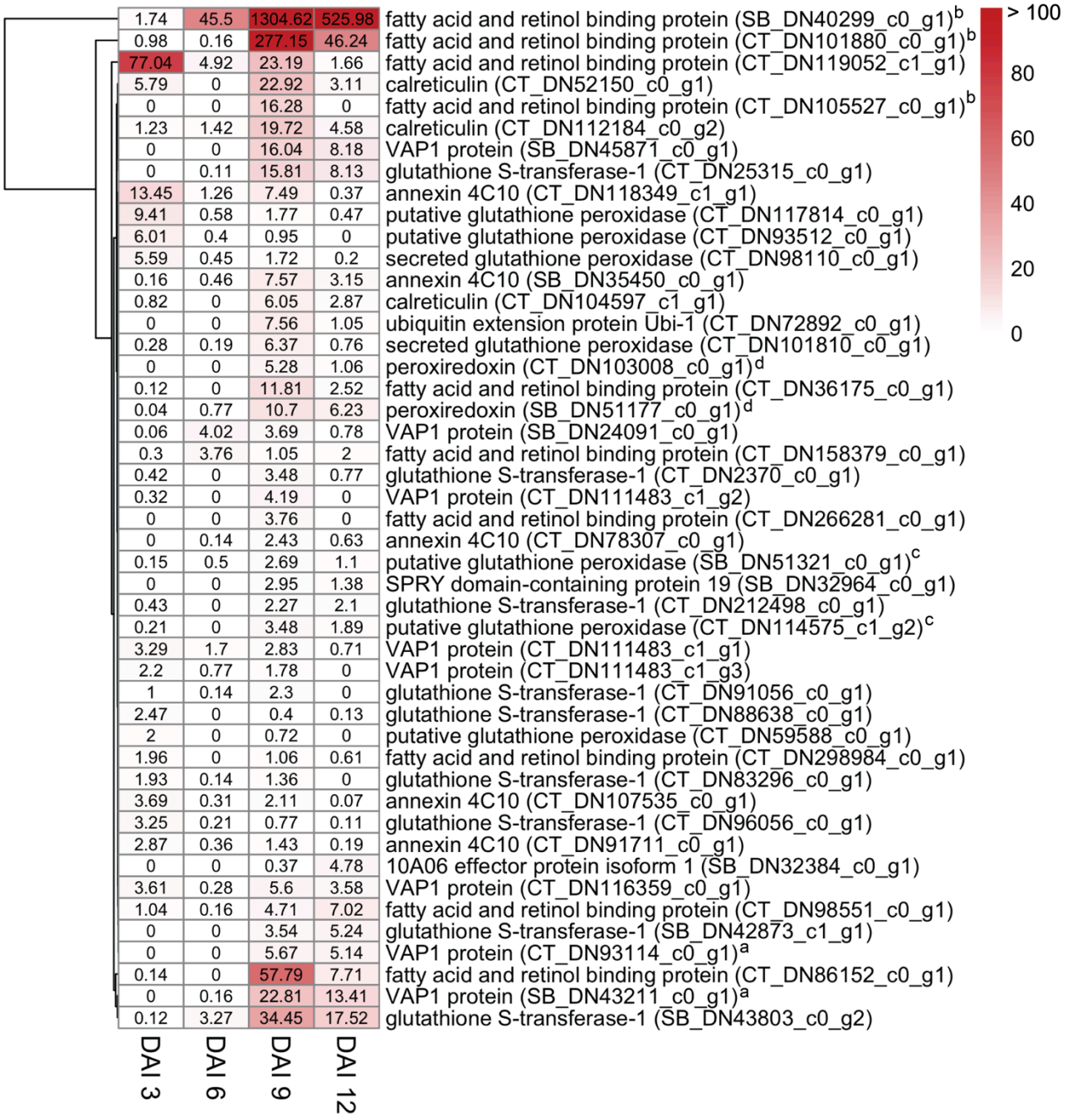

References

Abad, P., Gouzy, J., Aury, J., Castagnone-Sereno, P., Danchin, E. G. J., Deleury, E., Perfus-Barbeoch, L., Anthouard, V., Artiguenave, F., Blok, V. C., Caillaud, M., Coutinho, P. M., Dasilva, C., De Luca, F., Deau, F., Esquibet, M., Flutre, T., Goldstone, J. V., Hamamouch, N., Hewezi, T., Jaillon, O., Jubin, C., Leonetti, P., Magliano, M., Maier, T. R., Markov, G. V., McVeigh, P., Pesole, G., Poulain, J., Robinson-Rechavi, M., Sallet, E., Segurens, B., Steinbach, D., Tytgat, T., Ugarte, E., van Ghelder, C., Veronico, P., Baum, T. J., Blaxter, M., Bleve-Zacheo, T., Davis, E. L., Ewbank, J. J., Favery, B., Grenier, E., Henrissat, B., Jones, J. T., Laudet, V., Maule, A. G., Quesneville, H., Rosso, M., et al. 2008. Genome sequence of the metazoan plant-parasitic nematode *Meloidogyne incognita*. Nat. Biotechnol. 26(8):909-915.

Agudelo, P., Robbins, R. T., Kim, K. S., and Stewart, J. M. 2005. Histological changes in *Gossypium hirsutum* associated with reduced reproduction of *Rotylenchulus reniformis*. J. Nematol. 37(2):185-189.

Ali, S., Magne, M., Chen, S., Cote, O., Stare, B. G., Obradovic, N., Jamshaid, L., Wang, X., Belair, G., Moffett, P. 2015. Analysis of Putative apoplastic effectors from the nematode, *Globodera rostochiensis*, and identification of an expansin-like protein that can induce and suppress host defenses. Plos One 10:e0115042.

Almenara, D. P., de Moura, J. P., Scarabotto, C. P., Zingali, R. B., and Winter, C. E. 2013. The molecular and structural characterization of two vitellogenins from the free-living nematode *Oscheius tipulae*. Plos One 8(1):e53460.

Bakhetia, M., Urwin, P. E., and Atkinson, H. J. 2007. qPCR analysis and RNAi define pharyngeal gland cell-expressed genes of *Heterodera glycines* required for initial interactions with the host. Mol. Plant-Microbe Interact. 20(3):306-312.

Banerjee, S., Gill, S. S., Gawade, B. H., Jain, P. K., Subramaniam, K., and Sirohi, A. 2018. Host delivered RNAi of two cuticle collagen genes, Mi-col-1 and Lemmi-5 hampers structure and fecundity in *Meloidogyne incognita*. Front. Plant Sci. 8:2266.

Bird, D. M., Jones, J. T., Opperman, C. H., Kikuchi, T., and Danchin, E. G. J. 2015. Signatures of adaptation to plant parasitism in nematode genomes. Parasitology 142:S71-84.

Blasingame, D., and Patel, M. V. 2012. Cotton disease loss estimate committee report. Proceedings of the 2012 Beltwide Cotton Conferences, 3-6 January 2012, Orlando, FL:341–344.

Bolger, A. M., Lohse, M., and Usadel, B. 2014. Trimmomatic: A flexible trimmer for Illumina sequence data. Bioinformatics 30(15):2114-2120.

Boraston, A., Bolam, D., Gilbert, H., and Davies, G. 2004. Carbohydrate-binding modules: Fine-tuning polysaccharide recognition. Biochem. J. 382:769-781.

Chen, Q., Rehman, S., Smant, G., and Jones, J. 2005. Functional analysis of pathogenicity proteins of the potato cyst nematode *Globodera rostochiensis* using RNAi. Mol. Plant-Microbe Interact. 18(7):621-625.

Chronis, D., Chen, S., Lu, S., Hewezi, T., Carpenter, S. C. D., Loria, R., Baum, T. J., and Wang, X. 2013. A ubiquitin carboxyl extension protein secreted from a plant-parasitic nematode *Globodera rostochiensis* is cleaved *in planta* to promote plant parasitism. Plant J. 74(2):185-196.

Conesa, A., Gotz, S., Garcia-Gomez, J., Terol, J., Talon, M., and Robles, M. 2005. Blast2GO: A universal tool for annotation, visualization and analysis in functional genomics research. Bioinformatics 21(18):3674-3676.

Cosgrove, D. 2000. Loosening of plant cell walls by expansins. Nature 407(6802):321-326.

Davies, K. G., and Curtis, R. H. C. 2011. Cuticle surface coat of plant-parasitic nematodes. Annu. Rev. Phytopathol. 49:135-156.

Davis, E. L., Hussey, R. S., Mitchum, M. G., and Baum, T. J. 2008. Parasitism proteins in nematode-plant interactions. Curr. Opin. Plant Biol. 11(4):360-366.

de Boer, J., McDermott, J., Davis, E., Hussey, R., Popeijus, H., Smant, G., and Baum, T. 2002a. Cloning of a putative pectate lyase gene expressed in the subventral esophageal glands of *Heterodera glycines*. J. Nematol. 34(1):9-11.

de Boer, J., McDermott, J., Wang, X., Maier, T., Qu, F., Hussey, R., Davis, E., and Baum, T. 2002b. The use of DNA microarrays for the developmental expression analysis of cDNAs from the oesophageal gland cell region of *Heterodera glycines*. Mol. Plant Pathol. 3(4):261-270.

Doyle, E., and Lambert, K. 2002. Cloning and characterization of an esophageal-gland-specific pectate lyase from the root-knot nematode *Meloidogyne javanica*. Mol. Plant-Microbe Interact. 15(6):549-556.

Dubreuil, G., Magliano, M., Deleury, E., Abad, P., and Rosso, M. N. 2007. Transcriptome analysis of root-knot nematode functions induced in the early stages of parasitism. New Phytol. 176(2):426-436.

Eves-Van den Akker, S., Lilley, C. J., Yusup, H. B., Jones, J. T., and Urwin, P. E. 2016. Functional C-TERMINALLY ENCODED PEPTIDE (CEP) plant hormone domains evolved *de novo* in plant parasite *Rotylenchulus reniformis*. Mol. Plant Pathol. 17(8):1265-1275.

Ganji, S., Jenkins, J. N., and Wubben, M. J. 2014. Molecular characterization of the reniform nematode C-type lectin gene family reveals a likely role in mitigating environmental stresses during plant parasitism. Gene 537(2):269-278.

Gao, B., Allen, R., Davis, E., Baum, T., and Hussey, R. 2004. Developmental expression and biochemical properties of a beta-1,4-endoglucanase family in the soybean cyst nematode, *Heterodera glycines*. Mol. Plant Pathol. 5(2):93-104.

Gardner, M., Verma, A., and Mitchum, M. G. 2015. Chapter eleven – Emerging roles of cyst nematode effectors in exploiting plant cellular processes. Plant Nematode Interactions: A View on Compatible Interrelationships, 73:259-291.

Gheysen, G., and Mitchum, M. G. 2011. How nematodes manipulate plant development pathways for infection. Curr. Opin. Plant Biol. 14(4):415-421.

Grant, B., and Hirsh, D. 1999. Receptor-mediated endocytosis in the *Caenorhabditis elegans* oocyte. Mol. Biol. Cell 10(12):4311-26.

Guo, X., Chronis, D., De La Torre, C. M., Smeda, J., Wang, X., and Mitchum, M. G. 2015. Enhanced resistance to soybean cyst nematode *Heterodera glycines* in transgenic soybean by silencing putative CLE receptors. Plant Biotechnol. J. 13(6):801-810.

Haas, B. J., Papanicolaou, A., Yassour, M., Grabherr, M., Blood, P. D., Bowden, J., Couger, M. B., Eccles, D., Li, B., Lieber, M., MacManes, M. D., Ott, M., Orvis, J., Pochet, N., Strozzi, F., Weeks, N., Westerman, R., William, T., Dewey, C. N., Henschel, R., Leduc, R. D., Friedman, N., and Regev, A. 2013. *De novo* transcript sequence reconstruction from RNA-seq using the trinity platform for reference generation and analysis. Nat. Protoc. 8(8):1494-1512.

Haegeman, A., Bauters, L., Kyndt, T., Rahman, M. M., and Gheysen, G. 2013. Identification of candidate effector genes in the transcriptome of the rice root knot nematode *Meloidogyne graminicola*. Mol. Plant Pathol. 14(4):379-390.

Hao, Y., Montiel, R., Abubucker, S., Mitreva, M., and Simoes, N. 2010. Transcripts analysis of the entomopathogenic nematode *Steinernema carpocapsae* induced in vitro with insect haemolymph. Mol. Biochem. Parasitol. 169(2):79-86.

Heald, C., and Robinson, A. 1990. Survey of current distribution of *Rotylenchulus reniformis* in the United States. J. Nematol. 22(4):695-699.

Hoeckendorf, A., and Leippe, M. 2012. SPP-3, a saposin-like protein of *Caenorhabditis elegans*, displays antimicrobial and pore-forming activity and is located in the intestine and in one head neuron. Dev. Comp. Immunol. 38(1):181-186.

Iberkleid, I., Vieira, P., Engler, J. d. A., Firester, K., Spiegel, Y., and Horowitz, S. B. 2013. Fatty acid-and retinol-binding protein, Mj-FAR-1 induces tomato host susceptibility to root-knot nematodes. Plos One 8(5):e64586.

Jaouannet, M., Magliano, M., Arguel, M. J., Gourgues, M., Evangelisti, E., Abad, P., and Rosso, M. N. 2013. The root-knot nematode calreticulin mi-CRT is a key effector in plant defense suppression. Mol. Plant-Microbe Interact. 26(1):97-105.

Jenkins, W. R. 1964. A rapid centrifugal-flotation technique for separating nematodes from soil. Plant Dis. Rep. 48(9):692.

Jones, J., Reavy, B., Smant, G., and Prior, A. 2004. Glutathione peroxidases of the potato cyst nematode *Globodera rostochiensis*. Gene 324:47-54.

Jones, M. G. K., and Dropkin, V. H. 1975. Cellular alterations induced in soybean roots by three endoparasitic nematodes. Physiol. Plant Pathol. 5(2):119-124.

Kosinski, M., McDonald, K., Schwartz, J., Yamamoto, I., and Greenstein, D. 2005. *C. elegans* sperm bud vesicles to deliver a meiotic maturation signal to distant oocytes. Development 132(15):3357-3369.

Kuwabara, P. 2003. The multifaceted *C. elegans* major sperm protein: An ephrin signaling antagonist in oocyte maturation. Genes Dev. 17(2):155-161.

Ledger, T. N., Jaubert, S., Bosselut, N., Abad, P., and Rosso, M. 2006. Characterization of a new beta-1,4-endoglucanase gene from the root-knot nematode *Meloidogyne incognita* and evolutionary scheme for phytonematode family 5 glycosyl hydrolases. Gene 382:121-128.

Li, B., and Dewey, C. N. 2011. RSEM: Accurate transcript quantification from RNA-seq data with or without a reference genome. BMC Bioinformatics 12:323.

Lozano-Duran, R., and Robatzek, S. 2015. 14-3-3 proteins in plant-pathogen interactions. Mol Plant-Microbe Interact 28(5):511-8.

Lozano-Torres, J. L., Wilbers, R. H. P., Gawronski, P., Boshoven, J. C., Finkers-Tomczak, A., Cordewener, J. H. G., America, A. H. P., Overmars, H. A., Van 't Klooster, J. W., Baranowski, L., Sobczak, M., Ilyas, M., van der Hoorn, R. A. L., Schots, A., de Wit, P. J. G. M., Bakker, J., Goverse, A., and Smant, G. 2012. Dual disease resistance mediated by the immune receptor cf-2 in tomato requires a common virulence target of a fungus and a nematode. Proc. Natl. Acad. Sci. USA 109(25):10119-10124.

Lu, S., Chen, S., Wang, J., Yu, H., Chronis, D., Mitchum, M. G., and Wang, X. 2009. Structural and functional diversity of CLAVATA3/ESR (CLE)-like genes from the potato cyst nematode *Globodera rostochiensis*. Mol. Plant-Microbe Interact. 22(9):1128-1142.

Ma, G. X., Zhou, R. Q., Hu, L., Luo, Y. L., Luo, Y. F., and Zhu, H. H. 2018. Molecular characterization and transcriptional analysis of the female-enriched chondroitin proteoglycan 2 of *Toxocara canis*. J. Helminthol. 92(2):154-160.

Mantelin, S., Thorpe, P., and Jones, J. T. 2015. Chapter thirteen - Suppression of plant defences by plant-parasitic nematodes. Plant Nematode Interactions: A View on Compatible Interrelationships, 73:325-337.

Mitchum, M. G., Wang, X., Wang, J., and Davis, E. L. 2012. Role of nematode peptides and other small molecules in plant parasitism. Annu. Rev. Phytopathol. 50:175-195.

Mitchum, M. G., Hussey, R. S., Baum, T. J., Wang, X., Elling, A. A., Wubben, M., and Davis, E. L. 2013. Nematode effector proteins: An emerging paradigm of parasitism. New Phytol. 199(4):879-894.

Nielsen, H. 2017. Predicting secretory proteins with SignalP. Methods Mol. Biol. 1611:59-73.

Nguyen, C., Perfus-Barbeoch, L., Quentin, M., Zhao, J., Magliano, M., Marteu, N., da Rocha, M., Nottet, N., Abad, P., and Favery, B. 2018. A root-knot nematode small glycine and cysteine-rich secreted effector, MiSGCR1, is involved in plant parasitism. New Phytol. 217(2):687-699.

Ohyama, K., Ogawa, M., and Matsubayashi, Y. 2008. Identification of a biologically active, small, secreted peptide in Arabidopsis by *in silico* gene screening, followed by LC-MS-based structure analysis. Plant J. 55(1):152-160.

Olson, S., Bishop, J., Yates, J., Oegema, K., and Esko, J. 2006. Identification of novel chondroitin proteoglycans in *Caenorhabditis elegans*: Embryonic cell division depends on CPG-1 and CPG-2. J Cell Biol. 173(6):985-994.

Patel, N., Hamamouch, N., Li, C., Hussey, R., Mitchum, M., Baum, T., Wang, X., and Davis, E. L. 2008. Similarity and functional analyses of expressed parasitism genes in *Heterodera schachtii* and *Heterodera glycines*. J. Nematol. 40(4):299-310.

Patel, N., Hamamouch, N., Li, C., Hewezi, T., Hussey, R. S., Baum, T. J., Mitchum M. G., Davis, E. L. 2010. A nematode effector protein similar to annexins in host plants. J. Exp. Bot. 61(1):235-248.

Qin, L., Kudla, U., Roze, E., Goverse, A., Popeijus, H., Nieuwland, J., Overmars, H., Jones, J., Schots, A., Smant, G., Bakker, J., and Helder, J. 2004. Plant degradation: A nematode expansin acting on plants. Nature 427(6969):30.

Rebois, R. V. 1980. Ultrastructure of a feeding peg and tube associated with Rotylenchulus reniformis in cotton. Nematologica 26(4):396-405.

Rebois, R. V., Madden, P. A., and Eldridge, B. J. 1975. Some ultrastructural changes induced in resistant and susceptible soybean roots following infection by Rotylenchulus reniformis. J. Nematol. 7(2):122-139.

Redding, N. W., Agudelo, P., and Wells, C. E. 2018. Multiple nodulation genes are up-regulated during establishment of reniform nematode feeding sites in soybean. Phytopathology 108(2):275-291.

Robinson, A. F., Inserra, R. N., Caswell-Chen, E. P., Vovlas, N., and Troccoli, A. 1997. Rotylenchulus species: Identification, distribution, host ranges, and crop plant resistance. Nematropica 27(2):127-180.

Robinson, A. F. 2007. Reniform in US cotton: When, where, why, and some remedies. Annu. Rev. Phytopathol. 45:263-288.

Rodriguez, A., McKay, K., Graham, M., Dittrich, J., and Holgado, A. M. 2014. Analysis of differential gene expression profiles in *Caenorhabditis elegans* knockouts for the v-SNARE master protein 1. J. Neurosci. Res. 92(6):772-782.

Roeder, T., Stanisak, M., Gelhaus, C., Bruchhaus, I., Groetzinger, J., and Leippe, M. 2010. Caenopores are antimicrobial peptides in the nematode *Caenorhabditis elegans* instrumental in nutrition and immunity. Dev. Comp. Immunol. 34(2):203-209.

Roze, E., Hanse, B., Mitreva, M., Vanholme, B., Bakker, J., and Smant, G. 2008. Mining the secretome of the root-knot nematode *Meloidogyne chitwoodi* for parasitism genes. Mol. Plant Pathol. 9(1):1-10.

Sacco, M. A., Koropacka, K., Grenier, E., Jaubert, M. J., Blanchard, A., Goverse, A., Smant, G., and Moffett, P. 2009. The cyst nematode SPRYSEC protein RBP-1 elicits Gpa2-and RanGAP2-dependent plant cell death. Plos Pathog. 5(8):e1000564.

Schneider, W. 1996. Vitellogenin receptors: Oocyte-specific members of the low-density lipoprotein receptor supergene family. Int. Rev. Cytol. 166:103-137.

Semblat, J., Rosso, M., Hussey, R., Abad, P., and Castagnone-Sereno, P. 2001. Molecular cloning of a cDNA encoding an amphid-secreted putative avirulence protein from the root-knot nematode *Meloidogyne incognita*. Mol. Plant-Microbe Interact. 14(1):72-79.

Sivakumar, C. V., and Seshadri, A. R. 1971. Life history of the reniform nematode, *Rotylenchulus reniformis* Linford and Oliveira, 1940. Indian Journal of Nematology 1:7-20

Smant, G., Stokkermans, J. P. W. G., Yan, Y., de Boer, J. M., Baum, T. J., Wang, X., Hussey, R. S., Gommers, F. J., Henrissat, B., Davis, E. L., Helder, J., Schots, A., and Bakker, J. 1998. Endogenous cellulases in animals: Isolation of β-1,4-endoglucanase genes from two species of plant-parasitic cyst nematodes**.** PNAS 95(9):4906-4911.

Smeds, L., and Kunstner, A. 2011. CONDETRI - A content dependent read trimmer for Illumina data. Plos One 6(10):e26314.

Truong, N. M., Nguyen, C. N., Abad, P., Quentin, M., and Favery, B. 2015. Chapter twelve - function of root-knot nematode effectors and their targets in plant parasitism. Plant Nematode Interactions: A View on Compatible Interrelationships, 73:293-324.

Vanholme, B., Van Thuyne, W., Vanhouteghem, K., De Meutter, J., Cannoot, B., and Gheysen, G. 2007. Molecular characterization and functional importance of pectate lyase secreted by the cyst nematode *Heterodera schachtii*. Mol. Plant Pathol. 8(3):267-278.

Wang, X. Mitchum, M. G., Gao, B., Li, C., Diab, H., Baum, T. J., Hussey, R. S., and Davis, E. L. 2005. A parasitism gene from a plant-parasitic nematode with function similar to CLAVATA3/ESR (CLE) of *Arabidopsis thaliana*. Mol. Plant Pathol. 6(2):187-191.

Wang, J., Lee, C., Replogle, A., Joshi, S., Korkin, D., Hussey, R., Baum, T. J., Davis, E. L., Wang, X., and Mitchum, M. G. 2010. Dual roles for the variable domain in protein trafficking and host-specific recognition of *Heterodera glycines* CLE effector proteins. New Phytol. 187(4):1003-1017.

Weis, W. I., Taylor, M. E., and Drickamer, K. 1998. The C-type lectin superfamily in the immune system. Immunol. Rev. 163:19-34.

Wieczorek, K. 2015. Chapter three - Cell wall alterations in nematode-infected roots. Plant Nematode Interactions: A View on Compatible Interrelationships, 73:61-90.

Wubben, M. J., Callahan, F. E., and Scheffler, B. S. 2010a. Transcript analysis of parasitic females of the sedentary semi-endoparasitic nematode *Rotylenchulus reniformis*. Mol. Biochem. Parasitol. 172(1):31-40.

Wubben, M. J., Ganji, S., and Callahan, F. E. 2010b. Identification and molecular characterization of a beta-1,4-endoglucanase gene (Rr-eng-1) from *Rotylenchulus reniformis*. J. Nematol. 42(4):342-351.

Wubben, M. J., Gavilano, L., Baum, T. J., and Davis, E. L. 2015. Sequence and spatiotemporal expression analysis of CLE-motif containing genes from the reniform nematode (*Rotylenchulus reniformis* Linford & Oliveira). J. Nematol. 47(2):159-165.

CONCLUSIONS

I. We report transcriptomes of reniform nematode infected and uninfected roots from a soybean split-root system across a twelve-day time course. The overall pattern of gene expression shares features with transcriptomes from better-studied nematode-host interactions. Many genes affected by reniform nematode infection also share similarities with mutualistic belowground symbioses such as nodulation and mycorrhization, suggesting overlap in pathways manipulated by multiple belowground symbionts and parasites.

II. Reniform nematode induced changes in lateral root initiation and the concomitant up-regulation of multiple genes associated with lateral root production and auxin dynamics suggests that there is mechanistic overlap between the feeding sites organogenesis and the initiation of lateral roots. Both reniform nematode syncytia and lateral roots develop from pericycle cells, and the processes might therefore be expected to interfere or promote one another. If lateral root genes are indeed a direct target of reniform nematode effectors, this would support the hypothesis that parasites and symbionts have co-opted normal root developmental programs to construct novel belowground organs.

III. *Rotylenchulus reniformis* is a generalist parasite that causes damage to a wide range of host species. Despite its importance, there remains relatively little information on the molecular biology of the species. Our work contributes to reniform nematode biology by identifying many putative effectors, including pectate lyases, annexins, calreticulins,

VAPs, FARs, ROS detoxifying agents, and homologs of several cyst and root-knot nematode effectors. The time course provided insight into highly expressed genes that may be necessary for the nematode to mature and reproduce.

Taken together, the nematode and plant genes we have identified will enable future studies to characterize putative effectors and their targets for a role in parasitism. Breeding and genetic engineering efforts can focus on disrupting molecular events that are unique to nematode infection while avoiding pathways that function in normal organogenesis and beneficial symbiose.

REFERENCES

Abad, P., Gouzy, J., Aury, J., Castagnone-Sereno, P., Danchin, E. G. J., Deleury, E., Perfus-Barbeoch, L., Anthouard, V., Artiguenave, F., Blok, V. C., Caillaud, M., Coutinho, P. M., Dasilva, C., De Luca, F., Deau, F., Esquibet, M., Flutre, T., Goldstone, J. V., Hamamouch, N., Hewezi, T., Jaillon, O., Jubin, C., Leonetti, P., Magliano, M., Maier, T. R., Markov, G. V., McVeigh, P., Pesole, G., Poulain, J., Robinson-Rechavi, M., Sallet, E., Segurens, B., Steinbach, D., Tytgat, T., Ugarte, E., van Ghelder, C., Veronico, P., Baum, T. J., Blaxter, M., Bleve-Zacheo, T., Davis, E. L., Ewbank, J. J., Favery, B., Grenier, E., Henrissat, B., Jones, J. T., Laudet, V., Maule, A. G., Quesneville, H., Rosso, M., et al. 2008. Genome sequence of the metazoan plant-parasitic nematode *Meloidogyne incognita*. Nat. Biotechnol. 26(8):909-915.

Agudelo, P., Robbins, R. T., Kim, K. S., and Stewart, J. M. 2005. Histological changes in *Gossypium hirsutum* associated with reduced reproduction of *Rotylenchulus reniformis*. J. Nematol. 37(2):185-189.

Albrecht, C., Geurts, R., and Bisseling, T. 1999. Legume nodulation and mycorrhizae formation; two extremes in host specificity meet. EMBO J. 18(2):281-288.

Ali, S., Magne, M., Chen, S., Cote, O., Stare, B. G., Obradovic, N., Jamshaid, L., Wang, X., Belair, G., Moffett, P. 2015. Analysis of Putative apoplastic effectors from the nematode, *Globodera rostochiensis*, and identification of an expansin-like protein that can induce and suppress host defenses. Plos One 10:e0115042.

Almenara, D. P., de Moura, J. P., Scarabotto, C. P., Zingali, R. B., and Winter, C. E. 2013. The molecular and structural characterization of two vitellogenins from the free-living nematode *Oscheius tipulae*. Plos One 8(1):e53460.

Anders, S., Pyl, P. T., and Huber, W. 2015. HTSeq-a python framework to work with high-throughput sequencing data. Bioinformatics 31(2):166-169.

Bakhetia, M., Urwin, P. E., and Atkinson, H. J. 2007. qPCR analysis and RNAi define pharyngeal gland cell-expressed genes of *Heterodera glycines* required for initial interactions with the host. Mol. Plant-Microbe Interact. 20(3):306-312.

Banerjee, S., Gill, S. S., Gawade, B. H., Jain, P. K., Subramaniam, K., and Sirohi, A. 2018. Host delivered RNAi of two cuticle collagen genes, Mi-col-1 and Lemmi-5 hampers structure and fecundity in *Meloidogyne incognita*. Front. Plant Sci. 8:2266.

Bardgett, R., Denton, C., and Cook, R. 1999. Below-ground herbivory promotes soil nutrient transfer and root growth in grassland. Ecol. Lett. 2(6):357-360.

Bartlem, D. G., Jones, M. G. K., and Hammes, U. Z. 2014. Vascularization and nutrient delivery at root-knot nematode feeding sites in host roots. J. Exp. Bot. 65(7):1789-1798.

Baylis, T., Cierlik, I., Sundberg, E., and Mattsson, J. 2013. SHORT INTERNODES/STYLISH genes, regulators of auxin biosynthesis, are involved in leaf vein development in *Arabidopsis thaliana*. New Phytol 197(3):737-50.

Bellafiore, S., Shen, Z., Rosso, M., Abad, P., Shih, P., and Briggs, S. P. 2008. Direct identification of the *Meloidogyne incognita* secretome reveals proteins with host cell reprogramming potential. Plos Pathog. 4(10):e1000192.

Benkova, E., Michniewicz, M., Sauer, M., Teichmann, T., Seifertova, D., Jurgens, G., and Friml, J. 2003. Local, efflux-dependent auxin gradients as a common module for plant organ formation. Cell 115(5):591-602.

Benkova, E., and Bielach, A. 2010. Lateral root organogenesis - from cell to organ. Curr. Opin. Plant Biol. 13(6):677-683.

Bennett, T., van den Toorn, A., Sanchez-Perez, G. F., Campilho, A., Willemsen, V., Snel, B., and Scheres, B. 2010. SOMBRERO, BEARSKIN1, and BEARSKIN2 regulate root cap maturation in Arabidopsis. Plant Cell 22(3):640-654.

Bird, D. M., Jones, J. T., Opperman, C. H., Kikuchi, T., and Danchin, E. G. J. 2015. Signatures of adaptation to plant parasitism in nematode genomes. Parasitology 142:S71-84.

Blasingame, D., and Patel, M. V. 2012. Cotton disease loss estimate committee report. Proceedings of the 2012 Beltwide Cotton Conferences, 3-6 January 2012, Orlando, FL:341–344.

Bolger, A. M., Lohse, M., and Usadel, B. 2014. Trimmomatic: A flexible trimmer for Illumina sequence data. Bioinformatics 30(15):2114-2120.

Boraston, A., Bolam, D., Gilbert, H., and Davies, G. 2004. Carbohydrate-binding modules: Fine-tuning polysaccharide recognition. Biochem. J. 382:769-781.

Bybd, D., Kirkpatrick, T., and Barker, K. 1983. An improved technique for clearing and staining plant-tissues for detection for nematodes. J. Nematol. 15(1):142-143.

Cabrera, J., Diaz-Manzano, F. E., Sanchez, M., Rosso, M., Melillo, T., Goh, T., Fukaki, H., Cabello, S., Hofmann, J., Fenoll, C., and Escobar, C. 2014. A role for LATERAL ORGAN BOUNDARIES-DOMAIN 16 during the interaction *Arabidopsis*-

Meloidogyne spp. provides a molecular link between lateral root and root-knot nematode feeding site development. New Phytol. 203(2):632-645.

Cabrera, J., Díaz-Manzano, F. E., Fenoll, C., and Escobar, C. 2015. Chapter seven - Developmental pathways mediated by hormones in nematode feeding sites. Adv. Bot. Res. 73:167-188.

Catoira, R., Galera, C., de Billy, F., Penmetsa, R., Journet, E., Maillet, F., Rosenberg, C., Cook, D., Gough, C., and Denarie, J. 2000. Four genes of *Medicago truncatula* controlling components of a nod factor transduction pathway. Plant Cell 12(9):1647-1665.

Charrier, B., Champion, A., Henry, Y., and Kreis, M. 2002. Expression profiling of the whole *Arabidopsis* Shaggy-like kinase multigene family by real-time reverse transcriptase-polymerase chain reaction. Plant Physiol. 130(2):577-590.

Chen, Q., Rehman, S., Smant, G., and Jones, J. 2005. Functional analysis of pathogenicity proteins of the potato cyst nematode *Globodera rostochiensis* using RNAi. Mol. Plant-Microbe Interact. 18(7):621-625.

Chen, L., Hou, B., Lalonde, S., Takanaga, H., Hartung, M. L., Qu, X., Guo, W., Kim, J., Underwood, W., Chaudhuri, B., Chermak, D., Antony, G., White, F. F., Somerville, S. C., Mudgett, M. B., and Frommer, W. B. 2010. Sugar transporters for intercellular exchange and nutrition of pathogens. Nature 468(7323):527-U199.

Chevalier, D., Batoux, M., Fulton, L., Pfister, K., Yadav, R. K., Schellenberg, M., and Schneitz, K. 2005. *STRUBBELIG* defines a receptor kinase-mediated signaling pathway regulating organ development in Arabidopsis. PNAS 102(25):9074-9079.

Chronis, D., Chen, S., Lu, S., Hewezi, T., Carpenter, S. C. D., Loria, R., Baum, T. J., and Wang, X. 2013. A ubiquitin carboxyl extension protein secreted from a plant-parasitic nematode *Globodera rostochiensis* is cleaved in planta to promote plant parasitism. Plant J. 74(2):185-196.

Cnops, G., Wang, X., Linstead, P., Van Montagu, M., Van Lijsebettens, M., and Dolan, L. 2000. TORNADO1 and TORNADO2 are required for the specification of radial and circumferential pattern in the Arabidopsis root. Development 127(15):3385-3394.

Complainville, A., Brocard, L. Roberts, I., Dax, E., Sever, N., Sauer, N., Kondorosi, A., Wolf, S., Oparka, K., and Crespi, M. 2003. Nodule initiation involves the creation of a new symplasmic field in specific root cells of *Medicago* species. Plant Cell 15:2778-2791.

Conesa, A., Gotz, S., Garcia-Gomez, J., Terol, J., Talon, M., and Robles, M. 2005. Blast2GO: A universal tool for annotation, visualization and analysis in functional genomics research. Bioinformatics 21(18):3674-3676.

Cosgrove, D. 2000. Loosening of plant cell walls by expansins. Nature 407(6802):321-326.

Davies, K. G., and Curtis, R. H. C. 2011. Cuticle surface coat of plant-parasitic nematodes. Annu. Rev. Phytopathol. 49:135-156.

Davis, E. L., Hussey, R. S., Mitchum, M. G., and Baum, T. J. 2008. Parasitism proteins in nematode-plant interactions. Curr. Opin. Plant Biol. 11(4):360-366.

de Boer, J., McDermott, J., Davis, E., Hussey, R., Popeijus, H., Smant, G., and Baum, T. 2002a. Cloning of a putative pectate lyase gene expressed in the subventral esophageal glands of *Heterodera glycines*. J. Nematol. 34(1):9-11.

de Boer, J., McDermott, J., Wang, X., Maier, T., Qu, F., Hussey, R., Davis, E., and Baum, T. 2002b. The use of DNA microarrays for the developmental expression analysis of cDNAs from the oesophageal gland cell region of *Heterodera glycines*. Mol. Plant Pathol. 3(4):261-270.

Denance, N., Szurek, B., and Noel, L. D. 2014. Emerging functions of nodulin-like proteins in non-nodulating plant species. Plant Cell Physiol. 55(3):469-474.

Desbrosses, G. J., and Stougaard, J. 2011. Root nodulation: A paradigm for how plant-microbe symbiosis influences host developmental pathways. Cell Host Microbe 10(4):348-358.

Dharmasiri, N., Dharmasiri, S., and Estelle, M. 2005. The F-box protein TIR1 is an auxin receptor. Nature 435(7041):441-445.

Dharmasiri, S., Swarup, R., Mockaitis, K., Dharmasiri, N., Singh, S., Kowalchyk, M., Marchant, A., Mills, S., Sandberg, G., Bennett, M., and Estelle, M. 2006. AXR4 is required for localization of the auxin influx facilitator AUX1. Science 312(5777):1218-1220.

Doyle, E., and Lambert, K. 2002. Cloning and characterization of an esophageal-gland-specific pectate lyase from the root-knot nematode *Meloidogyne javanica*. Mol. Plant-Microbe Interact. 15(6):549-556.

Du, Y., and Scheres, B. 2018. Lateral root formation and the multiple roles of auxin. J. Exp. Bot. 69(2):155-167.

Dubreuil, G., Magliano, M., Deleury, E., Abad, P., and Rosso, M. N. 2007. Transcriptome analysis of root-knot nematode functions induced in the early stages of parasitism. New Phytol. 176(2):426-436.

Edgar, B. A., Zielke, N., and Gutierrez, C. 2014. Endocycles: A recurrent evolutionary innovation for post-mitotic cell growth. Nat. Rev. Mol. Cell Biol. 15(3):197-210.

Endre, G., Kereszt, A., Kevei, Z., Mihacea, S., Kalo, P., and Kiss, G. 2002. A receptor kinase gene regulating symbiotic nodule development. Nature 417(6892):962-966.

Engler, J. d. A., and Gheysen, G. 2013. Nematode-induced endoreduplication in plant host cells: Why and how? Mol. Plant-Microbe Interact. 26(1):17-24.

Engler, J. d. A., Vieira, P., Rodiuc, N., Grossi de Sa, M. F., and Engler, G. 2015. Chapter four - the plant cell cycle machinery: Usurped and modulated by plant-parasitic nematodes. Adv. Bot. Res. 73:91-118.

Eom, J., Chen, L., Sosso, D., Julius, B. T., Lin, I. W., Qu, X., Braun, D. M., and Frommer, W. B. 2015. SWEETs, transporters for intracellular and intercellular sugar translocation. Curr. Opin. Plant Biol. 25:53-62.

Eves-Van den Akker, S., Lilley, C. J., Yusup, H. B., Jones, J. T., and Urwin, P. E. 2016. Functional C-TERMINALLY ENCODED PEPTIDE (CEP) plant hormone domains evolved *de novo* in plant parasite *Rotylenchulus reniformis*. Mol. Plant Pathol. 17(8):1265-1275.

Favery, B., Complainville, A., Vinardell, J., Lecomte, P., Vaubert, D., Mergaert, P., Kondorosi, A., Kondorosi, E., Crespi, M., and Abad, P. 2002. The endosymbiosis-induced genes ENOD40 and CCS52a are involved in endoparasitic-nematode interactions in *Medicago truncatula*. Mol. Plant-Microbe Interact. 15(10):1008-1013.

Ferguson, B. J., Indrasumunar, A., Hayashi, S., Lin, M., Lin, Y., Reid, D. E., and Gresshoff, P. M. 2010. Molecular analysis of legume nodule development and autoregulation. J. Integr. Plant Biol. 52(1):61-76.

Flemetakis, E., Dimou, M., Cotzur, D., Efrose, R. C., Aivalakis, G. Colebatch, G., Udvardi, M., and Katinakis, P. 2003. A sucrose transporter, LjSUT4, is up-regulated during *Lotus japonicus* nodule development. J. Exp. Bot. 54(388):1789-1791.

Fu, Q., Li, S., and Yu, D. 2010. Identification of an Arabidopsis nodulin-related protein in heat stress. Mol. Cells 29(1)77-84.

Gamas, P., de Carvalho-Niebel, F., Lescure, N., and Cullimore, J. 1996. Use of a subtractive hybridization approach to identify new *Medicago truncatula* genes induced during root nodule development. Mol. Plant-Microbe Interact. 9(4):233-242.

Ganji, S., Jenkins, J. N., and Wubben, M. J. 2014. Molecular characterization of the reniform nematode C-type lectin gene family reveals a likely role in mitigating environmental stresses during plant parasitism. Gene 537(2):269-278.

Gao, B., Allen, R., Davis, E., Baum, T., and Hussey, R. 2004. Developmental expression and biochemical properties of a beta-1,4-endoglucanase family in the soybean cyst nematode, *Heterodera glycines*. Mol. Plant Pathol. 5(2):93-104.

Gardner, M., Verma, A., and Mitchum, M. G. 2015. Chapter eleven – Emerging roles of cyst nematode effectors in exploiting plant cellular processes. Plant Nematode Interactions: A View on Compatible Interrelationships, 73:259-291.

Gheysen, G., and Mitchum, M. G. 2011. How nematodes manipulate plant development pathways for infection. Curr. Opin. Plant Biol. 14(4):415-421.

Ghosh, R., and Bankaitis, V. A. 2011. Phosphatidylinositol transfer proteins: negotiating the regulatory interface between lipid metabolism and lipid signaling in diverse cellular processes. Biofactors 37(4):290-308.

Ghosh, R., de Campos, M. K. F., Huang, J., Huh, S. K., Orlowski, A., Yang, Y., Tripathi, A., Nile, A., Lee, H., Dynowski, M., Schaefer, H., Rog, T., Lete, M. G., Ahyayauch, H., Alonso, A., Vattulainen, I., Igumenova, T. I., Schaaf, G., and Bankaitis, V. A. 2015. Sec14-nodulin proteins and the patterning of phosphoinositide landmarks for developmental control of membrane morphogenesis. Mol. Biol. Cell 26(9):1764-1781.

Gil, P., Dewey, E., Friml, J., Zhao, Y., Snowden, K., Putterill, J., Palme, K., Estelle, M., and Chory, J. 2001. BIG: A calossin-like protein required for polar auxin transport in Arabidopsis. Genes Dev. 15(15):1985-1997.

Goto-Yamada, S., Mano, S., Nakamori, C., Kondo, M., Yamawaki, R., Kato, A., and Nishimura, M. 2014. Chaperone and protease functions of LON protease 2 modulate the peroxisomal transition and degradation with autophagy. Plant and Cell Physiol. 55(3):482-96.

Goverse, A., Overmars, H., Engelbertink, J., Schots, A., Bakker, J., and Helder, J. 2000. Both induction and morphogenesis of cyst nematode feeding cells are mediated by auxin. Mol. Plant-Microbe Interact. 13(10):1121-1129.

Grant, B., and Hirsh, D. 1999. Receptor-mediated endocytosis in the *Caenorhabditis elegans* oocyte. Mol. Biol. Cell 10(12):4311-26.

Grunewald, W., Cannoot, B., Friml, J., and Gheysen, G. 2009. Parasitic nematodes modulate PIN-mediated auxin transport to facilitate infection. Plos Pathog. 5(1):e1000266.

Grunewald, W., De Smet, I., Lewis, D. R., Loefke, C., Jansen, L., Goeminne, G., Bossche, R. V., Karimi, M., De Rybel, B., Vanholme, B., Teichmann, T., Boerjan, W., Van Montagu, M. C. E., Gheysen, G., Muday, G. K., Friml, J., and Beeckman, T. 2012. Transcription factor WRKY23 assists auxin distribution patterns during Arabidopsis root development through local control on flavonol biosynthesis. Proc. Natl. Acad. Sci. USA 109(5):1554-1559.

Guo, W., Bundithya, W., and Goldsbrough, P. 2003. Characterization of the Arabidopsis metallothionein gene family: Tissue-specific expression and induction during senescence and in response to copper. New Phytol. 159(2):369-381.

Guo, X., Chronis, D., De La Torre, C. M., Smeda, J., Wang, X., and Mitchum, M. G. 2015. Enhanced resistance to soybean cyst nematode *Heterodera glycines* in transgenic soybean by silencing putative CLE receptors. Plant Biotechnol. J. 13(6):801-810.

Haas, B. J., Papanicolaou, A., Yassour, M., Grabherr, M., Blood, P. D., Bowden, J., Couger, M. B., Eccles, D., Li, B., Lieber, M., MacManes, M. D., Ott, M., Orvis, J., Pochet, N., Strozzi, F., Weeks, N., Westerman, R., William, T., Dewey, C. N., Henschel, R., Leduc, R. D., Friedman, N., and Regev, A. 2013. *De novo* transcript sequence reconstruction from RNA-seq using the trinity platform for reference generation and analysis. Nat. Protoc. 8(8):1494-1512.

Haase, S., Ruess, L., Neumann, G., Marhan, S., and Kandeler, E. 2007. Low-level herbivory by root-knot nematodes (*Meloidogyne incognita*) modifies root hair morphology and rhizodeposition in host plants (*Hordeum vulgare*). Plant Soil 301(1-2):151-164.

Haegeman, A., Bauters, L., Kyndt, T., Rahman, M. M., and Gheysen, G. 2013. Identification of candidate effector genes in the transcriptome of the rice root knot nematode *Meloidogyne graminicola*. Mol. Plant Pathol. 14(4):379-390.

Hao, Y., Montiel, R., Abubucker, S., Mitreva, M., and Simoes, N. 2010. Transcripts analysis of the entomopathogenic nematode *Steinernema carpocapsae* induced in vitro with insect haemolymph. Mol. Biochem. Parasitol. 169(2):79-86.

Heald, C., and Robinson, A. 1990. Survey of current distribution of *Rotylenchulus reniformis* in the United States. J. Nematol. 22(4):695-699.

Helariutta, Y., Fukaki, H., Wysocka-Diller, J., Nakajima, K., Jung, J., Sena, G., Hauser, M., and Benfey, P. 2000. The SHORT-ROOT gene controls radial patterning of the Arabidopsis root through radial signaling. Cell 101(5):555-67.

Hewezi, T., Piya, S., Richard, G., and Rice, J. H. 2014. Spatial and temporal expression patterns of auxin response transcription factors in the syncytium induced by the beet cyst nematode *Heterodera schachtii* in Arabidopsis. Mol. Plant Pathol. 15(7):730-736.

Hoeckendorf, A., and Leippe, M. 2012. SPP-3, a saposin-like protein of *Caenorhabditis elegans*, displays antimicrobial and pore-forming activity and is located in the intestine and in one head neuron. Dev. Comp. Immunol. 38(1):181-186.

Hou, H., Erickson, J., Meservy, J., and Schultz, E. A. 2010. FORKED1 encodes a PH domain protein that is required for PIN1 localization in developing leaf veins. Plant J. 63(6):960-973.

Huang, G., Allen, R., Davis, E. L., Baum, T. J., and Hussey, R. S. 2006a. Engineering broad root-knot resistance in transgenic plants by RNAi silencing of a conserved and essential root-knot nematode parasitism gene. Proc. Natl. Acad. Sci. USA 103(39):14302-14306.

Huang, G., Dong, R., Allen, R., Davis, E., Baum, T., and Hussey, R. 2006b. A root-knot nematode secretory peptide functions as a ligand for a plant transcription factor. Mol. Plant-Microbe Interact. 19(5):463-470.

Huang, P., Catinot, J., and Zimmerli, L. 2016. Ethylene response factors in Arabidopsis immunity. J. Exp. Bot. 67(5):1231-1241.

Hundertmark, M., and Hincha, D. K. 2008. LEA (late embryogenesis abundant) proteins and their encoding genes in *Arabidopsis thaliana*. BMC Genomics 9:118.

Hutangura, P., Mathesius U., Jones, M. G. K., and Rolfe B. G. 1999. Auxin induction is a trigger for root gall formation caused by root-knot nematodes in white clover and is associated with the activation of the flavonoid pathway. Aust. J. Plant Physiol. 26(3):221-231.

Iberkleid, I., Vieira, P., Engler, J. d. A., Firester, K., Spiegel, Y., and Horowitz, S. B. 2013. Fatty acid-and retinol-binding protein, Mj-FAR-1 induces tomato host susceptibility to root-knot nematodes. Plos One 8(5):e64586.

Imin, N., Mohd-Radzman, N. A., Ogilvie, H. A., and Djordjevic, M. A. 2013. The peptide-encoding CEP1 gene modulates lateral root and nodule numbers in *Medicago truncatula*. J. Exp. Bot. 64(17):5395-5409.

Jaouannet, M., Magliano, M., Arguel, M. J., Gourgues, M., Evangelisti, E., Abad, P., and Rosso, M. N. 2013. The root-knot nematode calreticulin mi-CRT is a key effector in plant defense suppression. Mol. Plant-Microbe Interact. 26(1):97-105.

Jenkins, W. R. 1964. A rapid centrifugal-flotation technique for separating nematodes from soil. Plant Dis. Rep. 48(9):692.

Jin, S., Xu, C., Li, G., Sun, D., Li, Y., Wang, X., and Liu, S. 2017. Functional characterization of a type 2 metallothionein gene, SsMT2, from alkaline-tolerant *Suaeda salsa*. Sci. Rep. 7:17914.

Jones, M. G. K., and Dropkin, V. H. 1975. Cellular alterations induced in soybean roots by three endoparasitic nematodes. Physiol. Plant Pathol. 5(2):119-124.

Jones, J., Reavy, B., Smant, G., and Prior, A. 2004. Glutathione peroxidases of the potato cyst nematode *Globodera rostochiensis*. Gene 324:47-54.

Juergensen, K., Scholz-Starke, J., Sauer, N., Hess, P., van Bel, A., and Grundler, F. 2003. The companion cell-specific Arabidopsis disaccharide carrier AtSUC2 is expressed in nematode-induced syncytia. Plant Physiol. 131(1):61-69.

Karczmarek, A., Overmars, H., Helder, J., and Goverse, A. 2004. Feeding cell development by cyst and root-knot nematodes involves a similar early, local and transient activation of a specific auxin-inducible promoter element. Mol. Plant Pathol. 5(4):343-346.

Kassaw, T., Bridges, W.,Jr., and Frugoli, J. 2015. Multiple autoregulation of nodulation (AON) signals identified through split root analysis of *Medicago truncatula sunn* and *rdn1* mutants. Plants-Basel 4(2):209-224.

Kennedy, M., Niblack, T., and Krishnan, H. 1999. Infection by *Heterodera glycines* elevates isoflavonoid production and influences soybean nodulation. J. Nematol. 31(3):341-347.

Koizumi, K., Hayashi, T., Wu, S., and Gallagher, K. L. 2012. The SHORT-ROOT protein acts as a mobile, dose-dependent signal in patterning the ground tissue. Proc. Natl. Acad. Sci. USA 109(32): 13010-13015.

Kosinski, M., McDonald, K., Schwartz, J., Yamamoto, I., and Greenstein, D. 2005. *C. elegans* sperm bud vesicles to deliver a meiotic maturation signal to distant oocytes. Development 132(15):3357-3369.

Krichevsky, A., Zaltsman, A., Kozlovsky, S. V., Tian, G., and Citovsky, V. 2009. Regulation of root elongation by histone acetylation in Arabidopsis. J. Mol. Biol. 385(1):45-50.

Kuusk, S., Sohlberg, J. J., Eklund, D. M., and Sundberg, E. 2006. Functionally redundant SHI family genes regulate Arabidopsis gynoecium development in a dose-dependent manner. Plant J. 47(1):99-111.

Kuwabara, P. 2003. The multifaceted *C. elegans* major sperm protein: An ephrin signaling antagonist in oocyte maturation. Genes Dev. 17(2):155-161.

Langmead, B., and Salzberg, S. 2012. Fast gapped-read alignment with Bowtie 2. Nat. Methods 9(4):357-359.

Laskowski, M., Biller, S., Stanley, K., Kajstura, T., and Prusty, R. 2006. Expression profiling of auxin-treated Arabidopsis roots: Toward a molecular analysis of lateral root emergence. Plant and Cell Physiol. 47(6):788-792.

Lavenus, J., Goh, T., Roberts, I., Guyomarc'h, S., Lucas, M., De Smet, I., Fukaki, H., Beeckman, T., Bennett, M., and Laplaze, L. 2013. Lateral root development in Arabidopsis: Fifty shades of auxin. Trends Plant Sci. 18(8):455-463.

Ledger, T. N., Jaubert, S., Bosselut, N., Abad, P., and Rosso, M. 2006. Characterization of a new beta-1,4-endoglucanase gene from the root-knot nematode *Meloidogyne incognita* and evolutionary scheme for phytonematode family 5 glycosyl hydrolases. Gene 382:121-128.

Lee, C., Chronis, D., Kenning, C., Peret, B., Hewezi, T., Davis, E. L., Baum, T. J., Hussey, R., Bennett, M., and Mitchum, M. G. 2011. The novel cyst nematode effector protein 19C07 interacts with the Arabidopsis auxin influx transporter LAX3 to control feeding site development. Plant Physiol. 155(2):866-880.

Lee, H. W., Cho, C., and Kim, J. 2015. Lateral organ boundaries Domain16 and 18 act downstream of the AUXIN1 and LIKE-AUXIN3 auxin influx carriers to control lateral root development in Arabidopsis. Plant Physiol. 168(4):1792-U1177.

Lefebvre, B., Timmers, T., Mbengue, M., Moreau, S., Herve, C., Toth, K., Bittencourt-Silvestre, J., Klaus, D., Deslandes, L., Godiard, L., Murray, J. D., Udvardi, M. K., Raffaele, S., Mongrand, S., Cullimore, J., Gamas, P., Niebel, A., and Ott, T. 2010. A

remorin protein interacts with symbiotic receptors and regulates bacterial infection. Proc. Natl. Acad. Sci. USA 107(5):2343-2348.

Li, J., and Nam, K. H. 2002. Regulation of brassinosteroid signaling by a GSK3/SHAGGY-like kinase. Science 295(5558):1299-1301.

Li, B., and Dewey, C. N. 2011. RSEM: Accurate transcript quantification from RNA-seq data with or without a reference genome. BMC Bioinformatics 12:323.

Li, R., Rashotte, A. M., Singh, N. K., Lawrence, K. S., Weaver, D. B., and Locy, R. D. 2015. Transcriptome analysis of cotton (*Gossypium hirsutum* L.) genotypes that are susceptible, resistant, and hypersensitive to reniform nematode (*Rotylenchulus reniformis*). PLoS One 10(11):e0143261.

Lingard, M. J., and Bartel, B. 2009. Arabidopsis LON2 is necessary for peroxisomal function and sustained matrix protein import. Plant Physiol. 151(3):1354-1365.

Liu, C.W., and Murray, J. D. 2016. The role of flavonoids in nodulation host-range specificity: an update. Plants-Basel 5(33).

Lohar, D., and Bird, D. 2003. *Lotus japonicus*: A new model to study root-parasitic nematodes. Plant Cell Physiol. 44(11):1176-1184.

Lohar, D., Schaff, J., Laskey, J., Kieber, J., Bilyeu, K., and Bird, D. 2004. Cytokinins play opposite roles in lateral root formation, and nematode and rhizobial symbioses. Plant J. 38(2):203-214.

Lopez-Bucio, J., Hernandez-Abreu, E., Sanchez-Calderon, L., Perez-Torres, A., Rampey, R., Bartel, B., and Herrera-Estrella, L. 2005. An auxin transport independent pathway is involved in phosphate stress-induced root architectural alterations in Arabidopsis. Identification of BIG as a mediator of auxin in pericycle cell activation. Plant Physiol. 137(2):681-691.

Love, M. I., Huber, W., and Anders, S. 2014. Moderated estimation of fold change and dispersion for RNA-seq data with DESeq2. Genome Biol. 15(12):550.

Lozano-Duran, R., and Robatzek, S. 2015. 14-3-3 proteins in plant-pathogen interactions. Mol Plant-Microbe Interact 28(5):511-8.

Lozano-Torres, J. L., Wilbers, R. H. P., Gawronski, P., Boshoven, J. C., Finkers-Tomczak, A., Cordewener, J. H. G., America, A. H. P., Overmars, H. A., Van 't Klooster, J. W., Baranowski, L., Sobczak, M., Ilyas, M., van der Hoorn, R. A. L., Schots, A., de Wit, P. J. G. M., Bakker, J., Goverse, A., and Smant, G. 2012. Dual disease resistance mediated by the immune receptor cf-2 in tomato requires a

common virulence target of a fungus and a nematode. Proc. Natl. Acad. Sci. USA 109(25):10119-10124.

Lu, S., Chen, S., Wang, J., Yu, H., Chronis, D., Mitchum, M. G., and Wang, X. 2009. Structural and functional diversity of CLAVATA3/ESR (CLE)-like genes from the potato cyst nematode *Globodera rostochiensis*. Mol. Plant-Microbe Interact. 22(9):1128-1142.

Ma, G. X., Zhou, R. Q., Hu, L., Luo, Y. L., Luo, Y. F., and Zhu, H. H. 2018. Molecular characterization and transcriptional analysis of the female-enriched chondroitin proteoglycan 2 of *Toxocara canis*. J. Helminthol. 92(2):154-160.

Madsen, E., Madsen, L., Radutoiu, S., Olbryt, M., Rakwalska, M., Szczyglowski, K., Sato, S., Kaneko, T., Tabata, S., Sandal, N., and Stougaard, J. 2003. A receptor kinase gene of the LysM type is involved in legume perception of rhizobial signals. Nature 425(6958):637-640.

Mantelin, S., Thorpe, P., and Jones, J. T. 2015. Chapter thirteen - Suppression of plant defences by plant-parasitic nematodes. Plant Nematode Interactions: A View on Compatible Interrelationships, 73:325-337.

Maroti, G., and Kondorosi, E. 2014. Nitrogen-fixing rhizobium-legume symbiosis: Are polyploidy and host peptide-governed symbiont differentiation general principles of endosymbiosis? Front. Microbiol. 5:326.

Mathesius, U. 2003. Conservation and divergence of signalling pathways between roots and soil microbes - the rhizobium-legume symbiosis compared to the development of lateral roots, mycorrhizal interactions and nematode-induced galls. Plant Soil 255(1):105-119.

Mazarei, M., Lennon, K., Puthoff, D., Rodermel, S., and Baum, T. 2003. Expression of an Arabidopsis phosphoglycerate mutase homologue is localized to apical meristems, regulated by hormones, and induced by sedentary plant-parasitic nematodes. Plant Mol. Biol. 53(4):513-530.

McCarter, J. P., Mitreva, M. D., Martin, J., Dante, M., Wylie, T., Rao, U., Pape, D., Bowers, Y., Theising, B., Murphy, C. V., Kloek, A. P., Chiapelli, B. J., Clifton, S. W., Bird, D. M., and Waterston, R. H. 2003. Analysis and functional classification of transcripts from the nematode Meloidogyne incognita. Genome Biol. 4(4):R26.

Mitchum, M. G., Wang, X., Wang, J., and Davis, E. L. 2012. Role of nematode peptides and other small molecules in plant parasitism. Annu. Rev. Phytopathol. 50:175-195.

Mitchum, M. G., Hussey, R. S., Baum, T. J., Wang, X., Elling, A. A., Wubben, M., and Davis, E. L. 2013. Nematode effector proteins: An emerging paradigm of parasitism. New Phytol. 199(4):879-894.

Mitra, R., Shaw, S., and Long, S. 2004. Six nonnodulating plant mutants defective for nod factor-induced transcriptional changes associated with the legume-rhizobia symbiosis. Proc. Natl. Acad. Sci. USA 101(27):10217-10222.

Ng, J. L. P., Perrine-Walker, F., Wasson, A. P., and Mathesius, U. 2015. The control of auxin transport in parasitic and symbiotic root–microbe interactions. Plants 4(3):606-643.

Nguyen, C., Perfus-Barbeoch, L., Quentin, M., Zhao, J., Magliano, M., Marteu, N., da Rocha, M., Nottet, N., Abad, P., and Favery, B. 2018. A root-knot nematode small glycine and cysteine-rich secreted effector, MiSGCR1, is involved in plant parasitism. New Phytol. 217(2):687-699.

Nielsen, H. 2017. Predicting secretory proteins with SignalP. Methods Mol. Biol. 1611:59-73.

Ohyama, K., Ogawa, M., and Matsubayashi, Y. 2008. Identification of a biologically active, small, secreted peptide in Arabidopsis by *in silico* gene screening, followed by LC-MS-based structure analysis. Plant J. 55(1):152-160.

Oldroyd, G., and Long, S. 2003. Identification and characterization of nodulation-signaling pathway 2, a gene of *Medicago truncatula* involved in nod factor signaling. Plant Physiol. 131(3):1027-1032.

Olson, S., Bishop, J., Yates, J., Oegema, K., and Esko, J. 2006. Identification of novel chondroitin proteoglycans in *Caenorhabditis elegans*: Embryonic cell division depends on CPG-1 and CPG-2. J Cell Biol. 173(6):985-994.

Ott, T., van Dongen, J., Gunther, C., Krusell, L., Desbrosses, G., Vigeolas, H., Bock, V., Czechowski, T., Geigenberger, P., and Udvardi, M. 2005. Symbiotic leghemoglobins are crucial for nitrogen fixation in legume root nodules but not for general plant growth and development. Curr. Biol. 15(6):531-535.

Patel, N., Hamamouch, N., Li, C., Hussey, R., Mitchum, M., Baum, T., Wang, X., and Davis, E. L. 2008. Similarity and functional analyses of expressed parasitism genes in *Heterodera schachtii* and *Heterodera glycines*. J. Nematol. 40(4):299-310.

Patel, N., Hamamouch, N., Li, C., Hewezi, T., Hussey, R. S., Baum, T. J., Mitchum M. G., Davis, E. L. 2010. A nematode effector protein similar to annexins in host plants. J. Exp. Bot. 61(1):235-248.

Peiro, A., Izquierdo-Garcia, A. C., Sanchez-Navarro, J. A., Pallas, V., Mulet, J. M., and Aparicio, F. 2014. Patellins 3 and 6, two members of the plant patellin family, interaction with the movement protein of alfalfa mosaic virus and interfere with viral movement. Mol. Plant Pathol. 15(9):881-891.

Peret, B., De Rybel, B., Casimiro, I., Benkova, E., Swarup, R., Laplaze, L., Beeckman, T., and Bennett, M. J. 2009. Arabidopsis lateral root development: An emerging story. Trends Plant Sci 14(7):399-408.

Peret, B., Middleton, A. M., French, A. P., Larrieu, A., Bishopp, A., Njo, M., Wells, D. M., Porco, S., Mellor, N., Band, L. R., Casimiro, I., Kleine-Vehn, J., Vanneste, S., Sairanen, I., Mallet, R., Sandberg, G., Ljung, K., Beeckman, T., Benkova, E., Friml, J., Kramer, E., King, J. R., De Smet, I., Pridmore, T., Owen, M., and Bennett, M. J. 2013. Sequential induction of auxin efflux and influx carriers regulates lateral root emergence. Mol. Syst. Biol. 9:699.

Peterman, T., Ohol, Y., McReynolds, L., and Luna, E. 2004. Patellin1, a novel Sec14-like protein, localizes to the cell plate and binds phosphoinositides. Plant Physiol. 136(2):3080-3094.

Petricka, J. J., Winter, C. M., and Benfey, P. N. 2012. Control of Arabidopsis root development. Annu. Rev. of Plant Biol. 63:563-590.

Preger, V., Tango, N., Marchand, C., Lemaire, S. D., Carbonera, D., Di Valentin, M., Costa, A., Pupillo, P., and Trost, P. 2009. Auxin-responsive genes AIR12 code for a new family of plasma membrane b-type cytochromes specific to flowering plants. Plant Physiol. 150(2):606-620.

Qin, L., Kudla, U., Roze, E., Goverse, A., Popeijus, H., Nieuwland, J., Overmars, H., Jones, J., Schots, A., Smant, G., Bakker, J., and Helder, J. 2004. Plant degradation: A nematode expansin acting on plants. Nature 427(6969):30.

Quentin, M., Abad, P., and Favery, B. 2013. Plant parasitic nematode effectors target host defense and nuclear functions to establish feeding cells. Front. Plant Sci. 4:53.

Rebois, R. V., Madden, P. A., and Eldridge, B. J. 1975. Some ultrastructural changes induced in resistant and susceptible soybean roots following infection by *Rotylenchulus reniformis*. J. Nematol. 7(2):122-139.

Rebois, R. V. 1980. Ultrastructure of a feeding peg and tube associated with *Rotylenchulus reniformis* in cotton. Nematologica 26(4):396-405.

Redding, N. W., Agudelo, P., and Wells, C. E. 2018. Multiple nodulation genes are up-regulated during establishment of reniform nematode feeding sites in soybean. Phytopathology 108(2):275-291.

Reddy, P., Aggarwal, R., Ramos, M., Ladha, J., Brar, D., and Kouchi, H. 1999. Widespread occurrence of the homologues of the early nodulin (ENOD) genes in Oryza species and related grasses. Biochem. Biophys. Res. Commun. 258(1):148-154.

Robinson, A. F., Inserra, R. N., Caswell-Chen, E. P., Vovlas, N., and Troccoli, A. 1997. *Rotylenchulus* species: Identification, distribution, host ranges, and crop plant resistance. Nematropica 27(2):127-180.

Robinson, A. F. 2007. Reniform in US cotton: When, where, why, and some remedies. Annu. Rev. Phytopathol. 45:263-288.

Rodriguez, A., McKay, K., Graham, M., Dittrich, J., and Holgado, A. M. 2014. Analysis of differential gene expression profiles in *Caenorhabditis elegans* knockouts for the v-SNARE master protein 1. J. Neurosci. Res. 92(6):772-782.

Roeder, T., Stanisak, M., Gelhaus, C., Bruchhaus, I., Groetzinger, J., and Leippe, M. 2010. Caenopores are antimicrobial peptides in the nematode *Caenorhabditis elegans* instrumental in nutrition and immunity. Dev. Comp. Immunol. 34(2):203-209.

Roze, E., Hanse, B., Mitreva, M., Vanholme, B., Bakker, J., and Smant, G. 2008. Mining the secretome of the root-knot nematode *Meloidogyne chitwoodi* for parasitism genes. Mol. Plant Pathol. 9(1):1-10.

Sacco, M. A., Koropacka, K., Grenier, E., Jaubert, M. J., Blanchard, A., Goverse, A., Smant, G., and Moffett, P. 2009. The cyst nematode SPRYSEC protein RBP-1 elicits Gpa2-and RanGAP2-dependent plant cell death. Plos Pathog. 5(8):e1000564.

Sakai, T., and Haga, K. 2012. Molecular genetic analysis of phototropism in Arabidopsis. Plant and Cell Physiol. 53(9):1517-34.

Schlicht, M., Ludwig-Mueller, J., Burbach, C., Volkmann, D., and Baluska, F. 2013. Indole-3-butyric acid induces lateral root formation via peroxisome-derived indole-3-acetic acid and nitric oxide. New Phytol. 200(2):473-482.

Schmutz, J., Cannon, S. B., Schlueter, J., Ma, J., Mitros, T., Nelson, W., Hyten, D. L., Song, Q., Thelen, J. J., Cheng, J., Xu, D., Hellsten, U., May, G. D., Yu, Y., Sakurai, T., Umezawa, T., Bhattacharyya, M. K., Sandhu, D., Valliyodan, B., Lindquist, E., Peto, M., Grant, D., Shu, S., Goodstein, D., Barry, K., Futrell-Griggs, M.,

Abernathy, B., Du, J., Tian, Z., Zhu, L., Gill, N., Joshi, T., Libault, M., Sethuraman, A., Zhang, X., Shinozaki, K., Nguyen, H. T., Wing, R. A., Cregan, P., Specht, J., Grimwood, J., Rokhsar, D., Stacey, G., Shoemaker, R. C., and Jackson, S. A. 2010. Genome sequence of the palaeopolyploid soybean. Nature 463(7278):178-183.

Schneider, W. 1996. Vitellogenin receptors: Oocyte-specific members of the low-density lipoprotein receptor supergene family. Int. Rev. Cytol. 166:103-137.

Schneider, C. A., Rasband, W. S., and Eliceiri, K. W. 2012. NIH image to ImageJ: 25 years of image analysis. Nat. Methods 9(7):671-675.

Semblat, J., Rosso, M., Hussey, R., Abad, P., and Castagnone-Sereno, P. 2001. Molecular cloning of a cDNA encoding an amphid-secreted putative avirulence protein from the root-knot nematode *Meloidogyne incognita*. Mol. Plant-Microbe Interact. 14(1):72-79.

Singh, S., Katzer, K., Lambert, J., Cerri, M., and Parniske, M. 2014. CYCLOPS, A DNA-binding transcriptional activator, orchestrates symbiotic root nodule development. Cell Host Microbe 15(2):139-152.

Sivakumar, C. V., and Seshadri, A. R. 1971. Life history of the reniform nematode, *Rotylenchulus reniformis* Linford and Oliveira, 1940. Indian Journal of Nematology 1:7-20

Smant, G., Stokkermans, J. P. W. G., Yan, Y., de Boer, J. M., Baum, T. J., Wang, X., Hussey, R. S., Gommers, F. J., Henrissat, B., Davis, E. L., Helder, J., Schots, A., and Bakker, J. 1998. Endogenous cellulases in animals: Isolation of β-1,4-endoglucanase genes from two species of plant-parasitic cyst nematodes. PNAS 95(9):4906-4911.

Smeds, L., and Kunstner, A. 2011. CONDETRI - A content dependent read trimmer for Illumina data. Plos One 6(10):e26314.

Smith, D., and Fedoroff, N. 1995. LRP1, a gene expressed in lateral and adventitious root primordia of Arabidopsis. Plant Cell 7(6):735-745.

Soyano, T., Hirakawa, H., Sato, S., Hayashi, M., and Kawaguchi, M. 2014. NODULE INCEPTION creates a long-distance negative feedback loop involved in homeostatic regulation of nodule organ production. Proc. Natl. Acad. Sci. USA 111(40):14607-14612.

Stepanova, A. N., Robertson-Hoyt, J., Yun, J., Benavente, L. M., Xie, D., Dolezal, K., Schlereth, A., Juergens, G., and Alonso, J. M. 2008. TAA1-mediated auxin biosynthesis is essential for hormone crosstalk and plant development. Cell 133(1):177-191.

Stracke, S., Kistner, C., Yoshida, S., Mulder, L., Sato, S., Kaneko, T., Tabata, S., Sandal, N., Stougaard, J., Szczyglowski, K., and Parniske, M. 2002. A plant receptor-like kinase required for both bacterial and fungal symbiosis. Nature 417(6892):959-962.

Subramanian, A., Tamayo, P., Mootha, V., Mukherjee, S., Ebert, B., Gillette, M., Paulovich, A., Pomeroy, S., Golub, T., Lander, E., and Mesirov, J. 2005. Gene set enrichment analysis: A knowledge-based approach for interpreting genome-wide expression profiles. Proc. Natl. Acad. Sci. USA 102(43):15545-15550.

Suzaki, T., Yoro, E., and Kawaguchi, M. 2015. Leguminous plants: Inventors of root nodules to accommodate symbiotic bacteria. Int. Rev. Cell Mol. Biol. 316:111-158.

Tapia-Lopez, R., Garcia-Ponce, B., Dubrovsky, J. G., Garay-Arroyo, A., Perez-Ruiz, R. V., Kim, S., Acevedo, F., Pelaz, S., and Alvarez-Buylla, E. R. 2008. An AGAMOUS-related MADS-box gene, XAL1 (AGL12), regulates root meristem cell proliferation and flowering transition in Arabidopsis. Plant Physiol. 146(3):1182-1192.

Trapnell, C., Roberts, A., Goff, L., Pertea, G., Kim, D., Kelley, D. R., Pimentel, H., Salzberg, S. L., Rinn, J. L., and Pachter, L. 2012. Differential gene and transcript expression analysis of RNA-seq experiments with TopHat and cufflinks. Nat. Protoc. 7(3):562-578.

Treonis, A. M., Cook, R., Dawson, L., Grayston, S. J., and Mizen, T. 2007. Effects of a plant parasitic nematode (*Heterodera trifolii*) on clover roots and soil microbial communities. Biol Fertility Soils 43(5):541-548.

Truernit, E. and Sauer, N. 1995. The promoter of the *Arabidopsis thaliana* SUC2 sucrose-H+ symporter gene directs expression of beta-glucuronidase to the phloem – Evidence for phloem loading and unloading by SUC2. Planta 196(3):564-570.

Truong, N. M., Nguyen, C. N., Abad, P., Quentin, M., and Favery, B. 2015. Chapter twelve - function of root-knot nematode effectors and their targets in plant parasitism. Plant Nematode Interactions: A View on Compatible Interrelationships, 73:293-324.

Ueda, M., Matsui, K., Ishiguro, S., Kato, T., Tabata, S., Kobayashi, M., Seki, M., Shinozaki, K., and Okada, K. 2011. Arabidopsis RPT2a encoding the 26S proteasome subunit is required for various aspects of root meristem maintenance, and regulates gametogenesis redundantly with its homolog, RPT2b. Plant and Cell Physiol. 52(9):1628-1640.

Vanholme, B., Van Thuyne, W., Vanhouteghem, K., De Meutter, J., Cannoot, B., and Gheysen, G. 2007. Molecular characterization and functional importance of pectate

lyase secreted by the cyst nematode *Heterodera schachtii*. Mol. Plant Pathol. 8(3):267-278.

Verma, D., Fortin, M., Stanley, J., Mauro, V., Purohit, S., and Morrison, N. 1986. Nodulins and nodulin genes of *Glycine max* - a perspective. Plant Mol. Biol. 7(1):51-61.

Vieira, P., Kyndt, T., Gheysen, G., and Engler, J. d. A. 2013. An insight into critical endocycle genes for plant-parasitic nematode feeding sites establishment. Plant Signal. Behav. 8(6):e24223.

Vieira-de-Mello, G. S., dos Santos, P. B., Soares-Cavalcanti, N. d. M., and Benko-Iseppon, A. M. 2011. Identification and expression of early nodulin in sugarcane transcriptome revealed by *in silico* analysis. Lect. Notes Bioinform. 6685:72-85.

Vilches-Barro, A., and Maizel, A. 2015. Talking through walls: Mechanisms of lateral root emergence in *Arabidopsis thaliana*. Curr. Opin. Plant Biol. 23:31-38.

Vinardell, J. M., Fedorova, E., Cebolla, A., Kevei, Z., Horvath, G., Kelemen, Z., Tarayre, S., Roudier, F., Mergaert, P., Kondorosi, A., and Kondorosi, E. 2003. Endoreduplication mediated by the anaphase-promoting complex activator CCS52A is required for symbiotic cell differentiation in *Medicago truncatula* nodules. Plant Cell 15(9):2093-2105.

Wan, Y., Jasik, J., Wang, L., Hao, H., Volkmann, D., Menzel, D., Mancuso, S., Baluska, F., and Lin, J. 2012. The signal transducer NPH3 integrates the Phototropin1 photosensor with PIN2-based polar auxin transport in Arabidopsis root phototropism. Plant Cell 24(2):551-565.

Wang, X. Mitchum, M. G., Gao, B., Li, C., Diab, H., Baum, T. J., Hussey, R. S., and Davis, E. L. 2005. A parasitism gene from a plant-parasitic nematode with function similar to CLAVATA3/ESR (CLE) of *Arabidopsis thaliana*. Mol. Plant Pathol. 6(2):187-191.

Wang, J., Lee, C., Replogle, A., Joshi, S., Korkin, D., Hussey, R., Baum, T. J., Davis, E. L., Wang, X., and Mitchum, M. G. 2010. Dual roles for the variable domain in protein trafficking and host-specific recognition of *Heterodera glycines* CLE effector proteins. New Phytol. 187(4):1003-1017.

Wasson, A. P., Ramsay, K., Jones, M. G. K., and Mathesius, U. 2009. Differing requirements for flavonoids during the formation of lateral roots, nodules and root knot nematode galls in *Medicago truncatula*. New Phytol. 183(1):167-179.

Weerasinghe, R., Bird, D., and Allen, N. 2005. Root-knot nematodes and bacterial nod factors elicit common signal transduction events in *Lotus japonicus*. Proc. Natl. Acad. Sci. USA 102(8):3147-3152.

Weis, W. I., Taylor, M. E., and Drickamer, K. 1998. The C-type lectin superfamily in the immune system. Immunol. Rev. 163:19-34.

Weise, A., Barker, L., Kuhn, C., Lalonde, S., Buschmann, H., Frommer, W., and Ward, J. 2000. A new subfamily of sucrose transporters, SUT4, with low affinity/high capacity localized in enucleate sieve elements of plants. Plant Cell 12(8):1345-1355.

Wieczorek, K. 2015. Chapter three - Cell wall alterations in nematode-infected roots. Plant Nematode Interactions: A View on Compatible Interrelationships, 73:61-90.

Won, C., Shen, X., Mashiguchi, K., Zheng, Z., Dai, X., Cheng, Y., Kasahara, H., Kamiya, Y., Chory, J., and Zhao, Y. 2011. Conversion of tryptophan to indole-3-acetic acid by TRYPTOPHAN AMINOTRANSFERASES OF ARABIDOPSIS and YUCCAs in Arabidopsis. Proc. Natl. Acad. Sci. USA 108(45):18518-18523.

Wu, G., Lewis, D. R., and Spalding, E. P. 2007. Mutations in Arabidopsis multidrug resistance-like ABC transporters separate the roles of acropetal and basipetal auxin transport in lateral root development. Plant Cell 19(6):1826-1837.

Wubben, M. J., Callahan, F. E., and Scheffler, B. S. 2010a. Transcript analysis of parasitic females of the sedentary semi-endoparasitic nematode *Rotylenchulus reniformis*. Mol. Biochem. Parasitol. 172(1):31-40.

Wubben, M. J., Ganji, S., and Callahan, F. E. 2010b. Identification and molecular characterization of a beta-1,4-endoglucanase gene (Rr-eng-1) from *Rotylenchulus reniformis*. J. Nematol. 42(4):342-351.

Wubben, M. J., Gavilano, L., Baum, T. J., and Davis, E. L. 2015. Sequence and spatiotemporal expression analysis of CLE-motif containing genes from the reniform nematode (*Rotylenchulus reniformis* Linford & Oliveira). J. Nematol. 47(2):159-165.

Xie, F., Murray, J. D., Kim, J., Heckmann, A. B., Edwards, A., Oldroyd, G. E. D., and Downie, A. 2012. Legume pectate lyase required for root infection by rhizobia. Proc. Natl. Acad. Sci. USA 109(2):633-638.

Xue, T., Li, X., Zhu, W., Wu, C., Yang, G., and Zheng, C. 2009. Cotton metallothionein GhMT3a, a reactive oxygen species scavenger, increased tolerance against abiotic stress in transgenic tobacco and yeast. J. Exp. Bot. 60(1):339-349.

Yamaguchi, N., Huang, J., Xu, Y., Tanoi, K., and Ito, T. 2017. Fine-tuning of auxin homeostasis governs the transition from floral stem cell maintenance to gynoecium formation. Nat. Commun. 8:1125.

Yang, H., and Murphy, A. S. 2009. Functional expression and characterization of Arabidopsis ABCB, AUX 1 and PIN auxin transporters in *Schizosaccharomyces pombe*. Plant J. 59(1):179-191.

Yano, K., Shibata, S., Chen, W., Sato, S., Kaneko, T., Jurkiewicz, A., Sandal, N., Banba, M., Imaizumi-Anraku, H., Kojima, T., Ohtomo, R., Szczyglowski, K., Stougaard, J., Tabata, S., Hayashi, M., Kouchi, H., and Umehara, Y. 2009. CERBERUS, a novel U-box protein containing WD-40 repeats, is required for formation of the infection thread and nodule development in the legume-rhizobium symbiosis. Plant J. 60(1):168-180.

Yu, L., Miao, Z., Qi, G., Wu, J., Cai, X., Mao, J., and Xiang, C. 2014. MADS-box transcription factor AGL21 regulates lateral root development and responds to multiple external and physiological signals. Mol. Plant 7(11):1653-1669.

Yuan, J., Chen, D., Ren, Y., Zhang, X., and Zhao, J. 2008. Characteristic and expression analysis of a metallothionein gene, OsMT2b, down-regulated by cytokinin suggests functions in root development and seed embryo germination of rice. Plant Physiol. 146(4):1637-1650.

Zazimalova, E., Murphy, A. S., Yang, H., Hoyerova, K., and Hosek, P. 2010. Auxin transporters - Why so many? Cold Spring Harb. Perspect. Biol. 2(3):a001552.

Zhang, H., and Forde, B. G. 2000. Regulation of Arabidopsis root development by nitrate availability. J. Exp. Bot. 51(342):51-59.

Zhao, Y., Christensen, S., Fankhauser, C., Cashman, J., Cohen, J., Weigel, D., and Chory, J. 2001. A role for flavin monooxygenase-like enzymes in auxin biosynthesis. Science 291(5502):306-309.

Zhao, J. 2015. Phospholipase D and phosphatidic acid in plant defence response: From protein-protein and lipid-protein interactions to hormone signaling. J. Exp. Bot. 66(7):1721-1736.